Somatosensory two-photon calcium imaging of nociceptive neuron populations in rodent *ex vivo* spinal cord

by

Joseph Salsovic

Submitted to the Graduate Faculty of the

School of Medicine in partial fulfillment

of the requirements for the degree of

Doctor of Philosophy

University of Pittsburgh

2022

UNIVERSITY OF PITTSBURGH

SCHOOL OF MEDICINE

This dissertation was presented

by

Joseph Salsovic

It was defended on

December 9, 2022

and approved by

Sarah Ross, Associate Professor, Department of Neurobiology & Anesthesiology

Kathryn Albers, Professor, Department of Neurobiology

Stephen Meriney, Professor and Chairman, Department of Neuroscience

Brian Davis, Professor, Department of Neurobiology

Mark Baccei, Professor, Department of Anesthesiology, University of Cincinnati

Thesis Advisor: H. Richard Koerber, Professor, Department of Neurobiology

Somatosensory two photon calcium imaging of nociceptive neuron populations in rodent *ex vivo* cord

Joseph Salsovic

University of Pittsburgh, 2022

Spinal dorsal horn disinhibition occurs in both development and painful neuropathies. In the naïve condition, heterogenous polymodal nociceptors of multiple tissue-types input into superficial lamina of the spinal dorsal horn, where local nociceptive neurons are controlled by inhibitory networks. However, it's unknown how inhibitory networks carve out distinct excitatory population responses from these heterogenous peripheral inputs. To address this knowledge gap, we used two-photon calcium imaging of populations of excitatory neurons in the mouse superficial dorsal horn. We identify the cutaneous modalities and tissue-type convergence in populations of superficial excitatory neurons. We find that, in the naïve condition, a majority of superficial excitatory neurons are polymodal and respond to two or more modalities. These polymodal neurons however are a heterogenous group composed of neurons with distinct modality tunings. Next, we determine the level of tissue-type convergence in superficial excitatory neurons. We identify a population of neurons responsive to both cutaneous and musculoskeletal stimulation and find that they are mechanical, heat, and cold (MHC) responsive and mechanical-tuned. Finally, to determine the role of inhibitory networks in shaping these naïve populations, we pharmacologically instate spinal disinhibition and find an increase in polymodality with mechanical population tuning driven by low-threshold mechanical inputs. In summary, during disinhibition, heterogenous, multi-functional naïve populations with distinct modality tunings become strictly polymodal with mechanical tuning resulting in a loss of the neural organization that may drive normal pain percepts.

Table of Contents

List of Tables

List of Figures

List of Supplemental Figures

1.0 Introduction

1.1 Premise

Naïve Cutaneous Modalities and Tunings of SDH Neuron Subpopulations

Somatosensation is often perceived in terms of its stimulus modality, intensity, duration and location on the body. Modalities are a principal feature of stimuli and are usually either mechanical, thermal, or chemical. Clinically, injuries can result in different pain modalities, sometimes preferential to one modality over another[93]. In addition, it's well established that pain arises from the somatosensory nervous system[34]. Thus, there is considerable interest in identifying the somatosensory neuron populations that drive different pain modalities for different injuries.

Since spinal dorsal horn neurons integrate peripheral somatosensory inputs and triage output to the brain, there's a significant effort in identifying the dorsal horn neurons that contribute to the nociceptive processing. In particular, spinal *superficial neurons* are thought to be part of a nociceptive pathway to the brain. Many polymodal nociceptors send their central projections primarily to superficial lamina of the cord[6;50-55], where nociceptive neurons project to the brainstem and thalamus[1-3;7;9;20;21;23;24;45;46;56;66;71;84]. In particular, lamina I spinoparabrachial neurons are thought to play an important role in driving pain behavior[26;33].

Given the importance of the response modalities of superficial dorsal horn (SDH) nociceptive neurons, the first section of this work starts with a thorough investigation on their *cutaneous modalities*. In the past, research has investigated the responses of individual SDH neurons evoked from various modalities of stimuli applied to the skin. It's known that a large

proportion of superficial neurons are nociceptive-specific and polymodal responding to two or more modalities[1-3;7;22;45;46;62;66;67]. Still, prior research has been met with two limitations that the current research expands on.

First, a cutaneous modality characterization of superficial neurons has never been done on *populations of neurons from individual animals*. Here, two-photon calcium imaging was used to determine the cutaneous modalities of SDH neuron populations of individual animals. This work provides the first comprehensive modality characterization of populations of SDH neurons. In doing so, one of the goals was to determine whether calcium population imaging can reproduce the nociceptive polymodality seen in prior electrophysiology work. Importantly, this method allowed for true statistics that samples individual animals (as opposed to neurons), increasing confidence and reducing the chance of sampling errors. Moreover, data collection on large numbers of neurons per animal can lead to the discovery of new neurons not yet observed in the prior studies that were limited to relatively few neurons per animal.

Second, while many nociceptive SDH neurons are known to be polymodal, their optimal stimuli are unknown, i.e. the modality of stimulation that a polymodal neuron responds to best. Here, an optimal stimulus is referred to as *primary modality preference* and *modality tuning*. For the first time, a *modality population tuning* methodology that identifies uni-, bi-, and tri-tuned polymodal neurons is purposefully developed for SDH neurons.

Naïve Musculoskeletal and Cutaneous Convergence in SDH Neuron Populations

Among clinical pain conditions, musculoskeletal pain is reported as most frequent[18]. The second section of this work thus examines musculoskeletal-evoked calcium population responses in SDH neurons. Pain referral between different types of tissues and body locations has been

reported in some types of neuropathic pain[63;73]. Yet, relatively minimal information is known about the convergence of inputs from somatic tissues in the superficial dorsal horn. Thus, this work does a systematic characterization of the convergence in musculoskeletal and cutaneous sensory inputs in the SDH. Briefly in the 1960s, and in the '80s and '90s, spinal neurons responsive to both skin and musculoskeletal tissue, or *Cutaneous & Musculoskeletal (C&MS) convergence neurons*, had been identified in the cat and rodent across a few studies[24;41;42;85;95;96]. While these studies identified C&MS convergence neurons and described some aspects of their inputs (e.g. conduction velocity, mechanical-responsiveness), they were limited primarily to mechanical and electrical modalities in naïve animals. In addition, the number of neurons recorded was insufficient to determine the true proportion of neurons with convergence in the areas recorded. More recently, electrophysiological proprieties of C&MS convergence lamina I projection neurons were investigated during development.[65]

This work expands on prior knowledge in three ways. First, to determine a true proportion of neurons with convergent responses, SDH C&MS convergence is examined in *populations of neurons from individual animals*. Second, to expand on the convergence studies that used mechanical stimulation of the past, a *cutaneous modality characterization, inclusive of mechanical, heat and cold modalities,* is described for neurons with musculoskeletal responses. Lastly, to understand the role of spinal inhibition in shaping convergence, pharmacology is used to determine how disinhibition changes properties of convergence in the superficial dorsal horn.

Spinal Disinhibition of Musculoskeletal and Cutaneous Evoked Population Responses

The third section examines the role of spinal inhibitory neurons in shaping the modalities and population tuning of superficial excitatory neurons. In a naïve condition, spinal nociceptive

neurons are regulated by inhibitory neurons that control their nociceptive-specific properties and distinct modalities[86;93]. In superficial laminae, there is a barrage of heterogenous, polymodal nociceptive inputs. Generally, polymodal nociceptors with thermal and mechanical optimal stimuli input into lamina I and lamina II respectively[6;50-55]. In addition, low-threshold mechanical fibers input generally into lamina III-V[13]. During development, neuropathy, or pharmacological spinal disinhibition, reductions in mechanical thresholds and amplified evoked responses are observed[1;2;5;29;30;56;93].

Since spinal disinhibition produces pronounced mechanical allodynia, thermal hyperalgesia, and spontaneous behaviors[8;31;35;44;48;61;68;70;86;93;94;98], it's important to understand how inhibitory neurons affect the modalities of neuron populations that drive these behaviors. In particular, given the heterogeneity of polymodal nociceptor inputs and the close proximity of superficial laminae, it's unknown how inhibitory neurons integrate the *population modality tuning* of superficial excitatory neurons. Furthermore, with inhibition removed, it's unknown the extent to which SDH population modality tuning is affected by gains in low-threshold mechanical inputs from deeper laminae. Here, we use calcium imaging to examine superficial populations during a state of disinhibition. We take a look at how central disinhibition affects polymodality, population modality tuning, and musculoskeletal and cutaneous convergence amongst populations of neurons from individual animals.

1.2 Background

Organization in the Somatosensory Nervous System

Mechanism of Conscious Somatosensory Perception

It should be well known that properties of local stimuli are represented in the somatosensory nervous system. In the periphery, the spatiotemporal and intensity properties of a mechanical, thermal or chemical stimulus are first transduced into electrical signals by somatosensory afferent fibers. The transduced electrical signal then enters the spinal cord, where dorsal horn inhibitory circuits are organized to fine-tune the representation of the stimulus. Dorsal horn neurons then quickly output the stimulus' representation to the brain, where a conscious awareness of the stimulus occurs. In the brain, the stimulus neural representation, combined with associative learning from prior somatosensory experience, as well as inputs from other senses and environmental cues, all can help us discriminate the stimulus. The entire neural circuit – from stimulus transduction through to the dorsal horn and brain – is required for an acute somatosensory perception in a healthy, non-pathological state.

General Organization of the Spinal Dorsal Horn

In order to understand how spinal dorsal horn circuits mediate somatosensation, it's important to first understand its underlying anatomical organization. In the 1950s, Bor Rexed introduced a dorsal horn laminar scheme based on its cytoarchitecture[88;89]. While Rexed first

introduced the laminar scheme in the cat, it was subsequently described in rodents[78;79]. In brief, the lamina I marginal zone is characterized primarily by the morphology of resident neurons with long-ranging horizontal dendrites. Ventral to lamina I is lamina II, which is inclusive of the substantia gelatinosa and distinguished by the presence of small cells. Lamina II is further divided into outer lamina IIo (densely packed cells) and inner lamina IIi (less densely packed cells). Ventral to lamina II are laminae III-V, which are distinguished by the presence of myelinated afferent fibers.

More recently, dorsal horn neurons have been defined according to their neurochemical composition. Neurons with soma local to the dorsal horn can be divided into two main groups: inhibitory neurons (GABAergic and/or glycinergic) and excitatory (glutamatergic) neurons. In rodent laminae I-III, a majority of neurons are excitatory glutamatergic neurons. These neurons frequently express somatostatin (SST), neurotensin, neurokinin B (NKB), gastrin-releasing peptide (GRP), calretinin, and PKCg[36]. Inhibitory neurons, which make up a minority of SDH neurons have been found to make neuropeptide Y, parvalbumin, nNOS, galanin and dynorphin[11].

Cutaneous Somatotopy in the Dorsal Horn

In addition to the cytoarchitecture of the dorsal horn, dorsal horn neurons also display a somatotopic representation of the body. In the 1970s, Brown and Fuchs quantitatively mapped out the mediaolateral somatotopic representation of skin in the lumbosacral cord[14], which was found to be consistent across spinal segments[57].

The dorsal horn somatotopy depends on the organization of both primary afferents and local dorsal horn neurons. In the dorsal horn, the spatial aspects of a stimulus are first influenced by the location of the peripheral nerve fibers that transduced it. Cutaneous nerve fibers are centrally

arranged such that nerve fibers innervating distal skin terminate in the dorsal horn medially, and cutaneous nerve fibers innervating proximal skin terminate in the dorsal horn laterally. While the location of primary afferents alone provides for a crude somatotopy, the dorsal horn neurons establish a more refined somatotopy. For adjacent roots, there is overlapping projections in the skin and the spinal cord[25]; however, receptive fields of dorsal horn neurons in different spinal segments are largely non-overlapping[15;58]. In addition, when inhibitory circuits are weaker, both in early development and during injury, receptive fields of dorsal horn neurons expand and overlap[29;30;47;93;103;107]. This data taken together suggests that dorsal horn inhibitory circuits fine-tune the somatotopy in the dorsal horn.

Dorsal Horn Organization by Afferent Modalities

Unmyelinated high-threshold cutaneous mechanoreceptors (C-fiber nociceptors)

While cutaneous C-fiber nociceptors make up a diverse group of sensory neurons, many share several things in common. First, they are relatively small for peripheral neurons and are unmyelinated with slowly conducting broad inflected somatic action potentials[6;28;32;49;59]. In addition, most C-fiber nociceptors have higher thresholds compared to low-threshold mechanoreceptors[28]. Most are polymodal, code for intensity into the noxious range, and can become sensitized during injury[6;50-55]. Lastly, they innervate both the skin and cord superficially. Yet, C-fiber nociceptors as whole are still a heterogeneous group of sensory neurons. As a population, they come in a wide range of slow conduction velocities; demonstrate a wide range of thresholds, adequate stimuli, and optimal stimuli; and some may only become responsive during injury[6;28;32;49-55;59;87]. Importantly, unmyelinated nociceptors are heterogenous in their neurochemical phenotype and their role in hypersensitivity across various injuries.

In terms of phenotypic diversity, unmyelinated cutaneous afferents contain a large number of neurochemicals. Historically, C-fibers have been divided into two major groups[99]. The first group are sensitive to the neurotrophin nerve growth factor (NGF), express neurotrophin receptor, TrkA, and usually contain neuropeptides such as calcitonin gene-related peptide (CGRP), substance P and galanin[4;10;80]. The second group usually lack neuropeptides[4], but bind lectin IB4 and are responsive to glial cell line-derived neurotrophic factor (GDNF), express the receptor tyrosine kinase (RET), and usually express the purinergic receptor P2X3[81]. The central arborizations of these two populations (i.e. peptidergic and IB4+) are segregated in the superficial dorsal horn, with peptidergic fibers projecting to lamina I and lamina IIo, and IB4+ fibers projecting to central lamina[4;97;106].

Myelinated high-threshold cutaneous mechanoreceptors (Aδ Nociceptors)

Aδ nociceptors are a diverse group of myelinated nociceptors. They generally are medium sized and lightly myelinated with mid-ranged conduction velocities. They share characteristics of C-fiber nociceptors. For example, most Aδ nociceptors are polymodal and code for stimulus intensity into the noxious range and terminate centrally in lamina I and IIo[16;17;39;67]. Furthermore, myelinated nociceptors have broad inflected somatic action potentials similar to C-fibers [60;105]. Nevertheless, the group displays a wide range of neurochemical phenotypes[64;67;105]

Myelinated low-threshold cutaneous mechanoreceptors (LTMR)

Low-threshold mechanoreceptive fibers enter the spinal cord via the dorsolateral Lissauer's tract, diverge into ascending and descending branches, and terminate in laminae IIi-V[13]. During injury and a state of disinhibition, a gain in low-threshold mechanoreceptor inputs into lamina I is

thought to drive mechanical allodynia. Here, during disinhibition, we examine how low-threshold mechanoreceptors play a role in the shaping the modality tuning of SDH neurons.

Afferent fibers innervating musculoskeletal tissue

Afferent fibers innervating muscle, tendons and joints are also characterized by their adequate stimuli, conduction velocity, neurochemical phenotype, and location of central projections. Group III and IV fibers are can respond to mechanical, thermal, and chemical [27;43;52;72] modalities. Group III fibers conduct in the Aδ range and are most frequently responsive to mechanical stimuli and have had central projections found in both superficial and deep laminae[52]. In contrast, Group IV fibers conduct in the C-fiber range and are most frequently chemoresponsive with central projections limited to lamina I and lamina II[52].

Spinal Disinhibition

Inhibitory neurons establish organization in the dorsal horn and provide strong control over the function of nociceptive neurons. To maintain organization in the dorsal horn, they serve a number of functions. In the context of nociception, at least four functions have been identified in the past[93]. First, they temper responses in nociceptive neurons. When central inhibition is removed, peripheral nociceptors drive amplified action potentials in nociceptive dorsal horn neurons, which may correspond with hyperalgesia and early development. Second, they can prevent or reduce low-threshold afferent inputs into nociceptive neurons. Without central inhibition, nociceptive neuron thresholds drop[1;56], as seen with allodynia[8;31;44;68;70;94;98] and early development [29;30;103]. Third, they inhibit spontaneous activity in nociceptive neurons[12;92], as associated with

disinhibition-dependent spontaneous behaviors. And fourth, inhibitory neurons tighten the receptive field sizes of nociceptive neurons, preventing referred or expansive pain on the body.

The two major inhibitory neurotransmitters in CNS neurons are GABA and glycine. GABA and glycine are found throughout the dorsal horn, and have been found to be co-localized in interneurons in lamina I to lamina III[74;100-102]. In neuropathic nerve injury models, both pre-synaptic and post-synaptic changes can occur in local dorsal horn neurons. The immunoreactivity of both GABA and glycine is reduced, but perhaps in some cases without changes in the number of GABAergic and glycine neurons[48;93]. In addition, GABA and glycine vesicular transporters are hindered. Post-synaptically, $GABA_AR$ and GlyRs have been observed to be modified for less chloride conductance[93]. Since the 1980s, spinal administration of either $GABA_AR$ or GlyR antagonists have been reported to cause a reversable mechanical allodynia, thermal hyperalgesia, and spontaneous behaviors[8;31;44;61;68;70;94;98].

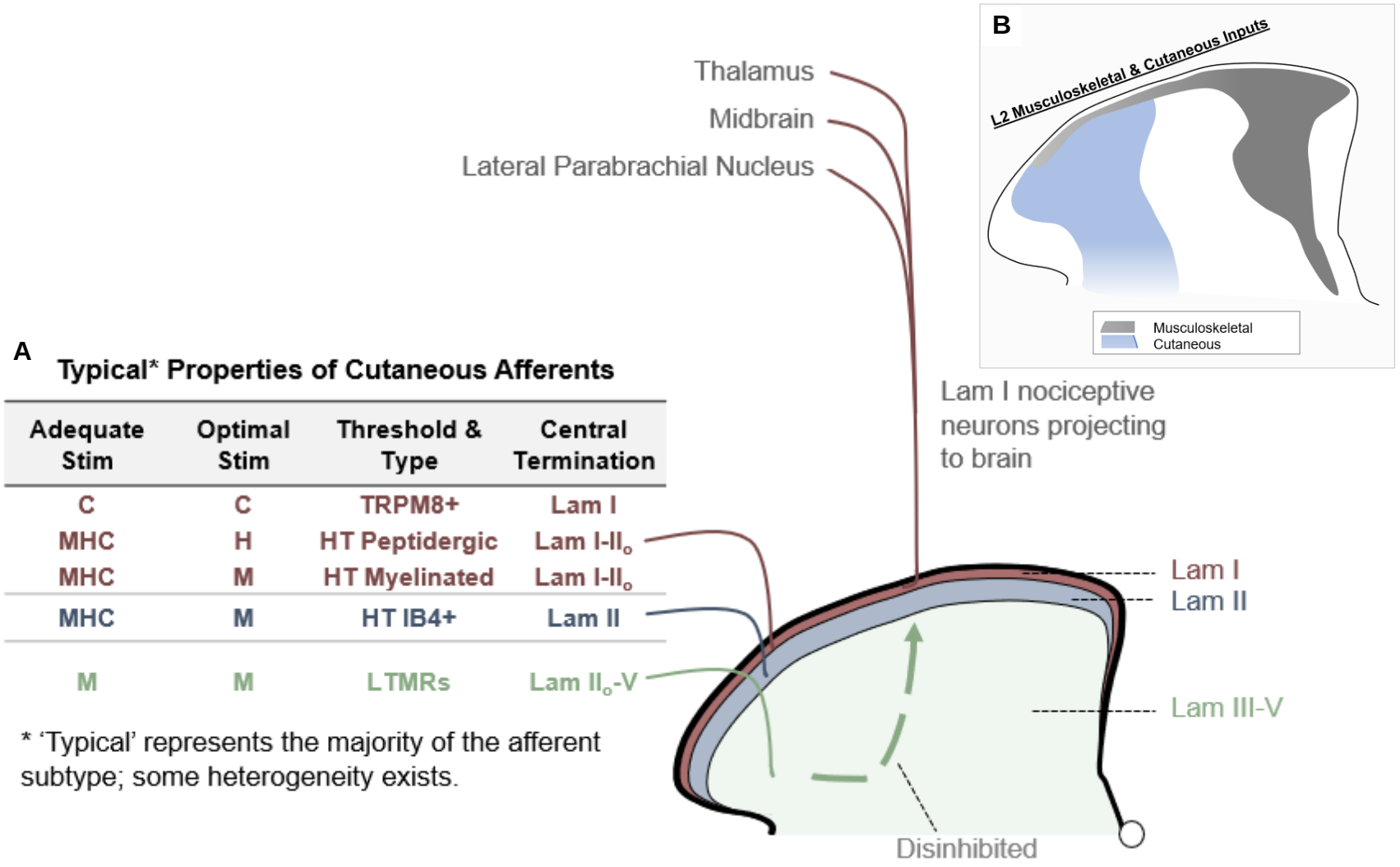

Figure 1: Organization in the Somatosensory Nervous System

Figure 1 Legend:

A: Heterogenous, polymodal somatosensory inputs into the superficial dorsal horn and intermediate and deep dorsal horn. TRPM+, peptidergic, myelinated, and IB4+ fibers terminate in laminae I-II_o, whereas low-threshold mechanical afferents terminate in laminae II_o -V. When inhibition is reduced, it's thought that low-threshold mechanical inputs input into lamina I nociceptive neurons that project to the brain.

B: Illustration of L2 cross section of dorsal horn showing overlap of femoral nerve (musculoskeletal) and lateral femoral cutaneous fiber projections. Musculoskeletal inputs generally are more medial in the dorsal horn compared to cutaneous. However, in L2, femoral fibers project more laterally in superficial laminae only.

2.0 Methods

2.1 Experiments

Animals

All experiments were performed with approval of the University of Pittsburgh's Institutional Animal Care and Use Committee (IACUC, Protocol Numbers 21100045 and 21038819). All mice used in experiments had a C57/BL6 background and were heterozygous for both the Vglut2-ires-cre allele (Jax Stock #016963) and the Ai96 allele (for Cre-dependent expression of GCaMP6s, Jax Stock # 028866). Mice were housed on a 12-hour light cycle with ad-libitum water and food in accordance with the United States National Institutes of Health guidelines for the care and use of laboratory animals. Relative humidity was kept between 30% and 70% and temperature was kept between 20 and 26°C. 10-15 fresh air changes per hour was provided for adequate ventilation. Daily observation of all animals was required, and bedding was changed at least weekly. Social housing was utilized with no more than 4 adult mice per cage was permitted. Single housing was not used except for cases of animal welfare, e.g., aggressive males being separated. Enrichment was provided in the form of soft bedding that can be burrowed within, plastic housing domes, and running wheels. Analysis was performed on 14 mice of both sexes.

Semi-intact Somatosensory Dissection

Mice were deeply anesthetized with a ketamine/xylazine mixture (1.75 mg ketamine and 0.25 mg xylazine per 20 g body weight). The entire dorsal side of the animal was shaved with an electric clipper leaving 2 - 3 mm of hair in place. Next, mice were transcardially perfused with 95%O_2/5%CO_2 saturated, chilled, sucrose-based artificial cerebrospinal fluid (ACSF). The sucrose-based ACSF contained (in mM): 234 sucrose, 2.5 KCl, 0.5 $CaCl_2$, 10 $MgSO_4$, 1.25 NaH_2PO_4, 26 $NaHCO_3$, and 11 Glucose. During the perfusion, a complete dorsal laminectomy from cervical to sacral segments was performed. Next, the spinal column, right hip, leg and foot as a single structure was cut out from the animal. The structure was immediately transferred into a dissection dish with circulating 234 sucrose, 2.5 KCl, 0.5 $CaCl_2$, 10 $MgSO_4$, 1.25 NaH_2PO_4, 26 $NaHCO_3$, and 11 Glucose. Over the course of two to three hours, the lateral femoral cutaneous nerve and skin, saphenous nerve and skin, and femoral nerve were each dissected out in continuum from the skin to the spinal cord. The dura was cut and removed from the entire spinal cord. After the dura was removed, the spinal cord was carefully lifted away from bone as dorsal and ventral roots were cut, leaving only the ipsilateral L1-L4 dorsal roots intact. Once the spinal cord was lifted away from the bone, any remaining dura was removed. The spinal cord was then pinned down so that the ipsilateral L2 visible grey matter was parallel to the ground. To do so, Minutien pins (FST Cat: 26002-20) were placed through the ventral horn parallel to the coronal axis at about every two spinal segments from the conus medullaris through cervical segments. No pins were placed near or under the L2 segment. Once the spinal cord was pinned in place, the L1 root was cut distally, pulled back gently to expose the entire L2 grey matter, and then fully excised from the cord. Pia was kept for imaging experiments. After the spinal cord was prepared, the skin was

also pinned down and the dissection was complete. The dish was transferred to the microscope rig. 5 liters of standard ACSF solution containing (in mM):

117 NaCl, 3.6 KCl, 2.5 $CaCl_2$, 1.2 $MgCl_2$, 1.2 NaH_2PO_4, 25 $NaHCO_3$, 11 glucose) was washed in and out for 30 min before recirculating. Next, the temperature of the bath solution was maintained at 26.5° C. Suction electrodes were positioned on nerves. Imaging began 30 - 60 min after completion of dissection.

Multiphoton Imaging

Ca^{2+} imaging was performed on a Leica SP5 MP microscope using a Leica 20x NA 1.0 water immersion lens with a Coherent Chameleon Ultra II Ti:Si femtosecond laser set to 940 nm for Ca^{2+} imaging. Fluorescence was captured with HyD detectors and standard FITC/TRITC emission filter sets with a 570 nm dichroic beam splitter. The scope was focused on the most superficial layer of neurons, scanning at 2.3 Hz with a 1.2x optical zoom at 1024 X 512 pixel resolution and a field size of 615.7 x 307.8 μm size yielding 1.6632 pixels per micron.

Since each animal's anatomy slightly differs, the grey matter location to image was functionally identified in each experiment. Before collecting data, to troubleshoot, a field of view within the L2 SDH was selected to image. Generally, the scope was always focused on the most superficial neurons that surfaced the cord (visible grey matter) spanning from the rostral end of the L2 root entry to the caudal end of the L1 root entry. Within this superficial L2 location, the exact location along the mediolateral axis of the surfaced grey mattered varied slightly across animals, however was always within the visible grey matter. This location was determined by success rates in population responses across multiple trials of mechanical, heat, cold skin stimulation and electrical nerve stimulation. If stimuli of each modality reliably evoked a

population response by eye to several trials each across a 30-minute period, then the location was selected to move forward to collect data. In other words, reliably achieving evoked population responses to all three modalities in the same location was a prerequisite to moving forward with the experiment. Data was not collected during this troubleshooting period. Imaging, stimuli controllers, feedback sensors (thermocouples, load cells, etc.), and event times were synchronized using a Power1401 and Signal (CED).

Natural Cutaneous Stimuli Application

All natural stimuli were applied to the same area of the skin for every animal, and centered on the skin innervated by the main trunk of the lateral femoral cutaneous nerve encompassing approximately 20 mm by 20 mm area. Each stimulation type was performed in 3 trials in the naïve period and 2 trials during the disinhibition period. 3 to 5 minutes of time was given in-between each trial.

High-threshold (HT) Mechanical cutaneous stimulation (referred to as "Mechanical" otherwise) was performed with a quantitative sensory testing brush (Somedic SenseLab AB, SENSELab Brush-05). HT Mechanical stimulation was applied for 3 seconds by placing a brush on the location of the skin where the main trunk of the lateral femoral cutaneous innervates, applying pressure, and then without lifting the brush, swirling and slightly moving the brush in a circular motion so that the entire patch of lateral femoral cutaneous skin was stretched while continuously applying pressure. Approximately a 20mm by 20mm area of the skin was stimulated.

Low-threshold Mechanical cutaneous stimulation was applied with an air puff for 3 seconds via a PicoSpritzer III (Parker Hannifin) through a 6mm diameter pipette, 0.7mm distance from the skin, with a pressure measured at 0.034 PSI (0.24kPA; 4.73 mN).

Heat stimulation was applied to the skin with 60° C saline applied through a 10mL syringe with a 18-gauge blunt needle moving slowly along the entire patch of lateral femoral cutaneous skin (approximately 20 mm by 20 mm area) for 5 seconds. Five seconds of stimulation was used to help maintain a constant temperature without cooling. Due to the cooling properties of saline, it's likely the average temperature of the skin was approximately 55° C. A one-second 50 degrees saline was noticeably less painful compared to 50° C Peltier applied to the experimenter's arm. Similarly, cold stimulation was applied to the skin with 0° C saline applied through a 10mL syringe with a 18-gauge blunt needle moving slowly along the entire patch of lateral femoral cutaneous skin (approximately 20 mm by 20 mm area) for 5 seconds.

Electrical Nerve Stimulation

To stimulate musculoskeletal nerve fibers, a suction electrode was placed on the cut end of the femoral nerve at the point in which the femoral nerve had entered the quadriceps. The femoral nerve was stimulated with 10, 1ms pulses at 15 Hz at either 2 μA, 5 μA, 10 μA, 50 μA, or 2 mA intensities.

Compound Action Potentials

Compound action potentials were used to determine the femoral nerve stimulation intensities that activated fibers of different conduction velocities. The femoral nerve was stimulated while compound action potentials were recorded from the whole L3 dorsal roots. Using the same dissection as described above, only the femoral nerve, L2 through L4 ganglia and roots, and cord were included. The L3 root was cut back halfway between the ganglia and entry zone of

the cord. Suction electrodes were placed on the cut ends of the femoral nerve and L3 dorsal roots. 10, 1 ms pulses at 15 Hz with intensities ranging from 1 μA to 2 mA were used for femoral nerve stimulation. 2 μA activated most if not all Group I and II fibers, 50 μA activated most if not all Group I-III fibers, and 2 mA stimulation activated most if not all Group I-IV fibers of the femoral nerve.

Musculoskeletal & Cutaneous Convergence Experiments

2 μA, 50 μA, and 2 mA femoral nerve stimulation intensities were used based upon the Type I-II, III, IV components respectively identified in femoral nerve-evoked compound action potential L2 root recordings (Supplemental Figure 4). The nerve stimulation frequency, 10, 1 msec pulses at 15 Hz, was determined from 2P imaging control experiments that showed a reproduction of responses at this frequency, count and pulse duration (Supplemental Figure 1J). 15 Hz 10 pulses was settled on as a moderate number and frequency of APs. This quantity of input seemed to consistently evoke a GCaMP response, but not big enough to cause over toxicity. While 2 μA (Group I-II) intensity easily and consistently evoked the early component of the compound action potential in several animals, in no 2P experiments was a 2 μA evoked GCaMP response in VGlut2+ superficial neurons observed in both naïve and disinhibition states. The threshold for an evoked GCaMP6s signal was observed typically in the range of 5-10 μA.

In this report, 50 μA (Group III) and 2 mA (Group IV) femoral nerve electrical stimulations were analyzed for responder numbers. A stimulus intensity of 2 mA nerve was sufficient to activate approximately 1.5 times the number that responded to a stimulus intensity of 50 μA (Supplemental 4D). Only 2 mA femoral nerve stimulation was further analyzed beyond responder number; and

all musculoskeletal and cutaneous convergence data herein is reflective of the 2mA femoral nerve stim.

Drug Applications

To instate disinhibition, 10uM bicuculine and 1uM strychnine was recirculated in the bath of the *ex vivo* dissection. These concentrations were based on the 10-20 μM bicuculine and 0.5-4 μM strychnine concentrations used in previous spinal cord slice electrophysiology and imaging experiments[5;12;83;92]. Bicuculine and strychnine were added to oxygenated 500 mL of aCSF and circulated into bath. Based on the flow rate, 2 minutes was given to wash out the existing circulating aCSF. Following 2 minutes, the aCSF with bicuculline and strychnine was recirculated continuously. Once recirculating, a 10-minute wait period was given before the first stimulation.

2.2 Data Analysis

Image Processing and Data Extraction

Suite2p (v0.10.0, HHMI Janelia) was used for image registration. Blinded to stimulation, the entire video was scrolled through to validate that the same plane, i.e. population of cells, were imaged throughout the two- to three-hour recording. If there was significant spinal cord swelling, drift or a change in microscope focal plane, then the registration wasn't completed and the experiment wasn't further analyzed. The regions of interest (ROIs) were drawn using a peripheral computer mouse in FIJI (V1.53i, ImageJ2) on a standard deviation intensity projection of an image stack along time.

Analysis of Evoked-Ca2+ Activity

In Microsoft Excel, the raw florescence traces were then normalized. For each frame (Fi), the 5th percentile of the surrounding 200 frames (or 87 seconds) was used as a baseline (Fb) in the rolling ball normalization calculation ((Fi- Fb)/Fb).

For each neuron, the evoked % ΔF/F and ΔF/SD was calculated in Microsoft Excel. To calculate evoked %ΔF/F and ΔF/SD, the mean basal fluorescence and standard deviation (SD) was taken from the 45 seconds immediately prior to each stimulation. The evoked increase in fluorescence was taken during the 3 (mechanical) or 5 (thermal) second stimulation. A Responder Threshold Methodology & Analysis, which determined a responder threshold greater than basal florescence, is described in Figure 3. For each modality, a neuron was considered a responder if it met the responder threshold requirement to at least one of three stimulation trials for each modality.

Vector Analysis

Vectors were calculated using the three-trial average Max % ΔF/F for mechanical, heat and cold skin stimulation. The vector angles were assigned 120° apart counter-clockwise from each other modality as follows: mechanical (+150), heat (+30) and cold (+270). Vectors calculations were automated in Microsoft Excel and then graphed in Matlab (R2021a, Mathworks). The Vector Modality Tuning Methodology created to identify uni-tuned, bi-tuned and tri-tuned neurons is described in Figure 5.

Statistical Analysis

An Excel tool was developed with Visual Basic Applications (VBA) code to automate the rolling ball normalization calculation, responder calculations, evoked Max %ΔF/F and ΔF/SD calculations, evoked response duration and AUC calculations, and responder, %ΔF/F and ΔF/SD heatmaps for each stimulation trial during the naïve and disinhibition periods. Screen shots and VBA code is provided in the Appendix C.

Statistical significance calculations, e.g. correlations and p values, were calculated in Matlab (R2021a, Mathworks).

2.3 Contributions

All components of this work, including the dissection, electrophysiology, 2-Photon imaging, video registration, coding, data analysis, and content development was performed by the author of this dissertation. In total, 14 animals were analyzed.

Charles Warwick provided training on Two-Photon microscopy and analysis and we discussed experimental concepts. Junichi Hachisuka provided training on the dissection and spinal cord patch clamp. Colleen Cassidy provided training on the dissection, DRG intracellular recordings, and optogenetic activation of sensory neurons. In addition, Emanual Loeza provided training on compound action potential recordings.

Lastly, Rick Koerber and Sarah Ross regularly provided mentorship, directional feedback, and resources.

2.4 Experimental Preparation

Dissection Design

Numerous approaches were considered (Supplemental Figure 1), but two dissections were prioritized for the final experiments used herein. The first approach is shown in Figure 2A, and it includes a continuous dissection of the cord, L2 and L3 roots and ganglia, lateral femoral cutaneous nerve, and the relatively proximal patch of skin it innervates. The lateral femoral cutaneous nerve was chosen because its fibers project to the relatively lateral region of the gray matter that surfaces the cord. In L2, this region is not covered by adjacent roots (Figure 2B-C). As a result, the L2 superficial lateral region of the cord is accessible to image inputs from the lateral femoral cutaneous nerve. In the mouse, the only other nerve to send dense cutaneous projections to dorsolateral L2 of the grey matter is the "proximal branch" of the saphenous nerve (Supplemental Figure 1). However, the saphenous branch's central projections are biased slightly more caudal and medial relative to projections of the lateral femoral cutaneous. As a result, the lateral femoral cutaneous nerve is a better candidate to capture cutaneous population responses in superficial lamina of lateral L2[75-77;90;91].

The second approach is introduced in Figure 6A, and it was used to characterize the convergence of musculoskeletal and cutaneous population responses in lateral L2 lamina I. It includes all of the same tissue components of the first dissection, plus the addition of the femoral nerve that mainly innervates the quadriceps (nerve only included). The femoral nerve was selected because it can be dissected out together with the lateral femoral cutaneous and/or saphenous

nerves, and its fiber projections overlap in the cord with the lateral femoral cutaneous nerve[70-72;84;85]. A more detailed review of the degree of overlap between the femoral nerve and lateral femoral cutaneous nerve in the cord is discussed in Section 3.3 as an introduction to the convergence results.

Experiment Design

The experiment design was separated into two periods: naïve (or baseline), and disinhibition (Figure 2D). Stimulation methods for high-threshold (HT) mechanical, low-threshold (LT) mechanical air-puff, heat, cold, and electrical stimulations are discussed in Methods 2.1. In the naïve period, 3 trials for each stimulation modality was used to ensure all responders were captured. In between each stimulation trial, three to five minutes of wait time was given for two reasons. The first was to let the spinal cord rest between stimulation trials to prevent over-stimulation. It was observed that over-stimulating the cord led more quickly to a state of higher basal fluorescence, blebbing, and irregular (unusually small or large) population responses overall. The second reason was that a stimulation-dependent "long-term network inhibition" was observed in which, immediately following a stimulation, it was difficult to evoke another response. This effect lasted not longer than one minute.

Following the stimulations during the naïve period, 10 micromolar bicuculine and 1 micromolar strychnine was circulated in bath (see Methods 2.1). During the disinhibition period, two trials per stimulation type were used. Two trials (instead of the three during the naïve period) were used to ensure all stimulations were performed in a relatively short period of time. It was observed that the disinhibition efficacy of the bicuculine and strychnine declined within an hour of circulation. The two trials appeared adequate during disinhibition as it was relatively easy to

evoke a response during disinhibition. Following the disinhibition period, in some experiments, bicuculine and strychnine were washed out and stimulations repeated again (Supplement Figure 7).

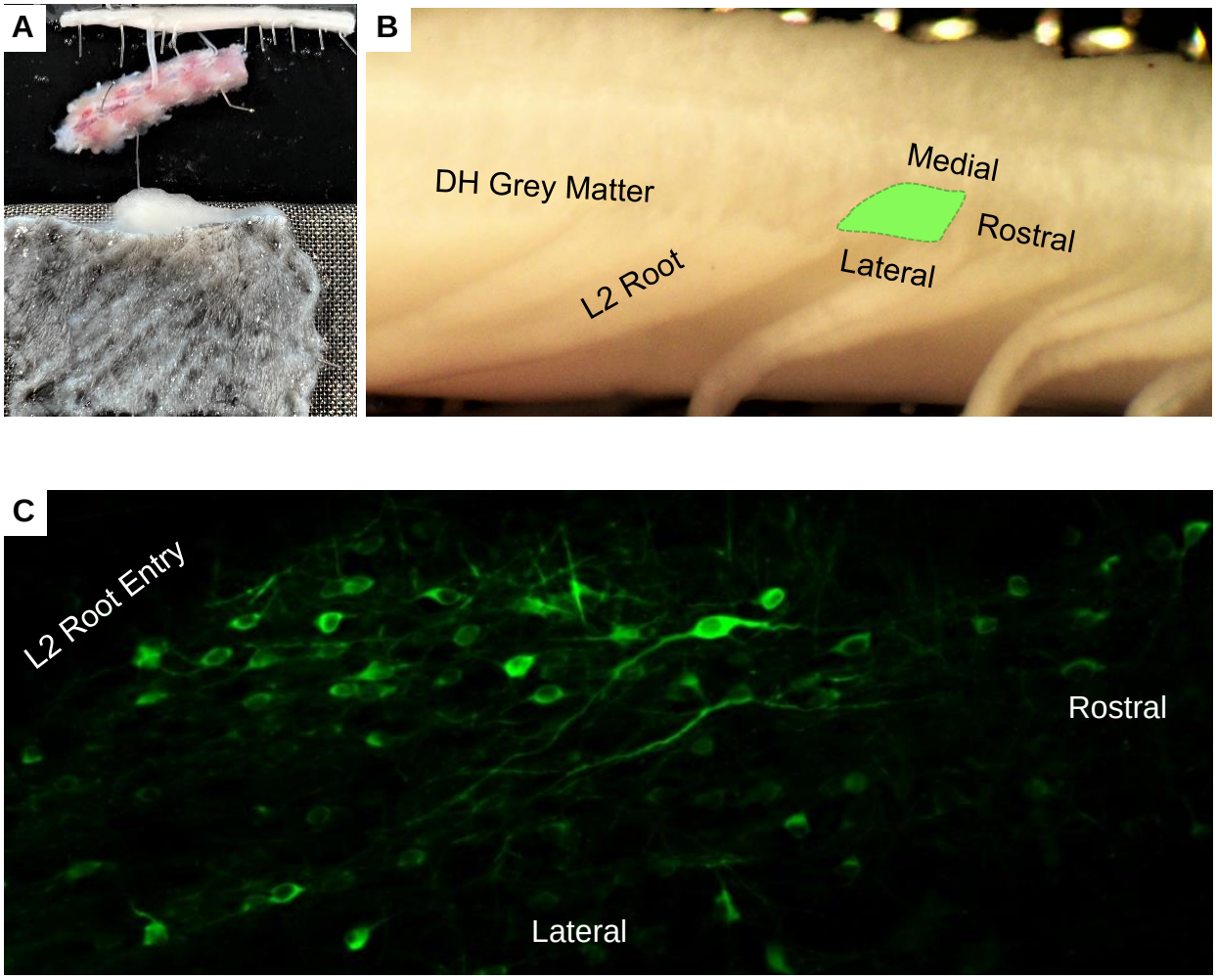

Figure 2: Experiment Design

Figure 2 Legend

A: Image of the *ex vivo* preparation used in experiments with cutaneous stimulation only. Spinal cord is shown with rostral to the right and caudal to the left, attached to the vertebrae, discs, ganglia, and muscle from approximately the mid-sacral to mid-lumbar segments. The lateral femoral cutaneous nerve connects the dorsal root ganglia to the skin, below which is the fat pad and hairy skin of the dorsal hind paw.

B: Under dissection microscope, a surfaced gray matter is visible as a darker ipsilateral region running rostral-caudally below the dorsal column mid-line. Because the superficial gray matter has surfaced here, and the L2 segment is not covered by roots, it is more accessible to image than more caudal enlarged regions. The L2 superficial gray matter that was imaged is shown in green, which corresponds to Figure 2C.

C: To express GCaMP6s in excitatory neurons, mice were heterozygous for both the Vglut2-ires-cre allele and the Ai96 allele (for Cre-dependent expression of GCaMP6s). The image shows a 615 μm by 307 μm image including the L2 gray matter with Vglut2+ neurons shown in green. The L2 root shown in Figure 2B is in the top left of this panel. Adjacent to the L2 root entry is the surfaced L2 segment imaged. The L1 root, before being cut back, had entered on the rostral (right) side of the image, and had covered about 20% of the entire image (on the far right). In other words, neurons on the far right had sat underneath the L1 root entry.

D: Experiment design used in experiments. Top: naïve stimulations on the left, disinhibition stimulations on the right. Bottom in gray: the time course of 3 stimulation trials in sequence.

3.0 Results

Results include analysis on the following number of animals and neurons:

- In total, experiments in 14 animals were analyzed, including 3,750 total excitatory neurons (averaging 268 neurons per animal).
- For the naïve cutaneous modality characterizations, 14 animals were analyzed; for disinhibition cutaneous modality characterizations, 13 of the same 14 animals were analyzed.
- For naïve and disinhibition-dependent musculoskeletal and cutaneous characterizations, femoral nerve stimulation was used in 8 of the same 14 animals.
- LT mechanical airpuff was used in 6 of the same 14 animals.

Results are broken down into four sections:

1. Responder threshold methodology & analysis
2. Naïve cutaneous modalities and population tunings
3. Naïve musculoskeletal and cutaneous convergence
4. Spinal disinhibition of cutaneous modalities and musculoskeletal convergence

3.1 Responder Threshold Methodology & Analysis

Responder Threshold Methodology

The lateral femoral cutaneous nerve gives way to dense projections to the lateral superficial L2 dorsal horn[91]. Stimulation of the lateral femoral cutaneous skin evokes action potentials in superficial neurons of the lateral L2 dorsal horn[37] (and see Appendix E). In addition, intracellular calcium changes can encode electrical activity[40;69]. However, in the current experiments, we cannot rule out the possibility of action potential-independent intracellular calcium changes. Furthermore, combining electrophysiology patch clamp with Two-photon GCaMP6s imaging was out of scope for the initial experiments of developing the new Two-photon technique in the *ex vivo* preparation. More details regarding the limitations of 2-photon imaging is provided in the discussion section.

Given the significant brightness of evoked fluorescence changes in VGlut2-cre animals, and the dendritic fluorescence noise that could accompany it, it was decided to use a responder threshold to minimize the probability of false positive responses. In the field, one method that's been used to determine a responder threshold is to select a threshold that is greater than the un-evoked, basal fluorescence[104]. For an experiment, a neuron's basal GCaMP6s florescence is influenced by its naïve calcium levels (including any spontaneous action potential-dependent changes), health of the cell (or lack there-of), and focal plane of the scope. Consequently, an individual neuron's basal florescence can vary over the length of a several hour recording. Therefore, for each naïve stimulation trial used in the experiments, the stimulation-evoked

response was measured against the 45 second “pre-stimulus” basal period immediately prior to a stimulation (Figure 3B-C).

Change in fluorescence can be expressed in at least two forms. The first is expressed as a percent change over mean basal florescence (%ΔF/F, Figure 3D-G). A second method to calculate a change in florescence is the number of standard deviations over mean basal florescence, or the z-score (ΔF/SD, Figure 3H-K). In order to prevent false positive responders, both expressions of change in florescence were used as a responder threshold. It should be noted, however, if only one criterion (% ΔF/F or ΔF/SD) is used, the results of the analysis are generally unaffected (Supplemental Figure 9). This is likely due to many of the evoked responses being several times greater than the responder thresholds (see next Figure 4B).

Responder Threshold Analysis

Responder thresholds were determined as a value greater than most neurons’ pre-stimulus, basal fluorescence. To determine the responder threshold, the pre-stimulus max basal florescence was measured during the 45 seconds before each stimulation trial for each neuron in 13 experiments (Figure 3A). In summary, each neuron’s max basal fluorescence was measured during the 45 seconds prior to 3 mechanical trials, 3 heat trials and 3 cold trials (9 total trials in each of 13 animals) (Figure 3A-C).

In an individual experiment, for each neuron, the max basal florescence was averaged across the 9 pre-stimulus trials (Figure 3D, 3H). Next, a histogram was made for this average max basal fluorescence across all neurons within an experiment (Figure 3E, 3I). Then, histograms of the average max basal florescence were created for each of 13 animals (Figure 3F, 3J). To reduce the chance of false positives, a responder threshold was selected as greater than most neurons’ pre-

stimulus max florescence. Therefore, in each experiment, the 95th percentile of all neurons' pre-stimulus max basal florescence was calculated. A responder threshold was then selected as the average 95th percentile across the 13 experiments (Figure 3G, 3K).

Based on this, 100% ΔF/F (average 95th percentile, Figure 3G) and 3.5 ΔF/SD (average 95th percentile, Figure 3K) was selected as the responder thresholds. For a neuron to be called a responder, it must respond during single frame greater than both 100% ΔF/F and 3.5 ΔF/SD of the 45 seconds immediately prior to the stimulation.

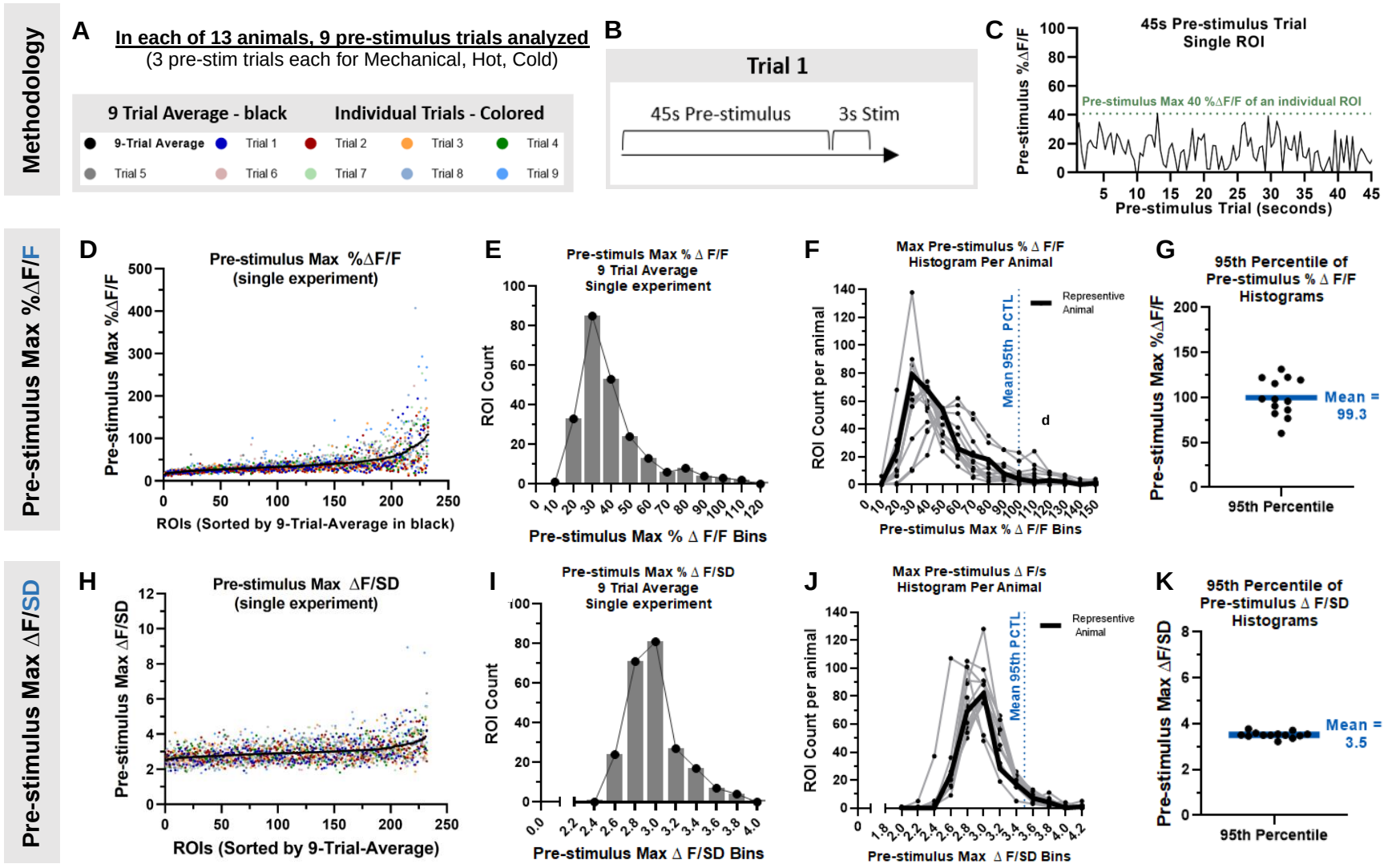

Figure 3: Responder Threshold Methodology & Analysis

Figure 3 Legend

A: In each of 13 animals, 9 pre-stimulus trials were used to analyze the max basal fluorescence absent of any stimulation. For each neuron, individual pre-stimulus trials are plotted as colors, and the 9-trial average is plotted as black.

B: For each individual trial, "pre-stimulus" refers to the 45 seconds prior to a stimulation. The 45 second pre-stimulus period was used to calculate mean basal fluorescence and standard deviation in the %ΔF/F and ΔF/SD calculations.

C: Example pre-stimulus basal trace expressed as %ΔF/F for an individual trial of a single neuron. For this neuron, the max pre-stimulus activity was 40% ΔF/F for an individual trial.

D: For each neuron in an individual animal, the pre-stimulus Max %ΔF/F is plotted for each of nine trials. Individual pre-stimulus trials are plotted in color, with the neurons on the x-axis sorted by their 9-trial average in black.

E: In the same experimental animal as Figure 3D, a histogram of the 9-trial average of Pre-stimulus Max %ΔF/F. Pre-stimulus Max 30% ΔF/F occurs most frequently across neuron in this individual experiment.

F: Histograms for the 9-trial average of Pre-stimulus Max %ΔF/F is plotted for each of 13 experimental animals, with the bold line being the example animal in Figure 3D-E.

G: For each experimental animal, the 95^{th} percentile of the histograms from Figure 3F is plotted. The average across animals is 99% ΔF/F.

H: For each neuron in an individual animal, the pre-stimulus Max ΔF/SD is plotted for each of nine trials. Individual pre-stimulus trials are plotted in color, with the neurons on the x-axis sorted by their 9-trial average in black.

I: In the same experimental animal as Figure 3H, a histogram of the 9-trial average of Pre-stimulus Max ΔF/SD. 3 ΔF/SD (number of SD over mean basal fluorescence, or z-score) occurs most frequently across neuron in the individual experiment.

J: Histograms for the 9-trial average of Pre-stimulus Max ΔF/SD is plotted for each of 13 experimental animals, with the bold line being the example animal in Figure 3H-I.

K: For each experimental animal, the 95^{th} percentile of the histograms from Figure 3J is plotted. The average across animals is 3.5 ΔF/SD.

3.2 Naïve cutaneous modalities and population tunings

Background: The Cutaneous Modalities of Superficial Spinal Neurons

In superficial laminae, there is a volley of heterogenous, polymodal nociceptive inputs. In a naïve condition, the modalities of spinal superficial nociceptive neurons are controlled by inhibition. The extent to which superficial excitatory neurons are polymodal or modality-specific was investigated.

Historically, while the modality of SDH neurons in Euarchontoglires has been studied, it has been met with a few challenges. First, statistical limitations are associated with data collected on a small number of neurons per animal. Questions posed on modality characterizations are questions of whether neuron modalities observed in individual animals are representative of a population of animals. In the past, due to technical limitations, neurons were pooled across animals. As a result, the *distributions of animal means and proportions*[82] have been unknown.

Despite these statistical limitations, research on spinal nociceptive polymodality has spanned both decades and labs throughout the second half of the 20th century, and it consistently reproduced the observation of *polymodal nociceptive-specific* neurons in superficial lamina. However, while some studies have reported a high degree of polymodality and nociceptive-specificity in superficial lamina, some studies were incongruent and the level of polymodality and nociceptive specificity has varied in reports[1-3;7;21;43;44;60;64;65]. As a whole, it's unknown to what extent these experimental differences can be explained by statistical sampling errors, species differences, differences in laminar location of neurons, and/or differences in stimulation protocols.

Overall Population Responses (OPR) for Mechanical, Heat, and Cold Cutaneous Stimulations

While developing the experiments, one of the initial goals was to consistently get evoked population responses. During the experiments, this consisted of visually seeing a roughly equal number of neurons "light up" and with similar brightness (i.e. the O*verall Population Response (OPR)*). To ensure consistent OPR, a few considerations were made during the experiments. First, it was important to use only healthy preparations. Preparations were considered healthy based upon preliminary success rates in population responses across multiple trials of mechanical, heat, cold skin stimulation (see Methods 2.1). Second, it was important to give the cord time to rest between trials (3 to 5 minutes) in order prevent blebbing and irregular population responses. Third, it was important to ensure the skin was consistently stimulated sufficiently to capture most receptive fields within the visual field. Lastly, it was important to monitor how the bath temperature may influence the OPR.

As a result of these trials and errors, the first endpoint of interest was to measure the animal variance for both responder count (expressed as percent of responders) and peak response magnitude (expressed as Max %ΔF/F) for mechanical, heat and cold stimulations (Figure 4A-B) and electrical nerve stimulation. Averaged across 14 animals, mechanical and heat stimulation evoked roughly an equal number of responders, both greater than cold-evoked responders (Figure 4A). In the naïve state, mechanical and heat stimulation evoked approximately 70% of responders each, and cold stimulation evoked about 40% of responders. In terms of the magnitude of response, all three modalities evoked a similar Max %ΔF/F (Figure 4B). The average mechanical, heat and cold evoked response were approximately 300%ΔF/F, 300%ΔF/F, and 250%ΔF/F respectively (Figure 4), 2.5 to 3 times greater than the responder threshold (Figure 3).

In summary, while there were more mechanical and heat responders than cold responders in superficial lamina, each modality evoked a similar average Max %ΔF/F. Not only are modality-evoked OPRs important to determine in-between animal variance in these experiments, but it may correlate to specific modalities of pain (to the extent to which changes in intracellular calcium relate to pain). For example, if an injury results in a pain phenotype specific to a modality, an initial population imaging endpoint to examine is whether there is a change in the size of the modality's OPR after injury.

Cutaneous Modality Responder Subpopulations

To appreciate how convergence of heterogenous nociceptive inputs is integrated in the superficial dorsal horn, we next determined the modality heterogeneity in populations of superficial excitatory neurons in the naïve state. In Figure 4C, on average across animals, 40% of total neurons were MHC+ responsive, making it the largest *Cutaneous-Modality Responder Subpopulation*. MHs were the second largest subpopulation accounting for 24% of total responders (Figure 4C). Despite a high degree of polymodality, overall a wide array of modality combinations was found to be present and furthermore, populations with modality-specific responses were observed. Notably, mechano- and heat-specific neurons combined made up approximately 25% of neurons and were not significantly different from each other in size (Figure 4C).

Superficial Mechanical Wide-dynamic Range Neurons

In the naïve state, it's thought that inhibitory neurons prevent low-threshold mechanical inputs from entering the superficial laminae. In past studies, a small minority of superficial neurons have been reported to have lower mechanical thresholds with wide dynamic ranges into the

noxious range[1-3;7;21;43;44;60;64;65]. To demonstrate the wide-dynamic range (WDR) population composition of superficial excitatory neurons, we show that a majority of mechanical inputs into superficial laminae are high-threshold. Only about 10% of neurons were multi-receptive, wide-dynamic range neurons with both low-threshold and high-threshold mechanical responses. Interestingly, 80% of WDR neurons were MHC neurons (Figure 4C Insert).

Identification of the Powerhouse Cutaneous-MHC Subpopulation

Since the largest *Cutaneous Modality Responder Subpopulation* was the MHCs, their mechanical, heat and cold responses were further evaluated. An exclusive subpopulation of MHC neurons with large mechanical and heat responses were identified.

It was discovered that MHC neurons' mechanical- and heat- evoked Max %ΔF/F were unique compared to all other superficial excitatory neurons. The average MHC subpopulation response (across all MHC neurons per animal) to mechanical and heat stimulations was greater than that of Non-MHCs (Figure 4D, 4F), but not for cold-evoked responses (Supplemental Figure 2A). For both mechanical and heat-evoked responses, this was found for nearly all animals tested (Figure 4E, FG).

Given that the MHC average mechanical and heat population responses were greater than the remaining excitatory neurons, the distribution of peak responses across MHC neurons was further investigated. On average across animals, it was found that while a majority of Non-MHC neurons had peak mechanical and heat responses less than 200% ΔF/F, a majority of MHC neurons had peak responses greater than 200% ΔF/F (Figure 4H-I). Using this inflection point, approximately 64% of MHC neurons had uniquely large mechanical-evoked responses greater than 200% ΔF/F. MHC neurons with large mechanical responses accounted for 26% of total naïve

responders. Similarly, 64% of MHC neurons had uniquely large heat-evoked responses, and MHC neurons with large heat responses accounted for 26% of total naïve responders as well.

As a whole, about half of MHC neurons had uniquely large responses to both mechanical and heat modalities (Figure 4J), representing 19% of total naïve responders. These MHC neurons that responded well to both mechanical and heat modalities are dubbed, *Powerhouse MHCs*, and are likely involved in transmitting signals in more than one pain state.

Table 1: Powerhouse MHCs

Neuron Subtype	Definition	Frequency
Powerhouse MHCs	MHC neurons that were discovered to *respond well* to both mechanical and heat modalities, with peak responses to both modalities greater than 200% ΔF/F.	• 47% of MHCs • 19% of Total Naïve Responders

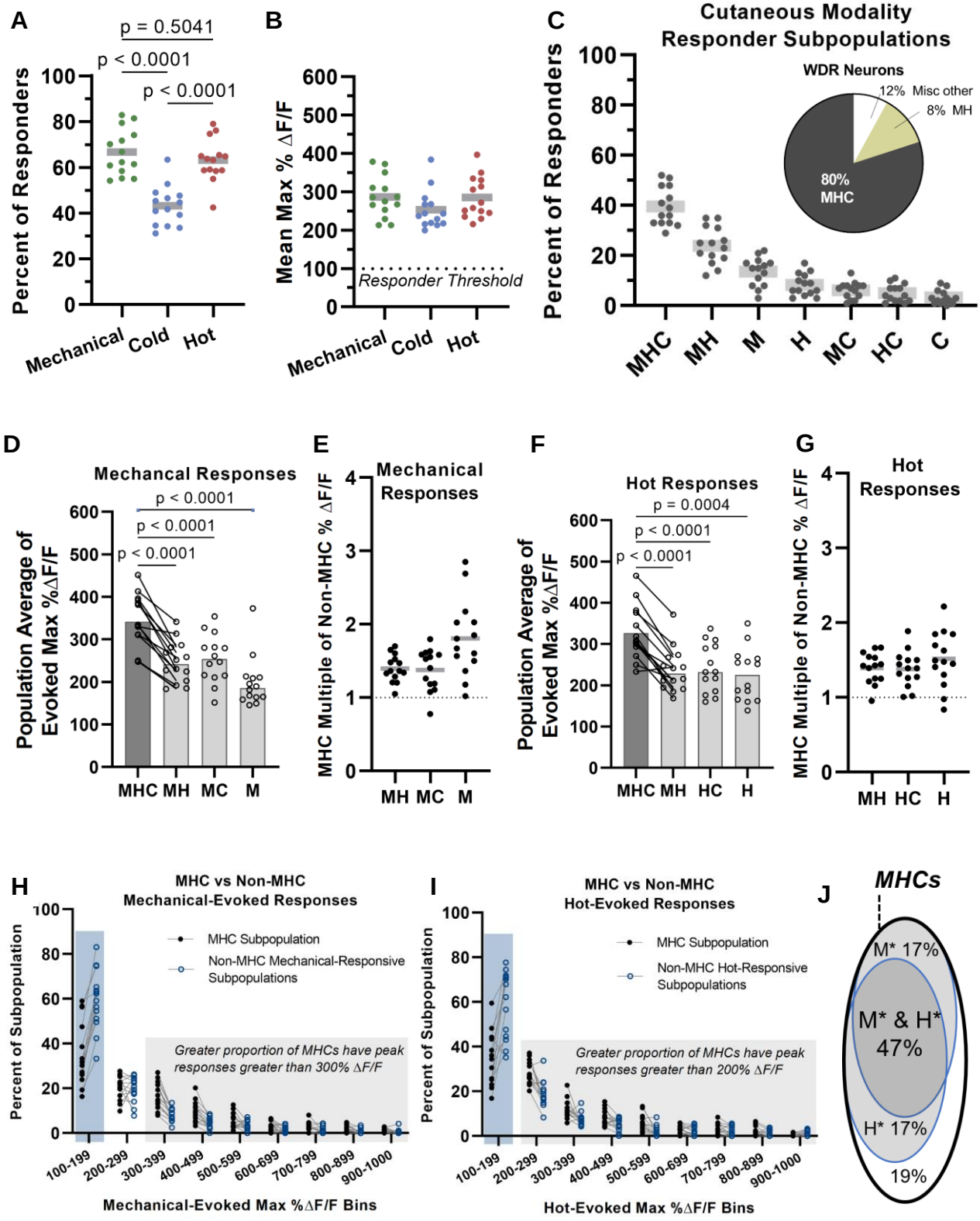

Figure 4: Cutaneous Polymodaly and the Powerhouse MHC Population

Figure 4 Legend

A: The percent of total responders during the naïve period, in superficial L2, that responded to mechanical, heat and cold stimulation of the lateral femoral cutaneous skin. On average across animals, there were more responders to mechanical and heat stimulation than cold stimulation. n=14 animals. One Way ANOVA with Repeated Measures and Tukey Multiple Comparisons

B: The average evoked Max %ΔF/F for mechanical, heat and cold stimulation of the skin. Max %ΔF/F is the endpoint for peak magnitude of response used in these experiments. The average Max %ΔF/F was not significantly different across modalities. n=14 animals. One Way ANOVA with Repeated Measures and Tukey Multiple Comparisons

C: The *Cutaneous Modality Responder Subpopulations*. The percent of total responders during the naïve period that responded to different combinations of modalities. The MHC subpopulation was the largest weighing in at 40%, followed by the MH subpopulation at 24%. Insert: The *cutaneous modality responder* breakdown of the Wide Dynamic Range neurons. The vast majority, or 80%, were polymodal MHCs, thereby creating a unique *MHC WDR* subpopulation.

D: The average mechanical-evoked responses of subpopulations that were mechanical-responsive (MHC, MH, MC, M). The MHC subpopulation on average responded with a greater magnitude to mechanical stimulation compared to Non-MHCs. One Way ANOVA with Repeated Measures and Tukey Multiple Comparisons

E: The average MHC mechanical responses expressed as a multiple of average Non-MHC mechanical responses.

F: The average heat-evoked population responses subpopulations that were heat-responsive (MHC, MH, MH, H). The MHC subpopulation on average responded with a greater magnitude to heat stimulation compared to Non-MHCs. One Way ANOVA with Repeated Measures and Tukey Multiple Comparisons

G: The average MHC heat responses expressed as a multiple of Non-MHC heat responses.

H: Histograms of mechanical responses of MHC and Non-MHC Mechanical-Responsive subpopulations. The proportion of MHC (black) and Non-MHC Mechanical-Responsive subpopulations (blue) with peak responses across bins of Max %ΔF/F. Note the inflection point around 200%-300% ΔF/F. A larger proportion of MHC neurons had mechanical responses greater than 300% ΔF/F, compared to Non-MHC subpopulations. n=14 animals.

I: Histograms of heat responses of MHC and Non-MHC Heat-Responsive subpopulations. The proportion of MHC (black) and Non-MHC Heat-Responsive subpopulations (blue) with peak responses across bins of Max %ΔF/F. Note the inflection point at 200% ΔF/F. A larger proportion of MHC neurons had heat responses greater than 200% ΔF/F, compared to Non-MHC subpopulations. n=14 animals

J: The percent of MHC neurons with uniquely large mechanical responses (as per > 200% ΔF/F inflection point in Figure 4H and I) (M*, 17%), uniquely large mechanical and heat responses (M* & H*, 47%), and uniquely large heat responses (H*, 17%).

Cutaneous Modality Tuning Background

In the previous section, under the naïve condition, many neurons were identified as polymodal, but heterogeneity was found with distinct populations that responded to different combinations of mechanical, heat and cold modalities, including modality-specific populations. In addition, MHC neurons with large responses to mechanical and heat were discovered.

But while many SDH neurons are polymodal and some may be *Powerhouse MHCs*, their responses to each modality *relative* to another modality is unknown. Since the dorsal horn maintains an organization of peripheral somatosensory inputs, we hypothesized a heterogeneity in the modality tunings of polymodal MHC neurons.

MHC Primary Modality Preference

To discover the optimal stimuli of SDH neuron populations, we first investigated the neurons' *primary modality preference*. Here, we asked what proportion of neurons *respond most* to mechanical, heat, or cold stimulation of the skin.

In the naïve state, roughly an equal number of neurons responded greatest to either mechanical or heat skin stimulation (Figure 5A). 41% of MHC neurons responded to mechanical stimulation greater than heat and cold. Similarly, 39% of MHC neurons responded to heat greater than mechanical and cold. Lastly, 20% of MHC neurons responded to cold greater than mechanical and heat. This is consistent with the mechanical and heat overall population response (OPR) from Figure 4A-B.

Modality Tuning Methodology

Since the *primary modality preference* of a neuron only determines the modality a neuron responds to most, a new modality tuning methodology was developed to examine the relative response magnitudes across the three modalities. Using a modality tuning methodology, neurons are identified as either *uni-tuned*, *bi-tuned* and *tri-tuned* neurons (Fig 5G, Table 2).

First, to determine a neuron's modality tuning, the average response magnitude for each modality was taken (Figure 5B). Next, each modality's response magnitude was plotted as a vector (Figure 5C). Then, the three modality vectors were summed, creating a single summed vector that represents a neuron's modality tuning (Figure 5D). Figure 5E shows the modality tuning vectors for all of the neurons within an individual animal; and Figure 5F for all the neurons in all experimental animals.

To understand modality tuning heterogeneity within tri-modal MHC neurons, we next determined the proportion of MHC neurons that are *uni-tuned*, *bi-tuned*, or *tri-tuned*. The tuning definitions are the following: *uni-tuned* neurons respond to a single modality greater than the average response of all three modalities; *bi-tuned* neurons response to two modalities greater than the average response of all three modalities; and *tri-tuned* neurons response to all three modalities relatively equally (Table 2). For tri-modal MHC neurons, uni-tuned and bi-tuned neurons geometrically plot in a section produced from six 60° central angles (Figure 5G-H, Table 2).

Table 2: Uni-Tuned, Bi-Tuned, and Tri-Tuned Neuron Population Subtypes

Neuron Subtype	Definition	Where will they plot?
Uni-tuned neurons	Neuron responds to a single modality with a response magnitude (Max %ΔF/F) greater than the average response magnitude of all three modalities	In one of the three 60 degrees central angle sections *surrounding* a modality
Bi-tuned neurons	Neuron responds to two modalities both with a response magnitude greater than the average response magnitude of all three modalities	In one of the three 60 degrees central angle sections *between* two modalities
Tri-tuned neurons	Neurons respond to all three modalities relatively equally with a vector magnitude less than 100 %ΔF/F	In a concentric circle with a radius of 100% ΔF/F

For *bi-modal* neurons (MH, MC, HC subpopulations), uni-tuned and bi-tuned neurons plot according to Supplemental Figure 3B.

Naïve Hetereogeneity of Tri-Modal MHC Modality Tuning

In the naïve condition, tri-modal MHC neurons were found to have heterogenous modality tunings. The modality tuning vectors of MHC neurons are plotted in Figure 5H and its quantification in Figure 5I. About half of polymodal MHCs were uni-tuned, most notably to either mechanical or heat. These neurons have a response to a single modality that's greater than the average response of all three modalities. In summary, four populations make up 87% of all MHCs, including **MHC** (tri-tuned), **M**hc (mechanical-tuned), m**H**c (heat-tuned), and **MH**c (mechano-heat bi-tuned) (Figure 5I).

We next determined the *degree to which neurons are tuned*. Here, the vector length magnitude measures the degree to which a modality's response is greater than the other modalities.

We found that MHC neurons, compared to non-MHC neurons, were more likely to having tuning to a high degree (Figure 5J-K).

In summary, while MHC neurons are tri-modal, they are a hetereogenous group of neurons that are highly tuned to distinct modalities, likely carving unique modality tuning pathways that help give rise to discrimination of stimuli in the brain.

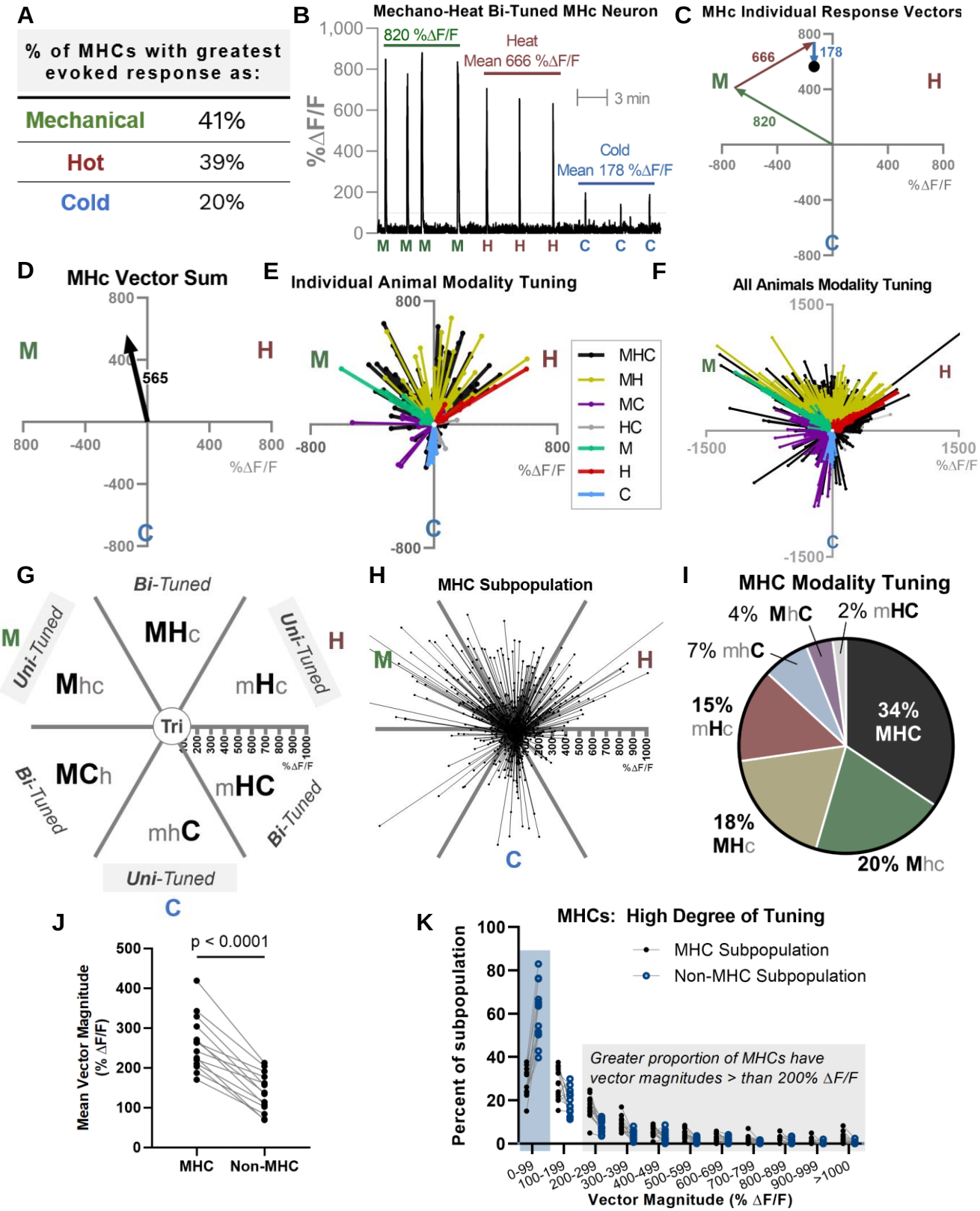

Figure 5: Cutaneous Modality Population Tuning

Figure 5 Legend

A: The percent of the MHC neurons with greatest Max %ΔF/F response as mechanical, heat or cold stimulation. In the naïve state, 41% of MHC neurons responded to mechanical with a greater %ΔF/F than to heat and cold. 39% of MHC neurons responded to heat with a greater response than mechanical and cold. Lastly, 20% of MHC neurons responded to cold with a greater response than mechanical and heat.

B: *An example trace of a tri-modal MHc neuron with mechano-heat bi-tuning*. As the first step of creating a modality tuning vector, the mechanicaal, heat and cold responses are averaged across their respective trials. This is an example of a tri-modal MHc neuron with bi-tuning to mechanical and heat.

C: *The second step of creating a modality tuning vector*. Each mechanical, heat and cold responses are plotted as individual vectors to create a final vector point represented as a black dot.

D: *The final step of creating a modality tuning vector*. A vector sum (sum of the three individual mechanical, heat and cold vectors) is plotted from the coordinate (0,0) to the black dot from Figure 5C.

E: The plotting of all neurons' naïve modality tuning vectors within an example animal. Vectors are color coded according to their Cutaneous Modality Responder Subpopulation identification.

F: The plotting of all neurons' naïve modality tuning vectors across all experimental animals. Since it is difficult to see all the vectors, see the heatmap of it in Supplemental Figure 3D.

G: Illustration of tri-modal MHC tuning methodology used to determine uni-tuning, bi-tuning, and tri-tuning. Uni-tuned neurons respond to a single modality with a Max %ΔF/F greater

than the average evoked Max %ΔF/F response of all three modalties. Bi-tuned neurons respond to two modalities with a Max %ΔF/F response greater than the average evoked Max %ΔF/F of all three modalties. Tri-tuned neurons have vector lengths less than 100 %ΔF/F with relatively equal responses to all three modalities.

H: The plotting of all naïve MHC modality tuning vectors across all experimental animals. Note that black vectors are the color for MHC neurons.

I: The proportion of naïve MHC neuron with modality tunings as uni-tuned, bi-tuned, and tri-tuned, as per the slices in Figure 5G.

J: The MHC average modality tuning magnitude is greater than the Non-MHC average modality tuning magnitude. Paired t Test.

K: The distribution of modality tuning magnitudes for MHC and non-MHC neurons. The magnitudes of MHC modality tunings are uniquely larger than 200% ΔF/F.

3.3 Naïve musculoskeletal and cutaneous convergence

Musculoskeletal & Cutaneous Convergence Background

In the previous section, in the naïve condition, we examined the convergence of cutaneous modalities in the SDH. We found that while many polymodal neurons were present, there were distinct *Cutaneous Modality Responder Subpopulations* (Figure 4) and *Population Modality Tunings* (Figure 5). In addition, we identified a unique polymodal cutaneous-MHC subpopulation with large tunings to mechanical and/or heat.

Since musculoskeletal pain is reported as most frequent[18], we next examine the musculoskeletal-evoked calcium population responses in SDH excitatory neurons. In particular, we describe the convergence of cutaneous and musculoskeletal inputs in the SDH.

Dorsal horn convergence of somatosensory inputs has been described for somatic and visceral tissues in adult and development. For somatic cutaneous and musculoskeletal convergence in the spinal cord, prior work has been primarily limited to mechanical and/or electrical modalities[24;41;42;85;95;96]. More recently, electrophysiological proprieties of C&MS convergence lamina I projection neurons were investigated during development.[65]

Since prior work has been limited in modalities, we take a systematic approach to determine the level C&MS convergence in the SDH. We identify a neuron functional subtype, *Cutaneous & Musculoskeletal (C&MS) Convergence Neurons*, and determine their cutaneous modalities and tunings.

Since there's a shift between cutaneous and muscular somatotopies, it's expected that the degree of C&MS convergence would likely vary based on the anatomical location of neurons. For example, holding the proximal-distal location of muscle and skin constant, musculoskeletal inputs tend to project more medial relative to cutaneous inputs in the dorsal horn. However, in rodent L1-L2, musculoskeletal femoral nerve fibers, which typically project medially, terminate laterally exclusively in superficial lamina (Figure 6B)[73-75;88;89]. While most musculoskeletal femoral nerve fibers terminate in the medial dorsal horn, there is a subset of femoral fibers that terminate laterally in lamina I, overlapping with the femoral cutaneous nerve's superficial projections (Figure 6B).

Therefore, I adapted the lateral femoral cutaneous *ex vivo* prep to include the femoral nerve as an add-on (Figure 6A). The lateral femoral cutaneous skin was included, and a suction electrode was placed on the cut end of the femoral nerve as it entered the quadriceps.

Identification of Cutaneous & Musculoskeletal (C&MS) Convergence Neurons

On average across the sample of animals, 26% of superficial excitatory neurons responded to both cutaneous stimulation and the musculoskeletal nerve stimulation (Figure 6C-D). These neurons are called *C&MS convergence neurons.* Of the C&MS convergence neurons, a quarter of them responded best to musculoskeletal stimulation (Figure 6E). Virtually the entire remainder of neurons that weren't C&MS convergence neurons were cutaneous-only responsive. Although never functionally shown, this cutaneous-heavy attribute of the dorsolateral L2 cord was expected, given that the lateral femoral cutaneous nerve inputs densely in this area.

Cutaneous-MHC C&MS Convergence Neurons

C&MS convergence neurons respond to both muscle and skin somatosensory inputs, but with which cutaneous modalities do they respond? We next determined the heterogeneity of C&MS convergence neurons according to their cutaneous modalities. Compared to non-convergence neurons, C&MS convergence neurons were more likely to be responsive to all three modalities: mechanical, heat and cold stimulation of the skin (Figure 6F-H). In addition, we found that a greater percent of C&MS convergence neurons were polymodal MHC. 60% of C&MS convergence neurons were cutaneous-MHC compared to 31% of non-C&MS convergence neurons (Figure 6I). And while 26% of all cutaneous responders were musculoskeletal responsive, 38% of cutaneous-MHC neurons were musculoskeletal responsive (Figure 6J). In total, 15% of the total naïve responder population were cutaneous-MHC C&MS convergence neurons (Figure 6K).

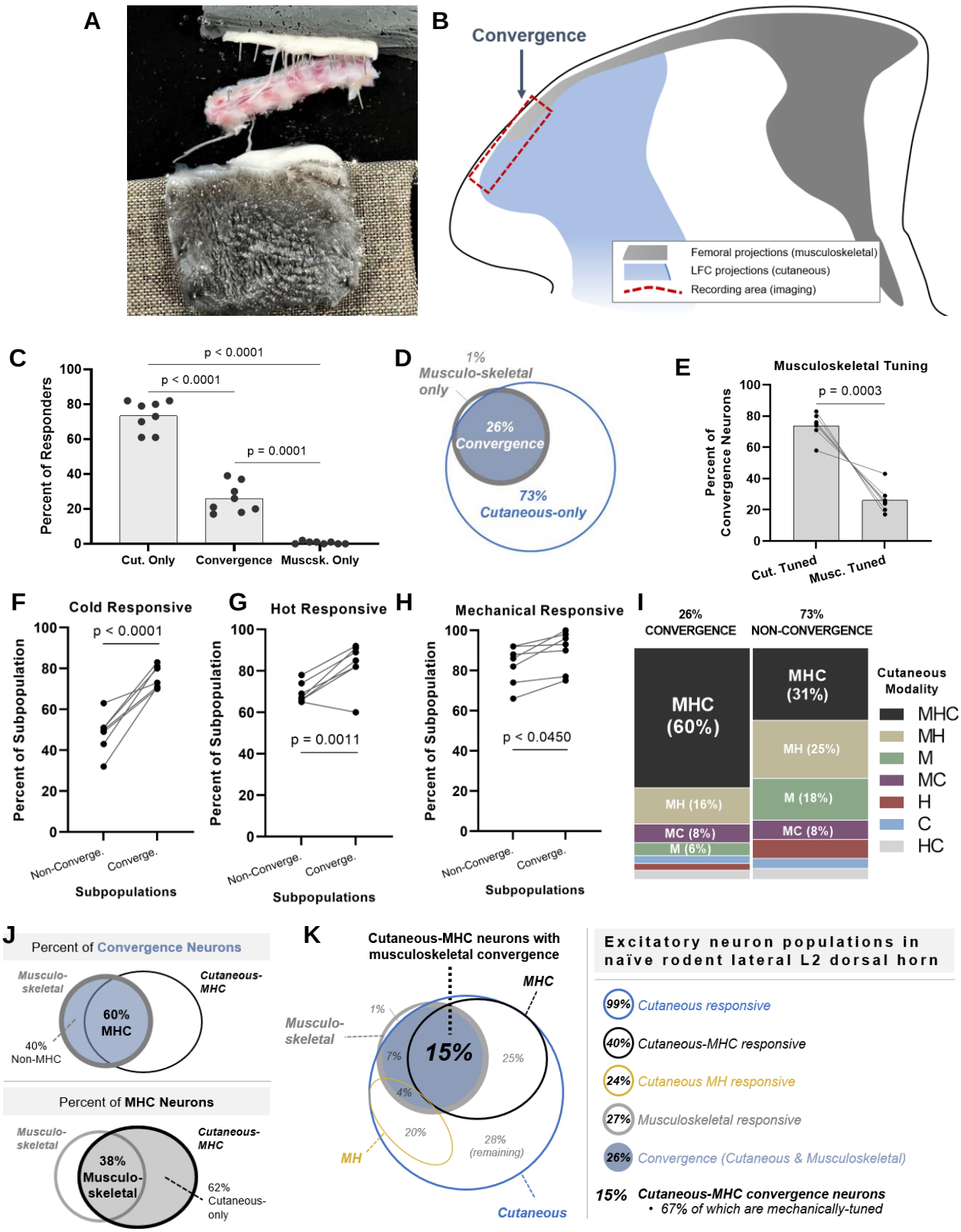

Figure 6: Polymodal Musculoskeletal and Cutaneous Convergence

Figure 6 Legend

A: Image of the *ex vivo* preparation used in experiments with cutaneous stimulation only. Spinal cord is shown with rostral to the right and caudal to the left, attached to the vertebrae, discs, ganglia, and muscle from approximately the mid-sacral to mid-lumbar segments. The lateral femoral cutaneous nerve connects the dorsal root ganglia to the skin, below which is the fat pad and hairy skin of the dorsal hindpaw. In addition, the femoral nerve is included to activate musculoskeletal fibers with a suction electrode.

B: Illustration of L2 cross section of dorsal horn showing overlap of femoral nerve (musculoskeletal) and lateral femoral cutaneous fiber projections. Musculoskeletal inputs generally are more medial in the dorsal horn compared to cutaneous. However, in L2, femoral fibers project more laterally in superficial lamina only.

C: The proportion of naïve responders that produce a convergence in musculoskeletal and cutaneous responses, cutaneous only, and musculoskeletal only. On average across n=8 animals, 26% of naïve responders were *C&MS convergence neurons*, 73% cutaneous only, and 1% musculoskeletal only. Repeated One Way ANOVA with Multiple Comparisons and Tukey Correction.

D: Venn diagram illustrating overlap of cutaneous and musculoskeletal inputs, based off of analysis in prior panel

E: On average across animals, 26% of C&MS convergence neurons responded best to musculoskeletal femoral nerve stimulation over mechanical, heat and cold cutaneous stimulation. This accounts for approximately 7% of total naïve responders in the area. Paired t Test.

F: The proportion of C&MS convergence neurons vs non-C&MS convergence neurons that are responsive to cutaneous cold stimulation. Neurons with musculoskeletal convergence are more likely to be *cold* responsive. Effect size is notably larger than heat (Figure 6G) and mechanical (Figure 6H). Standardized mean difference (divided by averaged SD) is 3.64% ΔF/F / SD. Figure 6 F, G, and H was tested together with a Repeated Measures Two-Way ANOVA with Multiple Comparisons and Holm-Sidak Correction.

G: The proportion of C&MS convergence neurons vs non-C&MS convergence neurons that are responsive to cutaneous heat stimulation. Neurons with musculoskeletal convergence are more likely to be *heat* responsive. Effect size is between cold (Figure 6F) and mechanical (Figure 6H). Standardized mean difference (divided by averaged SD) is 1.73% ΔF/F / SD. Figure 6 F, G, and H was tested together with a Repeated Measures Two-Way ANOVA with Multiple Comparisons and Holm-Sidak Correction.

H: The proportion of C&MS convergence neurons vs non-C&MS convergence neurons that are responsive to cutaneous *mechanical* stimulation. Neurons with musculoskeletal convergence are more likely to be mechanical responsive, but with an effect size that is notably smaller than heat (Figure 6G) and cold (Figure 6H). Standardized mean difference (divided by averaged SD) is 0.71%ΔF/F / SD. Figure 6 F, G, and H was tested together with a Repeated Measures Two-Way ANOVA with Multiple Comparisons and Holm-Sidak Correction.

I: The *Cutaneous Modality Responder Subpopulations* of C&MS convergence neurons vs non-C&MS convergence. C&MS convergence neurons are more likely to be MHC-responsive (60%) than non-C&MS convergence neurons (31%).

J: The intersection of C&MS convergence and cutaneous-MHC neuron populations. 60% of C&MS convergence neurons are cutaneous-MHC. 38% of cutaneous-MHC neurons receive musculoskeletal inputs, compared to 26% of the total naïve responder population (Figure 5).

K: Summary of major excitatory neuron populations in naïve rodent L2 SDH. C&MS convergence neurons are more likely to be MHC. Cutaneous-MHC neurons that are musculoskeletal-responsive make up a considerable 15% of total naïve responders.

The Primary Modality Preference of Cutaneous-MHC C&MS Convergence Neurons

Since approximately 60% of C&MS convergence neurons are cutaneous-MHC-responsive, we next determined their optimal stimuli to determine if there's any heterogeneity in their modality tunings.

To examine C&MS convergence neurons' optimal stimuli, we first investigated the neurons' *primary modality preference*. Here, we asked what proportion of cutaneous-MHC C&MS convergence neurons *respond most* to mechanical, heat, or cold stimulation of the skin.

In the naïve state, it was discovered that a majority of cutaneous-MHC C&MS convergence neurons respond best to mechanical stimulation of the skin. Two thirds of cutaneous-MHC convergence neurons respond best to mechanical stimulation of the skin (Figure 7A). In addition, 22% of cutaneous-MHC C&MS convergence neurons responded best to heat stimulation, and 11% responded best to cold stimulation of the skin (Figure 7A). In contrast, in the same 8 animals, 44% of cutaneous-MHC *non*-C&MS neurons responded best to mechanical stimulation of the skin, 34% responded best to heat stimulation, and 22% responded best to cold stimulation of the skin (Figure 7B).

The Modality Tuning of Cutaneous-MHC C&MS convergence neurons

Since the primary modality preference of a neuron doesn't reflect the *relative difference* in magnitudes between responses of different modalities, we next identified the modality tuning of polymodal C&MS convergence neurons using the tuning methodology shown in Figure 5. It was discovered that approximately half, or 46%, of cutaneous-MHC C&MS convergence neurons are mechanically uni-tuned, compared to 26% of cutaneous-MHC *non*-C&MS convergence neurons (Figure 7E-F).

Summary of C&MS Convergence Neurons

In summary, neurons that were responsive to skin and muscle make up about 26% of naïve responders. C&MS convergence neurons were uniquely cutaneous-MHC-responsive. Approximately 60% of C&MS convergence neurons were cutaneous-MHC compared to 31% of *non*-C&MS neurons. In addition, cutaneous-MHC neurons were particularly mechanical-tuned. Please see below a table for review.

Table 3: Naïve Convergence and Non-Convergence Neuron Subpoulations

Characteristics of Subpopulation	Convergence Neuron Subpopulation	Non-Convergence Neuron Subpopulation
Cutaneous-Responsive	Yes	Yes
Musculoskeletal-Responsive	Yes	No
Percent of Total Naïve Responders in L2 Lam I	26%	73%
MHC Polymodality	60% MHC	31% MHC
Primary Mechanical Preference	67% Mechanical Preferenced	44% Mechanical Preferenced
MHC Tuning	46% Mechanically Uni-Tuned	Various distinct tunings

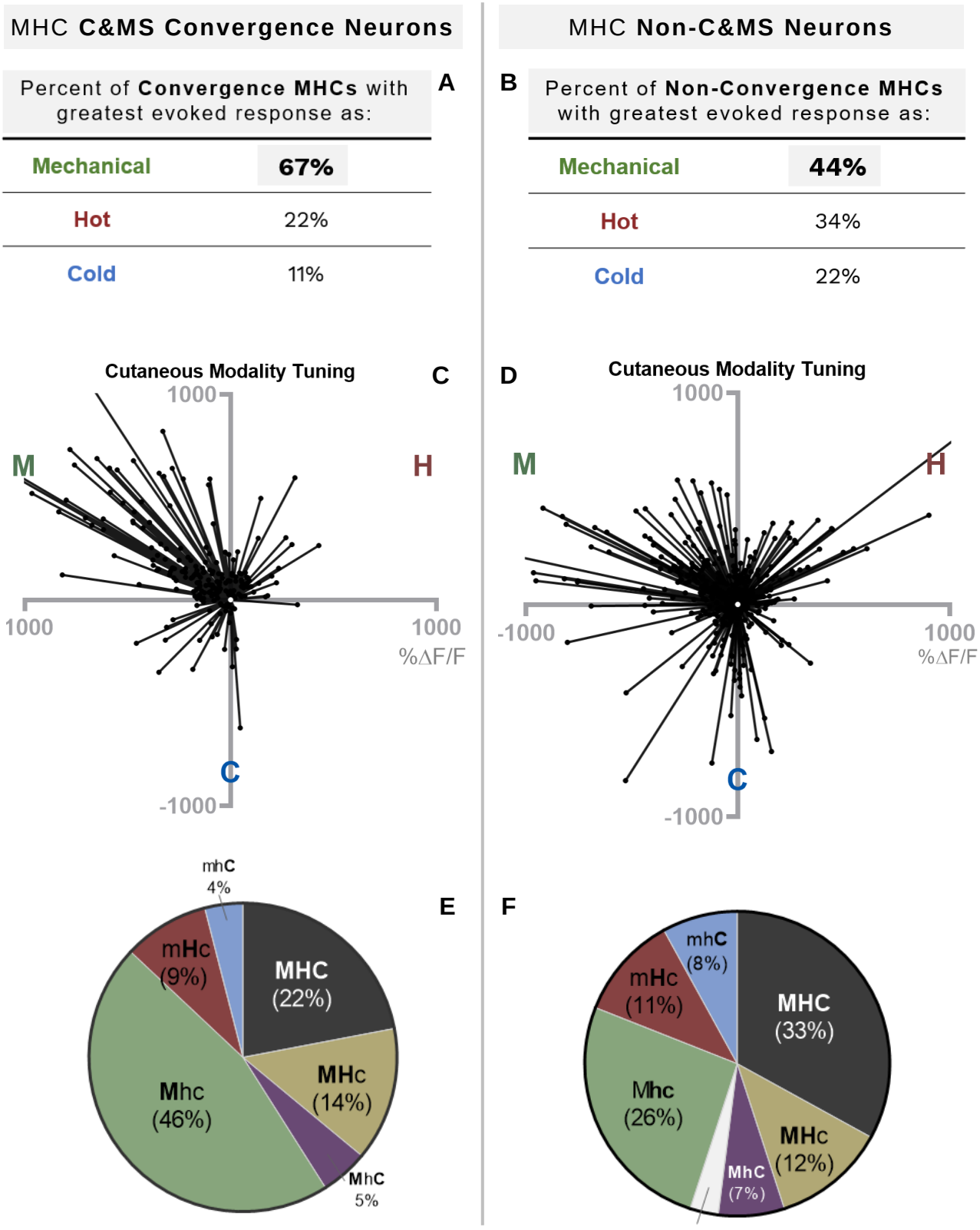

Figure 7: Cutaneous-Mechanical Tuning of Covergence Neurons

Figure 7 Legend

A: The percent of cutaneous-MHC *C&MS convergence neurons* with greatest response either to mechanical, heat, or cold cutaneous stimulation. Two thirds, or 67%, of cutaneous-MHC C&MS convergence neurons respond best to mechanical stimulation of the skin, compared to 44% of MHC non-C&MS convergence neurons in Figure 7B. n=8 animals.

B: The percent of cutaneous-MHC *non*-C&MS neurons (cutaneous-only responsive) with greatest response either to mechanical, heat, or cold. 44% of cutaneous-MHC non-C&MS convergence neurons respond best to mechanical stimulation of the skin, compared to 67% of MHC C&MS convergence neurons in Figure 7A.

C: The plotting of the cutaneous-modality tuning of MHC C&MS convergence neurons. Note that many neurons point in the direction of mechanical stimulation, compared to cutaneous-MHC non-C&MS convergence neurons in Figure 7D.

D: The plotting of cutaneous-modality tuning of MHC *non*-C&MS neurons in the same 8 animals as Figure 7A-C.

E: The proportion of cutaneous-MHC C&MS convergence neurons with of uni-, bi-, tri- tuning vectors. Approximately half, or 46%, of cutaneous-MHC C&MS convergence neurons are mechanically uni-tuned, compared to 26% of cutaneous-MHC non-C&MS convergence neurons shown in Figure 7F.

F: The proportion of cutaneous-MHC *non*-C&MS neurons with of uni-, bi-, tri- tuning vectors.

3.4 Spinal disinhibition of cutaneous modalities and musculoskeletal convergence

Central Disinhibition Background

In the prior section, in a naïve condition, populations of spinal nociceptive neurons were shown to be nociceptive-specific, responding to different combinations of modalities, and with distinct modality tunings. In addition, it's known that when central inhibition is removed, an increase in polymodality and a reduction in mechanical thresholds can occur[1;56]. Surprisingly, however, superficial polymodality characterizations during disinhibition seem to be minimally investigated in prior work. Since plasticity associated with disinhibition is thought to be a fundamental aspect of forms of pain hypersensitivity and allodynia, it's important to understand how populations of superficial excitatory neurons are affected. Therefore, we next used calcium population imaging to determine how central disinhibition affects polymodality, population modality tuning, and musculoskeletal and cutaneous convergence amongst populations of neurons from individual animals. By comparing population responses during naïve and disinhibited states, these data may provide insights into how inhibitory networks can shape distinct modality tunings and convergence patterns observed in the naïve condition.

Disinhibition-dependent Overall Population Responses (OPR)

In the naïve state, the overall population responses (OPR), as measured by both responder percentage and Max %ΔF/F, is compared across mechanical, heat and cold cutaneous stimulation in Figure 4. Here, for each modality, we start with comparing the naïve OPR against the

disinhibition OPR. During disinhibition, the disinhibition-dependent OPR increased for each of the modalities, including HT-mechanical (Figure 8A), heat (Figure 8B) and cold (Figure 8C) stimulation of the skin. Utilizing the bicuculline and strychnine concentrations that are typically near the lower range seen in spinal cord slice[5;12;83;92], HT-mechanical responders likely hit a near ceiling in generating GCaMP6s signals in excitatory neurons. HT-mechanical stimulation of the skin evoked calcium responses in 94%-100% (animal range) of total disinhibited responders. As an indicator of the responder count ceiling, these disinhibited-dependent mechanical population responses seem to mirror that of K+-evoked responses done in more recent experiments (data not analyzed). For heat cutaneous stimulation, the evoked population count was similar but slightly less at about 90% of total disinhibited responders. For cold-evoked responder count, there was an animal range from 60% to 99% of total disinhibition responders which correlated with spontaneous responders, indicating the possibility of a shared independent variable (Figure 8D) (see discussion).

As for the response magnitudes during disinhibition, HT-mechanical stimulation easily evoked the greatest average Max %ΔF/F, followed by heat, then cold (Figure 8A-C; Table 4; Figure 10A-B for direct comparison).

Disinhibited-dependent Polymodality

Next, we describe how a disinhibited-dependent increase in polymodality occurs across large populations of excitatory neurons (Figure 8E; Table 4). We found that population polymodality increased considerably. While the number of MHC neurons increased significantly in each animal, the number of MHC and MH neurons varied across animals and strongly correlated with the number of cold responders across animals (Supplemental Figure 5A). In other words, the

variance in cold responder count led to a variance in polymodal convergence and thus the percentages of neurons that are MHC and MH. The greater the number of cold responders, the more MHCs and less MHs. Lastly, the number of uni-modal and bi-modal neurons, except for MH neurons and mechano-specific neurons, went down to zero across all animals (Figure 8E).

Subpopulation Contributions to Disinhibited-Polymodality

It's important to understand how distinct modality-specific and tuning pathways may change during injury. Here we investigate which naïve *Cutaneous Modality Responder Subpopulations* (Figure 4) underwent change to become more polymodal during disinhibition. Given the breadth of MHC during disinhibition, which was near 100% in some animals, most of these naïve subpopulations from Figure 4 gained responses such that they became polymodal MHC. However, it was unknown to what extent the naïve responders as a whole, compared to the disinhibited-gained responders, contributed to the polymodality seen during disinhibition. In order to assess this, three general populations of excitatory neurons were defined: Naïve Responder Subpopulation, Disinhibited-dependent Gained Responder Subpopulation, and All Disinhibition Responders (Table 5) (Figure 8F-G).

In these calcium population imaging experiments, the naïve responder subpopulation accounted for 83% of all total disinhibition-dependent responders (Figure 8F). Gained responders during disinhibition accounted for 17% of Total Disinhibition Responders.

Next, the modalities of the Naïve Responder Subpopulation and Disinhibited-dependent Gained Responders were examined. Not only do naïve responders make up a majority of all disinhibited responders, but they are also more likely polymodal MHC during disinhibition. That is, during disinhibition, the naïve responder population went from 40% MHC to 79% MHC. In

contrast, the responders gained during disinhibition were only 54% MHC (Figure 8G). This suggests that the disinhibited-dependent pain sensitivity may be driven more so by changes in naïve responders than gains in new responders.

In summary, inhibitory neurons carve out diverse modality populations that may underly normal pain percepts. With inhibition is removed, there is an increase in overall population responses to all three modalities enabling multiple pain states. This increase in overall population responses results in an increase in cutaneous convergence onto individual neurons. The change to polymodal MHC during disinhibition is driven largely by changes in naïve responders. However, given that disinhibition causes expansive receptive fields, it's likely that gained responders outside of the visual field weren't captured in these experiments.

Table 4: Cutaneous-Modality Responses of Naive and Disinhibited Neurons

Characteristics		**Naïve**	**Disinhibition**
Percent of Responders	*Total*	83%	100%
	Mechanical	67%	98%
	Heat	62%	92%
	Cold	44%	76%
Average Max ΔF/F	*Mechanical*	284% Max ΔF/F	724% Max ΔF/F
	Heat	282% Max ΔF/F	499% Max ΔF/F
	Cold	248% Max ΔF/F	411% Max ΔF/F
Cutaneous-Modality Subpopulation	*MHC*	40%	74%
	MH	24%	18%
	M	13%	4%
	H	8%	-
	C	4%	-
	MC	6%	3%
	HC	5%	-

Table 5: Naive Responders, Gained Responders, Total Disinhibtion Responders

Neuron Subtype	Definition	Percent of Total Responders
Naïve Responder Subpopulation	All responders during the naïve period prior to bath application of bicuculline and strychnine	83%
Disinhibited Gained Responder Subpopulation	Neurons that did not respond during the naïve period, but did respond during disinhibition	17%
Total Disinhibited Population	Naïve Responder Subpopulation + Disinhibition Gained Responder Subpopulation	100%

Table 6: Disinhibited Modalities of Naive, Gained, and Total Responders

Property	Naïve Responders	Gained Responders	Total Responders
Percent of Responders	83%	17%	100%
Salient Characteristic	Majority MHC	Half MHC Uniquely Mechano-specific	Majority MHC
Largest Modality Subpopulations	79% MHC 16% MH	54% MHC 31% MH 11% M	74% MHC 19% MH 4% M

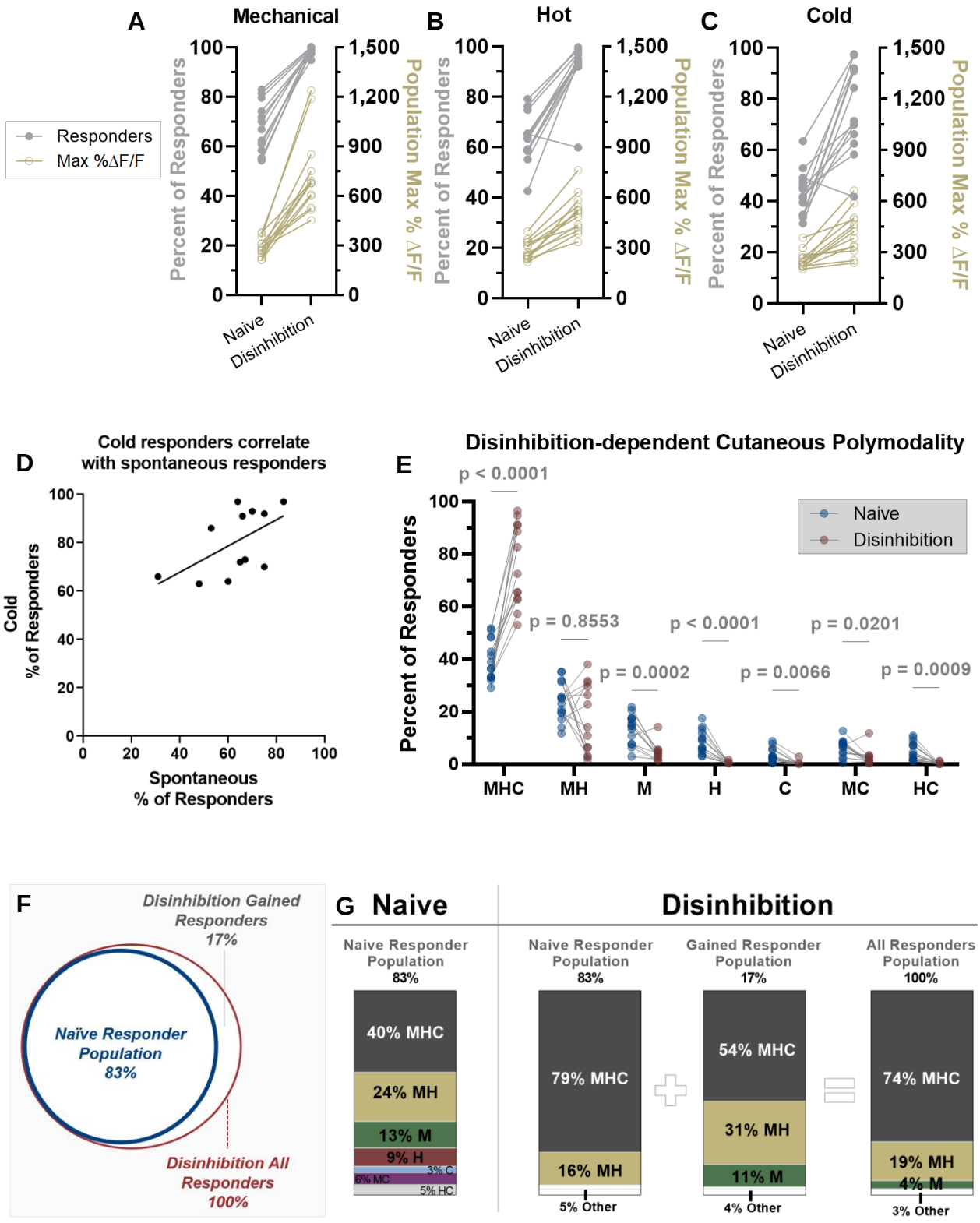

Figure 8: Disinhibited Polymodality Driven by Changes in Naïve Responders

Figure 8 Legend

A: Mechanical Overall Population Response (OPR): Percent of Responders and Average Max %ΔF/F during naïve and disinhibition periods. There was an increase in mechanical evoked responder numbers and average response magnitude.

B: Heat-evoked OPR: Percent of Responders and Average Max %ΔF/F during naïve and disinhibition periods. There was an increase in heat evoked responder numbers and average response magnitude.

C: Cold-evoked OPR: Percent of Responders and Average Max %ΔF/F during naïve and disinhibition periods. There was an increase in cold evoked responder numbers and average response magnitude.

D: During disinhibition, the number of spontaneous responders (as percent of total responders) plotted on the x-axis, and the number of cold responders (as percent of total responders) plotted on the y-axis. The cold responders, but not mechanical and heat, correlate with the spontaneous responders, indicating the possibility of a shared independent variable. Linear regression; R-squared = 0.31; p=0.05

E: The comparison of *Cutaneous-Modality Responder Subpopulations* during naïve and disinhibition periods. During disinhibition, there was an increase in polymodality. During disinhibition, % MHC animal variance is explained by the number of MHC neurons correlating strongly with number of cold responders (Supplemental Figure 5A). Repeated Measures Two-Way ANOVA with Multiple Comparisons and Bonferroni Correction.

F: Naïve Responders account for 89% of Total Disinhibition Responders. 19% of Total Disinhibition Responders are Disinhibition-dependent Gained Responders.

G: During disinhibition, the *Cutaneous Modality Responder Subpopulations* of the Naïve Responder Subpopulation, Disinhibition-dependent Gained Responder Subpopulation, and Total Disinhibition Responders. During disinhibition, polymodality is driven more by the naïve responder subpopulation than by gained responders.

Disinhibited Musculoskeletal & Cutaneous Convergence

We next show how inhibitory networks carve out musculoskeletal and cutaneous convergence. As inhibition is removed centrally, musculoskeletal and cutaneous convergence increases to 39% of total disinhibited responders (Figure 9A). The increase in convergence from 26% of naïve responders to 39% of disinhibited responders was found to be modest in comparison to the increase in cutaneous MHC from 40% to 74% (Figure 8).

Similar to how changes in the naïve responder subpopulation drive most of the disinhibited cutaneous polymodality overall (Figure 8), an increase in convergence in the naïve responder subpopulation was also found to drive most disinhibited convergence (Figure 9A). Convergence in the naïve responder subpopulation increased from 26% to 44%. In contrast, of the disinhibited-gained responders, only 18% had musculoskeletal and cutaneous convergence.

Disinhibited Polymodality of C&MS convergence neurons

In the naïve state, C&MS convergence neurons were found to be more likely responsive to mechanical, heat and cold stimulation of the skin. As a result, 60% of naïve C&MS convergence neurons were polymodal MHC (compared to 31% of non-C&MS neurons) (Figure 6). Similarly, during disinhibition, it was found that C&MS convergence neurons were also more likely to be

polymodal MHC compared to non-C&MS convergence neurons. On average across animals, 86% of C&MS convergence neurons were polymodal MHC-responsive during disinhibition (Figure 8B). This was the case for each animal, where C&MS convergence neurons were 1.4 times more like than non-C&MS neurons to be cutaneous MHC (Figure 8C).

In summary, during disinhibition, C&MS convergence neurons made up 39% of the total disinhibited responders, 86% of which were MHC-responsive. In contrast, non-C&MS neurons made up 61% of total responders, 62% of which were MHC-responsive (Figure 8D-E). The resultant summary of MHC C&MS convergence neurons during disinhibition is shown in Figure 8G: 34% of total responders were MHC C&MS convergence neurons driven mostly by an increase in convergence of the naïve responder subpopulation.

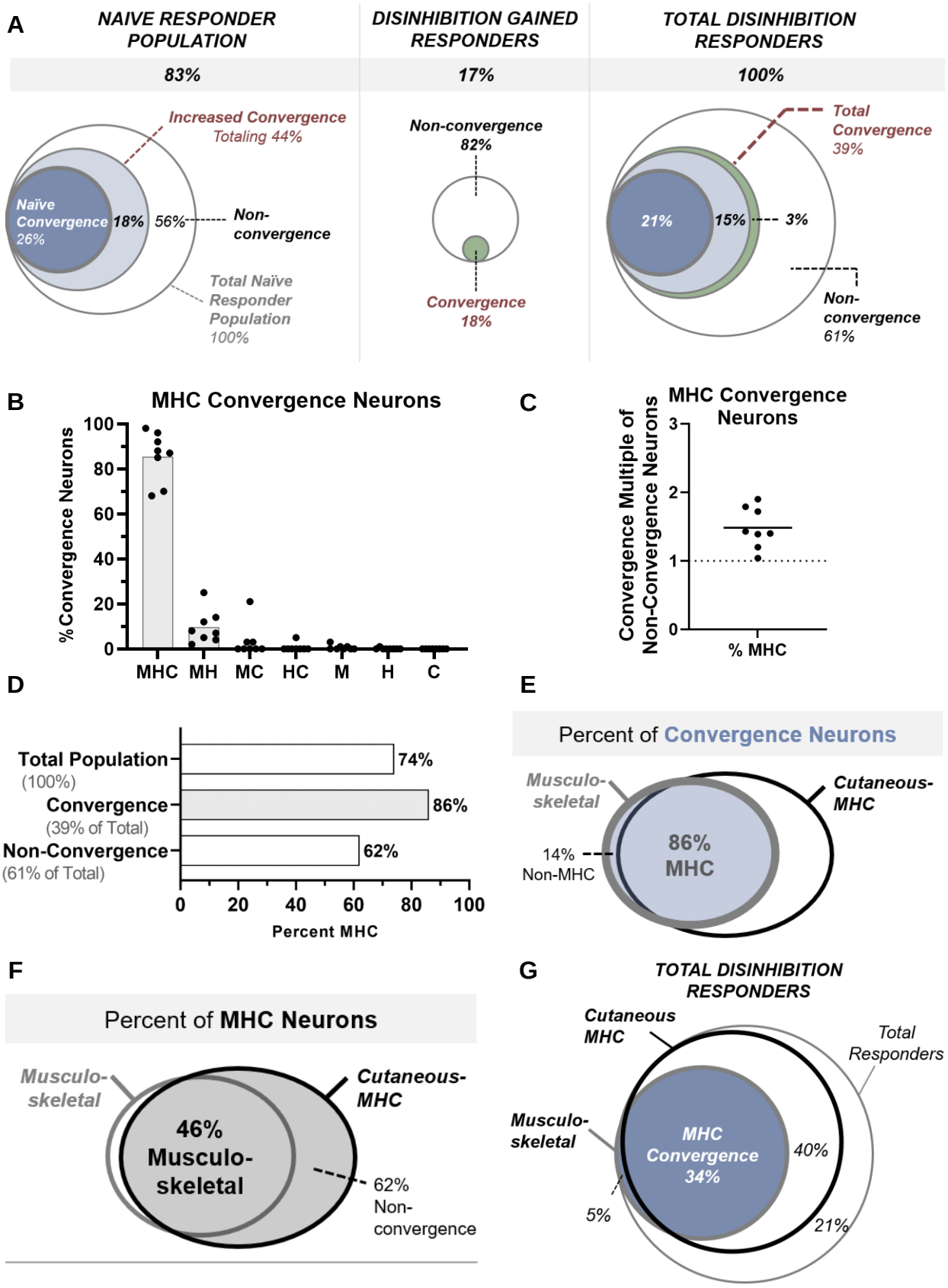

Figure 9: Disinhibition-dependent Musculoskeletal and Cutaneous Convergence

Figure 9 Legend

A: During disinhibition, the musculoskeletal and cutaneous convergence percent breakdown of the Naïve Responder Subpopulation, Disinhibited Gained Responder Subpopulation, and Total Disinhibited Responders. Note that the increase in convergence during disinhibition is driven mostly by changes in the Naïve Responder Subpopulation and not Disinhibited Gained Responders.

B: During disinhibition, the Cutaneous Modality breakdown of C&MS convergence neurons. On average across animals, 86% of C&MS convergence neurons are polymodal MHC-responsive.

C: During disinhibition, the percent of C&MS convergence neurons that are MHC as a multiple of the percent of *non*-C&MS neurons that are MHC. In each animal, there was a greater percentage of C&MS convergence neurons that were MHC compared to *non*-C&MS neurons. On average across animals, C&MS convergence neurons are 1.48 times more likely to be MHC than *non*-C&MS neurons.

D: During disinhibition, summary of MHC proportion of total responders, C&MS convergence neurons, and *non*-C&MS neurons. During disinhibition, 74% of all responders were MHC-responsive. 86% of C&MS convergence neurons were MHC-responsive compared to 62% of *non*-C&MS neurons.

E: During disinhibition, depiction showing 86% of C&MS convergence neurons as MHC-responsive.

F: During disinhibition, 46% of all MHC-responsive neurons were musculoskeletal-responsive, compared to 39% of all neurons.

G: During disinhibition, Venn diagram summary of polymodal MHC cutaneous and musculoskeletal convergence populations. 34% of total responders were MHC C&MS convergence neurons; 5% of total responders were non-MHC C&MS convergence neurons.

Disinhibition-dependent Population Tuning Background

In the prior sections, without inhibition, there was an increase in overall population responses, cutaneous polymodality, and musculoskeletal and cutaneous convergence. These changes may result from reductions in local inhibition within superficial lamina governing responses to C-fiber nociceptor inputs, as well as reductions in ventrodorsal inhibition governing responses to low-threshold mechanical inputs. However, it's unknown how inhibition in both superficial and deeper lamina preferentially affects population modality tuning in superficial excitatory neurons.

In behavioral assays with pharmacological central disinhibition, mechanical allodynia and spontaneous responses are often shown to be most pronounced[8;31;44;61;68;70;94;98]. Given the prominence of mechanical allodynia during central disinhibition, and the potential gain of many LT mechanical inputs from deeper lamina, it was hypothesized that the modality population tuning of superficial neurons may bias toward mechanical.

Disinhibited Mechanical-Tuning

With inhibition removed, it was found that the average HT-mechanical Max %ΔF/F was significantly greater than the average heat and cold-responses (Figure 10A). This was true for each

animal tested, in which the average mechanical response was 1.8 and 1.4 times greater than the average cold and heat responses (Figure 10B).

Because the average mechanical-evoked responses were greater than heat and cold, we next determined the proportion of disinhibited-MHC excitatory neurons had a mechanical optimal stimulus. It was found that during disinhibition, 71% of responders had a mechanical primary preference (Figure 10C), compared to 41% in the naïve state (Figure 5). To understand how these large mechanical responses affected the uni-, bi- and tri-tuning of MHC neurons, we plotted the modality tuning vectors of all disinhibited excitatory neurons (Figure 10D). For disinhibited-MHCs, which make up a large majority of neurons during disinhibition, it was found that close to half, or 46%, were mechanically uni-tuned. The remaining were predominately Mechano-Heat bi-tuned and MHC tri-tuned (Figure 10E). In contrast, in the naïve state, only 20% of MHCs are mechanical uni-tuned (Figure 5).

On The Origin of the Disinhibited Mechanical Population Tuning

To test whether low-threshold mechanical afferents drove the mechanical population tuning, a low-threshold air puff was used to stimulate the skin. In the naïve animals, LT-mechanical stimulation evoked approximately 10% of responders. During disinhibition, this increased to 78% of total disinhibited responders (Figure 10F). In both naïve and disinhibited states, these wide-dynamic range neurons were more likely to be polymodal MHC. During disinhibition, approximately 90% of the wide-dynamic range neurons were MHC-responsive (Figure 10G).

Next, to separate out the HTMR and LTMR responses for each neuron, the LT-mechanical Max %ΔF/F was subtracted out from the HT-mechanical response. It was found that with the LT-mechanical component removed, the average HTMR-evoked Max %ΔF/F was similar to that of

the average heat and cold response (Figure 10H). Moreover, only 38% of neurons had a primary preference to HTMR inputs, compared to heat 39% and cold 23% (Figure 10I). This suggests that the disinhibition-dependent change to mechanical population tuning may be driven by LT-mechanical inputs.

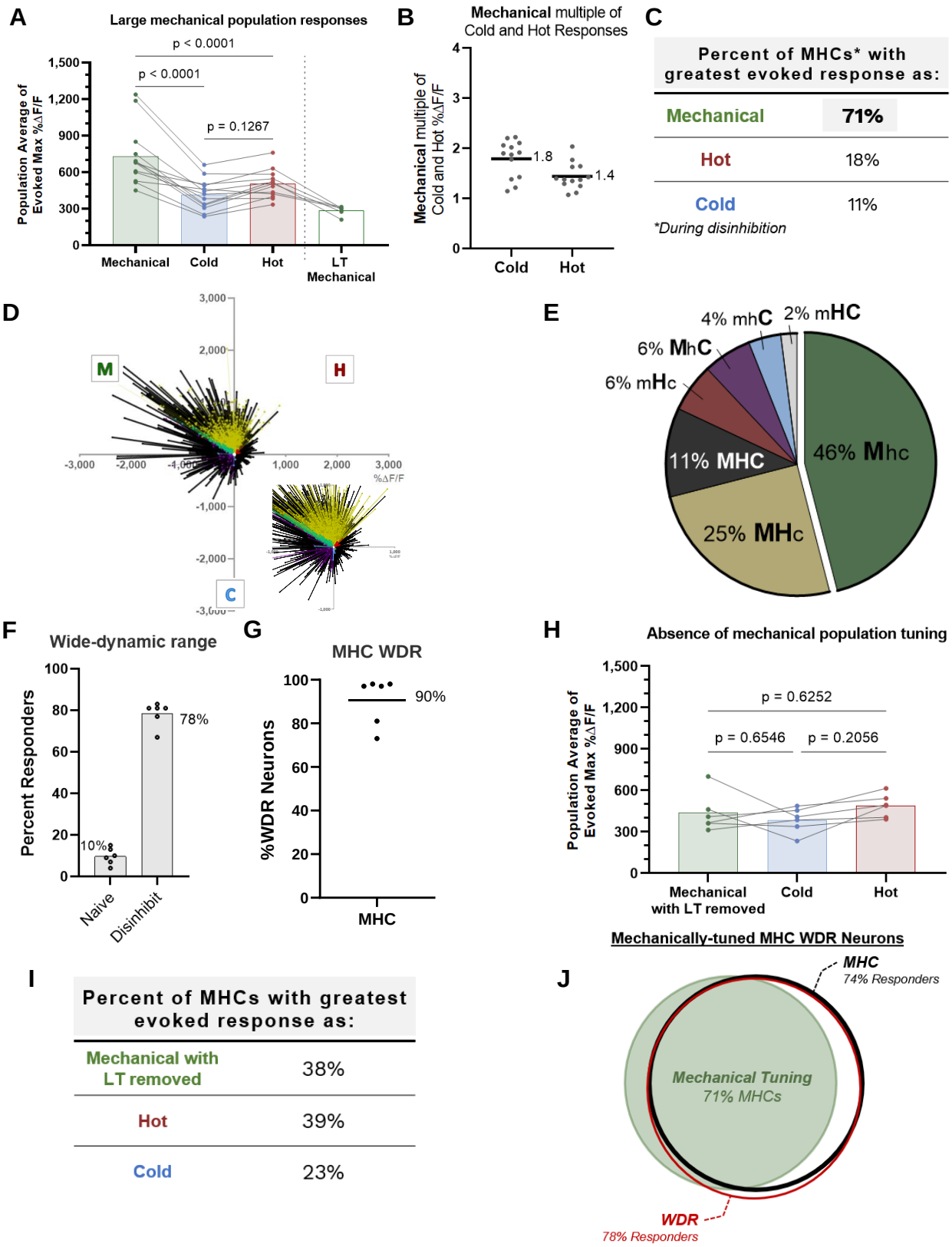

Figure 10: Disinhibition-dependent Mechanical Tuning Driven by LT-Mechanical Stim

Figure 10 Legend

A: The HT-Mechanical, Heat, Cold and LT-Mechanical average Max %ΔF/F during disinhibition. The average HT-mechanical evoked max response was greater than both heat and cold max responses. One Way ANOVA with Repeated Measures and Tukey Multiple Comparisons.

B: In each animal, the HT-mechanical-evoked average Max %ΔF/F was greater than heat and cold stimulation of the skin.

C: 71% of polymodal cutaneous-MHC neurons during disinhibition responded best to mechanical stimulation, greater than 41% in the naïve state (Figure 5).

D: The plotting of cutaneous-modality tunings of all neurons during disinhibition. Note the majority of neurons are tuned in the direction of mechanical stimulation. Note the scale goes up to 3,000% ΔF/F, which is over 3 times the magnitude of the scale of the insert and all other vector charts in the document.

E: The proportion of MHC neurons during disinhibition with cutaneous modality tunings either uni-, bi-, or tri-tuned. 46% of MHC neurons during disinhibition are uni-tuned to mechanical stimulation, compared to 20% in the naïve state (Figure 5).

F: On average across animals, the proportion of responders that are wide-dynamic range increased from 10% to 78% without inhibition.

G: On average across animals, 90% of WDR neurons are polymodal cutaneous-MHC without inhibition.

H: LT-mechanical stimulation drives disinhibition-dependent mechanical population tuning. For each neuron, when the LT-mechanical Max %ΔF/F component is removed from the HT-mechanical response, the mechanical average Max %ΔF/F is not significantly different than

heat and cold responses. One Way ANOVA with Repeated Measures and Tukey Multiple Comparisons

I: LT mechanical stimulation drives disinhibited mechanical population tuning. For each neuron, when the LT-mechanical Max %ΔF/F component is removed from the HT-mechanical response, 38% of MHC neurons responded best to mechanical, similar to 41% in the naïve state (Figure 5).

J: Venn diagram summarizing the general situation during disinhibition: mechanically-tuned MHC WDR range neurons. 74% of total responders were MHC, 71% of which were mechanically-tuned. 78% of responders were also WDR.

4.0 Discussion

In both naïve and disinhibition conditions, this work marks the first thorough cutaneous modality and musculoskeletal convergence characterization of populations of superficial excitatory dorsal horn neurons. We developed a modality tuning methodology to identify functional neuron subtypes according to their uni-, bi-, and tri-tunings. In the naïve condition, despite the presence of many polymodal neurons, we show heterogeneity in response combinations to different modalities (Figure 4) and in their modality tuning (Figure 5). We also identify the cutaneous modalities and tunings onto C&MS convergence neurons (Figure 6-7). In addition, we show how dorsal horn inhibitory networks shape this functional heterogeneity. With inhibition removed, we show an increase in both cutaneous polymodality and C&MS convergence driven largely by changes in a naïve responder subpopulation (Figure 7-8). Lastly, we found that disinhibition causes a change to pronounced mechanical population tuning in superficial excitatory neurons. This change to mechanical population tuning was driven largely by LT-mechanical inputs and may be a basis for mechanical allodynia observed in painful neuropathies.

Limitations of 2P GCaMP6s Imaging

It's acknowledged that there are limitations with 2P GCaMP6s imaging. First, it's possible that changes in intracellular calcium can occur independent of action potentials (APs). As a result, this calls into question the use of a responder threshold based on a GCaMP signal alone; and more importantly, it's unknown whether the calcium population responses represent neural activity that underly pain behavior. In addition, GCaMP6s doesn't completely encode for AP frequency. It's been reported that a high AP frequency can cause a GCaMP6s signal to plateau. This has

implications on all endpoints including the responder threshold, peak amplitude responses, and tuning vectors. Another potential concern in GCaMP imaging experiments is whether the data sampling can capture a single AP. However, in these experiments, GCaMP6s was used due to its slow decay time. The 2.3 Hz sampling rate can capture a GCaMP6s signal from a single AP[19]. Lastly, these endpoints are measuring a change in fluorescence from regions of interests (ROIs), which may not always be individual neurons. In particular, throughout a two-three hour recording, there's a risk of identifying false-positive responders. In Vglut2cre animals, there is a high quantity of GCaMP6s in superficial laminae. In healthy preparations that enable large evoked responses, there is sometimes an evoked background response across the entire visual field from GCaMP6s signals in dendrites and neuropil of deeper laminae.

Because these limitations have implications on all GCaMP endpoints, in my view, the only solution is to record from neurons in the same experiments. This would aide in the identification of responder thresholds and help determine the degree to which the GCaMP6s signal is encoding for APs with the inputs used in these experiments. In addition, it would be interesting whether an analysis of relatively few neurons recorded with electrophysiology would yield similar conclusions as a GCaMP population analysis.

The *ex vivo* preparation was used for four reasons. First, it enables access to image the spinal cord. Second, it allows for a consistent use of pharmacology. Third, it provides for superior imaging quality by eliminating breathing movement thereby maintaining a consistent optical plan. And lastly, it enables the separation of cutaneous and musculoskeletal stimulation by separating out skin from muscle. However, it is acknowledged that tissue and CNS damage occurs *ex vivo*. In addition, brainstem descending inputs that modulate superficial laminae are not included in the *ex vivo* preparation.

Naïve Overall Population Responses

Although results were generally consistent across animals, some in-between animal variance was present. Looking at the percent responders evoked from mechanical, heat, and cold cutaneous stimulation (Figure 4A), there was an animal range typically around plus/minus 10% of the mean excluding outliers. The variance in percent responders evoked from each modality may be the result of a number of factors, including differences in the health of individual preps, slight variance in depth of neurons imaged, and variation in manual stimulation.

Nevertheless, the large overall population responses (OPR) to mechanical and heat in superficial neurons (Figure 4) is consistent with nociceptive inputs into the region. The most prevalent type of cutaneous C-fiber found in mice are those that respond to both thermal and mechanical stimulations[55]. The cold-evoked OPR was slightly smaller, which is also consistent with cutaneous TRPM8-expressing sensory afferents as a small population[53].

Naïve Cutaneous Modalities & Population Tuning

The *Cutaneous Modality Responder Subpopulations* (Figure 4C) are generally in line with prior electrophysiology that identified the presence of polymodality in superficial neurons[1-3;7;22;45;46;62;66;67]. To that end, this work validates prior electrophysiology studies with the use of two-photon calcium population imaging. While the results of certain modality characterizations may merely reflect the mechanical pressures and thermal temperature used in a particular protocol, as well as the extent to which all receptive fields are stimulated for the neurons in a visual field, the current experiments instead sought to determine the true polymodal potential of superficial excitatory neurons. Therefore, the entire lateral femoral cutaneous skin was stimulated with high

pressure and temperature changes to maximize inputs and capture most receptive fields of the neurons resident to visual field imaged (Figure 2B).

As a whole, heterogeneity in functional population subtypes was found in terms of different response combinations to modalities as well as distinct modality tunings. Although many neurons were found to be polymodal in the naïve condition, we found that many were uniquely tuned to specific modalities (Figure 5). These distinct modality tuning profiles may help drive pathways of modality-specificity to the brain.

Naïve Cutaneous & Musculoskeletal Convergence

Research into the convergence of musculoskeletal and cutaneous convergence in dorsal horn had previously been relatively limited in scope[24;41;42;85;95;96]. These experiments mark the first comprehensive cutaneous modality characterization of superficial neurons also responsive to musculoskeletal stimulation. We find that about a quarter of lateral superficial neurons respond to both skin stimulation and musculoskeletal nerve stimulation. This is consistent with a few lines of prior work. First, transganglionic nerve tracing studies show that musculoskeletal nerve fibers typically terminate more medially while cutaneous fibers project more laterally in the dorsal horn[73-75;88;89]. Accordingly, we show that approximately three quarters of lateral superficial neurons are cutaneous-only responsive and virtually none are musculoskeletal-only. Similarly, a very important study recently demonstrated similar results and found that medial lamina I lumbar neurons are more likely to be C&MS convergence neurons than lateral neurons[65].

Spinal Disinhibition of Cutaneous Modalities and Musculoskeletal Convergence

The current work expands upon the existing knowledge of spinal disinhibition-dependent plasticity. First, it demonstrates the degree of polymodality that's observed at the bicuculline and strychnine concentrations that's been used in slice physiology[5;12;83;92]. Both mechanical and heat stimulation of the skin evoked responses in nearly all excitatory neurons.

The proportion of superficial excitatory neurons that were cutaneous-MHC-responsive ranged from 50 to 100% of total responders, depending on the size of the cold-evoked response. Cold-evoked responders ranged from 60% to 99% of total disinhibition responders. On an animal-by-animal basis, the number of cold responders (Figure 8D), but not the mechanical and heat responders (Supplemental Figure 5C-D), correlated with the number of spontaneous responders during disinhibition. One interpretation of this is that both cold-evoked and spontaneous responders may have been affected by the efficacy in disinhibition (e.g. differences in aliquot measurements, health of prep affecting disinhibition efficacy). Along those lines, maximal cold responses may have a higher EC50 and are controlled by inhibition more so than mechanical and heat. In addition to the variance in cold responses during disinhibition, the increase in musculoskeletal responses were limited compared to the increase in cutaneous polymodality and mechanical tuning. It's possible that there is a hard-coded excitatory segregation between musculoskeletal and cutaneous responses in the absence of inhibition in this particular region of the cord. Alternatively, musculoskeletal responses may be controlled by inhibition more than cutaneous mechanical and hot responses in this region of the dorsal horn.

In summary, bicuculline and strychnine concentration-dependent responses in new experiments could test whether cold responses, spontaneous activity, and musculoskeletal responses are controlled by inhibition more than cutaneous mechanical and hot stimulation. This

in turn may aide in the understanding of how central inhibitory networks differentially affect population responses to different modalities and tissue types.

With the disinhibition analyses, two other phenomena occurred. First, the increase in both polymodality and C&MS convergence was driven more so by changes in the naïve responder subpopulation than the disinhibition-dependent gained responders (Figure 8 and Figure 9). This was in terms of both the naïve responders being a large majority of total disinhibited responders, as well as the naïve responders during disinhibition being more polymodal with convergence responses. The responder threshold in principle can affect these percentages, i.e. a higher responder threshold can result in less naïve responders, but more gained responders. However, any reasonable responder threshold, e.g. less than 200% ΔF/F, results in a similar breakdown of naïve vs gained responders, given that the average naïve evoked response is 250-300% ΔF/F (Figure 4). However, given that disinhibition causes expansive receptive fields, it's likely that gained responders outside of the visual field weren't captured in these experiments. Nevertheless, the naïve responder subpopulation was more likely to be polymodal and C&MS during disinhibition.

Finally, we show a change in population tuning from distinct modality tunings in the naïve condition to primarily mechanical population tuning during disinhibition. The change to mechanical tuning was driven largely by gains in low-threshold mechanical inputs. This is consistent with the field's focus on investigating the ventro-dorsal circuits that may drive mechanical allodynia.

On The Notion of Neuron Subpopulation Multi-Functionality

Subpopulation convergence was found both in terms of a convergence in modalities and tissue types. There were three subpopulations identified which are uniquely multi-responsive, including C&MS convergence neurons (which can respond to multiple tissue types), Powerhouse

MHCs (which are tri-modal and respond well to both mechanical and heat), and tri-tuned MHCs (which respond to the three modalities roughly equally). Neuron populations with convergent responses may play a maladaptive role in referred pain[73].

But what's the function of such multi-responsive populations and how do they help define distinct somatosensory pathways that lead to sensory discrimination? It is apparent that these convergent, *multi-responsive* populations are likely *multi-functional*. For example, if there is a network of neurons that drive cutaneous pain, and another network of neurons that drive muscle pain, then C&MS neurons would be multi-functional in that they form a part of at least two networks that drive skin and muscle pain respectively. The same can be said for tri-tuned MHCs neurons, which may form a part in each of three neuron networks that drive mechanical, heat and cold pain.

Whether it's through traditional pharmacology, bioelectronics, or brain-computer interfaces[38], neuroscience is centering around the identification of specific neuron networks – whether by genetic markers, electrophysiological properties, anatomical location, etc. – that can drive different behaviors. Thus, the degree of overlap between populations of neurons that drive different behaviors is a critical question to get right. While there are technical challenges in teasing out precise overlap between neuron networks that drive different pain types (e.g. optogenetics, chemogenetics), this work provides a reference point for the degree of functional subpopulation overlap in the superficial dorsal horn. In addition, theoretical questions on the multi-functionality of neuron populations are important to address this gap. To which degree can neuron networks overlap such that any given individual network is uniquely functional? In that light, it is proposed here that population convergence be viewed through the lens of neuron subpopulation multi-functionality.

Page Break

Appendix A Supplemental Figures

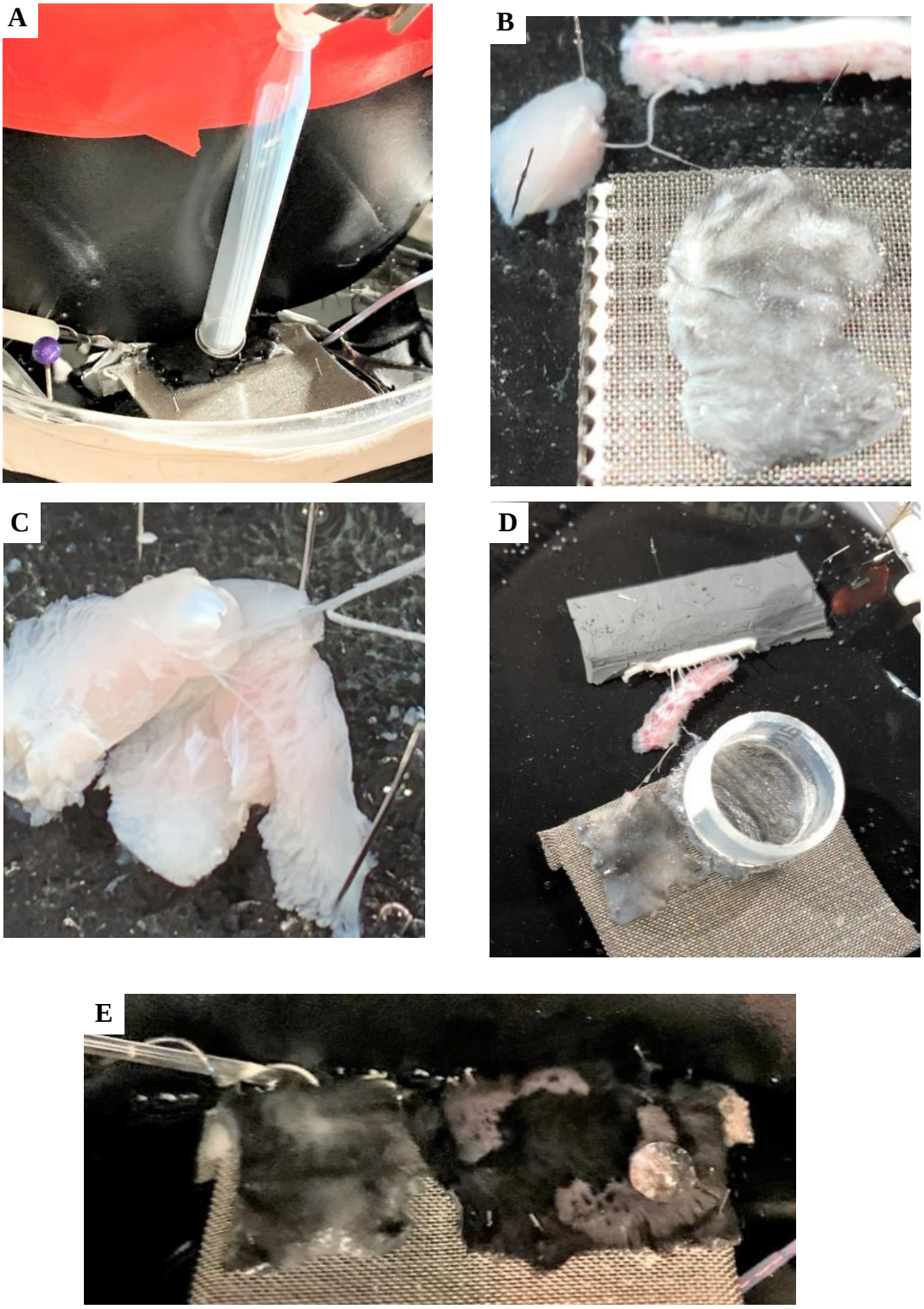

Supplemental Figure 1: Experimental Methods

F

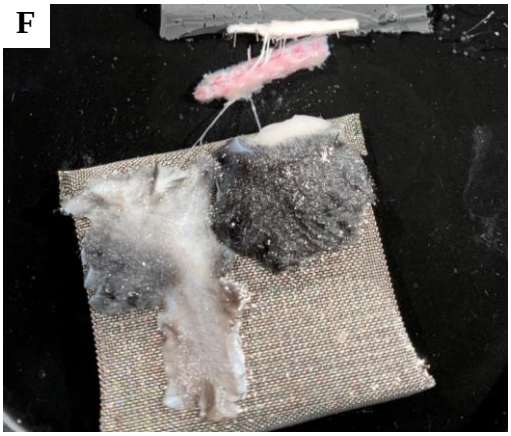

G

H Original proposed experimental design for recording convergence in GCaMP in dorsal horn

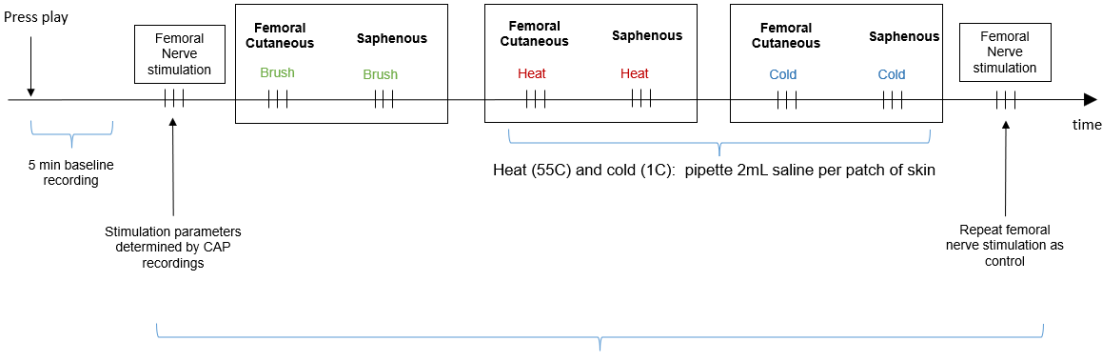

- **3 sweeps of each stimulation to determine if response is evoked or spontaneous**
- **2 minutes between each sweep to let the dorsal horn rest**

I

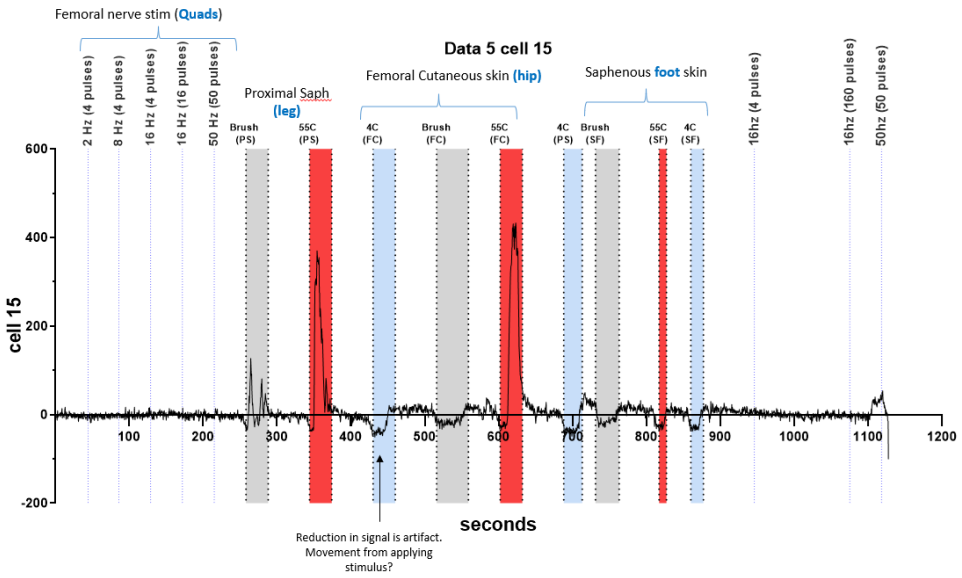

Supplemental Figure 1: Experimental Methods Continued

J

Control experiment: demonstrate reproducible GCaMP responses to **nerve** stimulation

1. In 1 animal, tested various stimulation frequencies (1mA intensity, 1ms pulse duration, 5 sweeps at 30s intervals)
2. Next steps:
   i. Do 3 more GCaMP experiments to quantify sweep fidelity for each stimulation frequency using the intensity determined from the CAP experiments

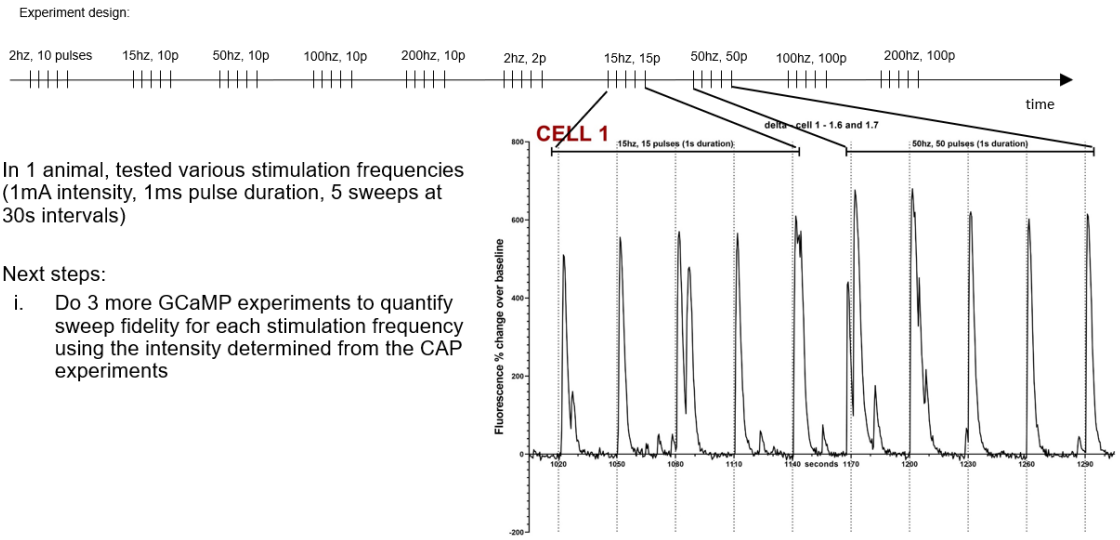

K

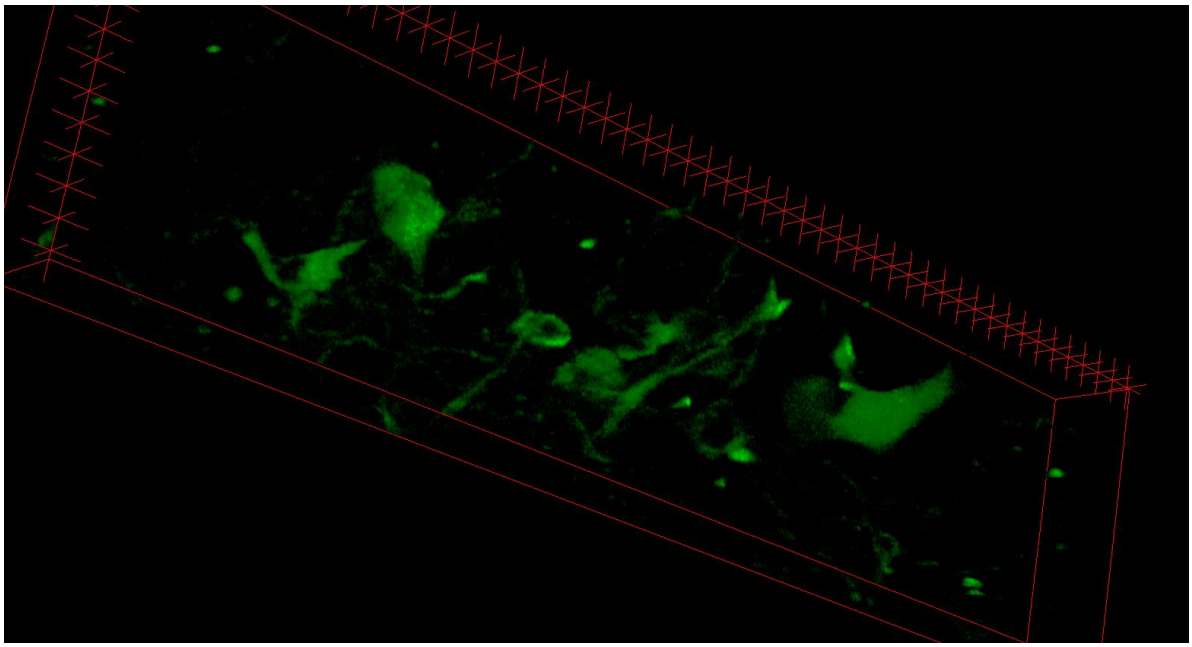

Supplemental Figure 1: Experimental Methods Continued

Supplemental Figure 1 Legend

A: Air puff set to stimulate skin with LT mechanical stim.

B: Experimental dissection considered to test the convergence musculoskeletal and cutaneous inputs into dorsal horn. Muscle included is quadriceps and skin is lateral femoral cutaneous.

C: An effort to open up the muscle to let the artificial CSF in while maintaining the main branches of the femoral nerve

D: Experimental setup with plastic section of centrifuge tube glued to skin to localize stimulation on skin. While it contained heat and cold saline for a few seconds, applying brush stimulation was difficult and caused movement of the prep and cord.

E: Example dissections showing unhealthy skin preventing the continuation of experiment. Ultra-hydrophobic dead skin preventing the spread of heat and cold water throughout the skin, likely caused by large air bubbles on the skin under water during the dissection.

F: Inclusion of skin from the proximal saphenous/main trunk of saphenous skin (left) and lateral femoral cutaneous skin (right) in the same prep. Both nerves input into lateral L2 and L3 dorsal horn, however with saphenous being slightly more caudal in L3 and LFC slightly more rostral in L2. Ultimately decision was made to move forward with one patch of skin, as only one was needed for experiments.

G: Inclusion of saphenous skin, lateral femoral cutaneous skin, and femoral nerve stimulation

H: Original experiment design not used in current experiments that included lateral femoral cutaneous skin, saphenous skin, and femoral nerve. The idea was to ensure we stimulated all of the receptive fields of L2 neurons with the inclusion of both lateral femoral cutaneous skin and saphenous skin. Image is screen shot from lab meeting presentation slide

I: A sample calcium response in prep that had both lateral femoral cutaneous skin and saphenous skin. Image is screen shot from lab meeting presentation slide. Note that the reduction in signal is an artifact from movement during cutaneous stimulation.

J: Control experiments testing various femoral nerve stimulation pulse durations and frequencies. Image is screen shot from lab meeting presentation slide.

K: A two step stack 15 microns in depth considered for original experiment design

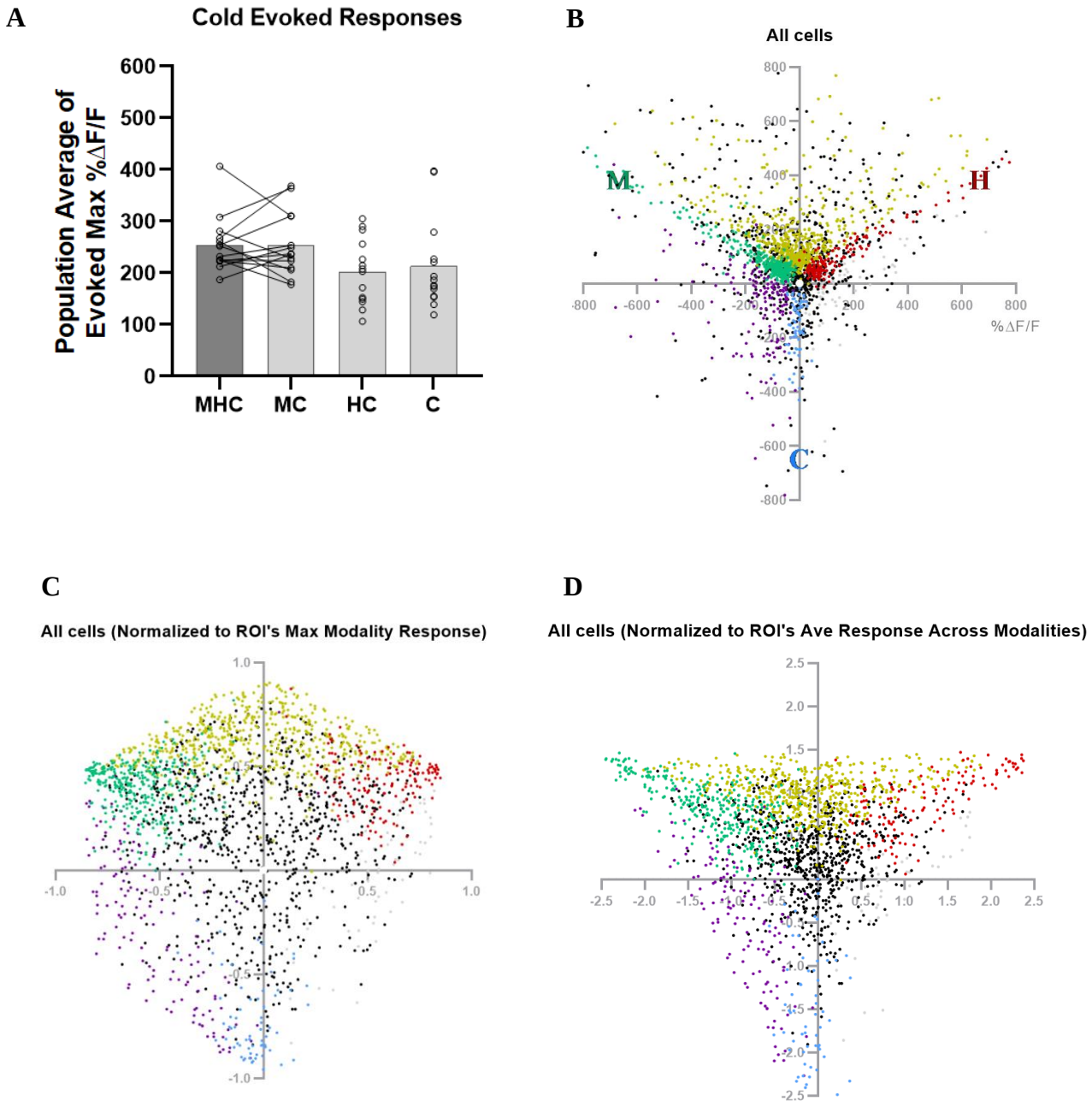

Supplemental Figure 2: Naïve Cutaneous Modality Responses & Tunings

Supplemental Figure 2 Legend

A: Average cold response was no different for MHC compared to Non-MHCs

B: Modality Tuning vectors during naïve state without the lines

C: Same cells as B, but normalizing each cell's response to the max response. Instead of plotting the vectors as df/f, each modalities response was normalized to the max response of the three.

D: Same cells as B and C, but normalizing each cell's response to the average response of the three modalities.

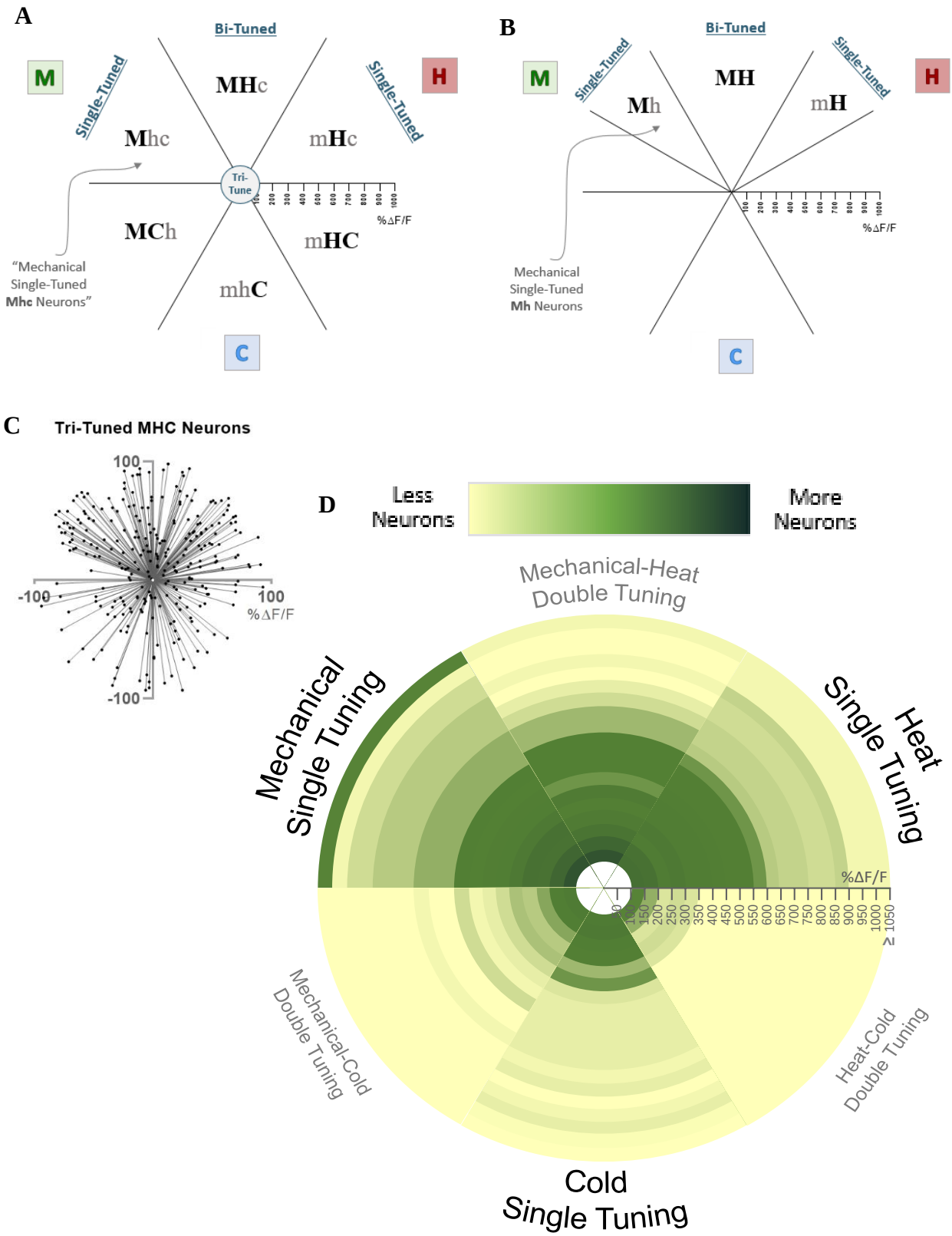

Supplemental Figure 3: Naïve Cutaneous Modality Tuning

Supplemental Figure 3 Legend

A: Illustration of tri-modal MHC tuning methodology to determine uni-tuning, bi-tuning, and tri-tuning. Uni-tuned neurons respond to a single modality with a %ΔF/F response greater than the average %ΔF/F response of all three modalties. Bi-tuned neurons respond to two modalities with a %ΔF/F response greater than the average %ΔF/F response of all three modalties. Tri-tuned neurons have vector lengths less than 100 %ΔF/F.

B: Illustration of bi-modal (MH, MC, HC) tuning methodology to determine uni-tuning or bi-tuning. For e.g. bi-modal MH neurons, vectors will plot in one of the three slices on the top of the graph depicted with **M**h, **MH**, and h**M**. Uni-tuned neurons respond to one modality with a %ΔF/F response greater than the average %ΔF/F response of the three modalities. Bi-tuned neurons respond to two modalities with a %ΔF/F response greater than the average %ΔF/F response of all three modalties.

C: A zoomed in view of MHC tri-tuned neurons. These neurons do not respond preferentially to any of the three modalities.

D: Since the plotting of all neuron's vectors across all animals on a single chart makes it difficult to see all the vectors, a heatmap was created to show were most vectors land. This is essentially a histogram of concentric circles. The vector chart was divided in concentric buckets of 50% ΔF/f. For each uni and bi tuning slice, the number of vectors in each concentric bucket was counted. The greener the concentric slice, the more neurons, the yellower the concentric slice, the less neurons. Viewing this illustration, one can see that most neurons in the naïve state have either mechanical and/or heat tuning. In addition, there's a cold tuning population, but with smaller vector magnitudes.

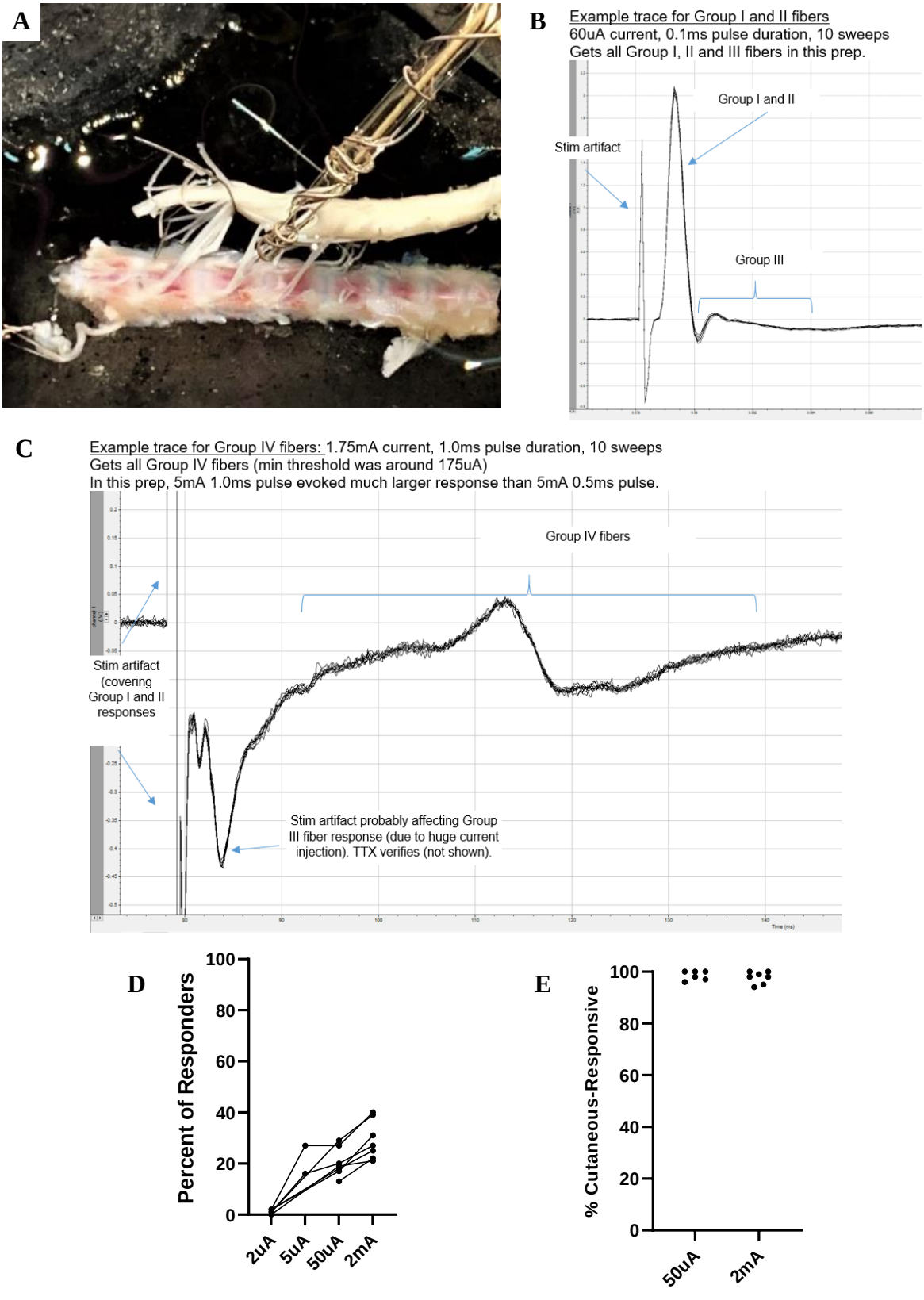

Supplemental Figure 4: Femoral Nerve Stimulation Intensities

Supplemental Figure

A: Mouse *ex vivo* prep used for dorsal root compound action potential recordings from femoral nerve stimulation. The purpose was to determine which stimulation intensities to use in the GCAMP experiments. Data obtained from approximately 5 animals. For each stimulation intensity ranging from 1uA to 2mA, the femoral nerve was stimulated with 10 sweeps, 0.1ms or 1ms pulse duration, with a range of frequencies from 10hz to 100hz. The compound action potential was recording on the L2 or L3 root.

B: An example L2 compound potential recording trace showing Group I, II, and III fibers. Compound response from Group I and II (A alpha and A beta) immediately followed the stimulus artifacts and could not be separated out from each other. The typical threshold for the Group I and II compound was 2uA. The typical threshold for Group III (A delta) was 50uA. Group I, II, and III components were easy to achieve in all animals.

C: The Group IV C-fiber component of an example compound action potential. The Group IV component was difficult to achieve since its peak voltage was small and lost in noise. The peak voltage was small due to the large spread in CVs for C-fibers, resulting in a short, long component. In some cases, the dipole would switch throughout the recording, as in this example. 1mA typically picked up the max component observed for Group IV fibers. 2mA stimulation was used in the GCaMP experiments to ensure all fibers were activated.

D: In the spinal cord GCaMP experiments, the percent of responders that were evoked from 2uA, 5uA, 50uA, and 2mA.

E: Virtually all neurons that responded to either 50uA and 2mA femoral nerve stimulation were also cutaneous-responsive.

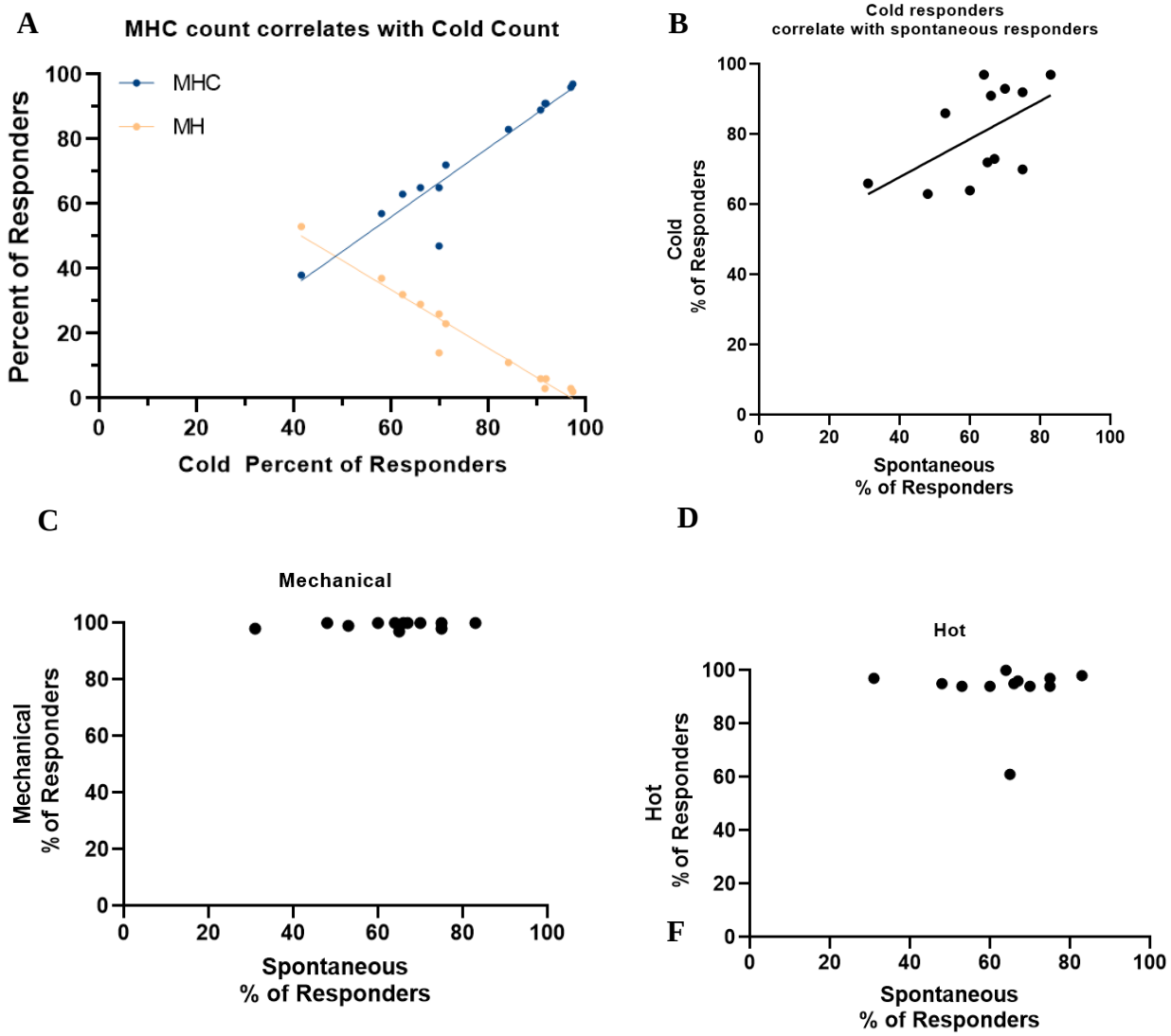

A: Disinhibition: MHC and MH Responders correlates with Percent Cold Responders. HC, MC and Cold-specific do not.

B: Disinhibition: Cold Responders correlate with Spontaneous Responders

C: Disinhibition: Mechanical Responders don't correlate with Spontaneous Responders

D: Disinhibition: Heat Responders don't correlate with Spontaneous Responders

Supplemental Figure 5: Disinhibition Characterizations

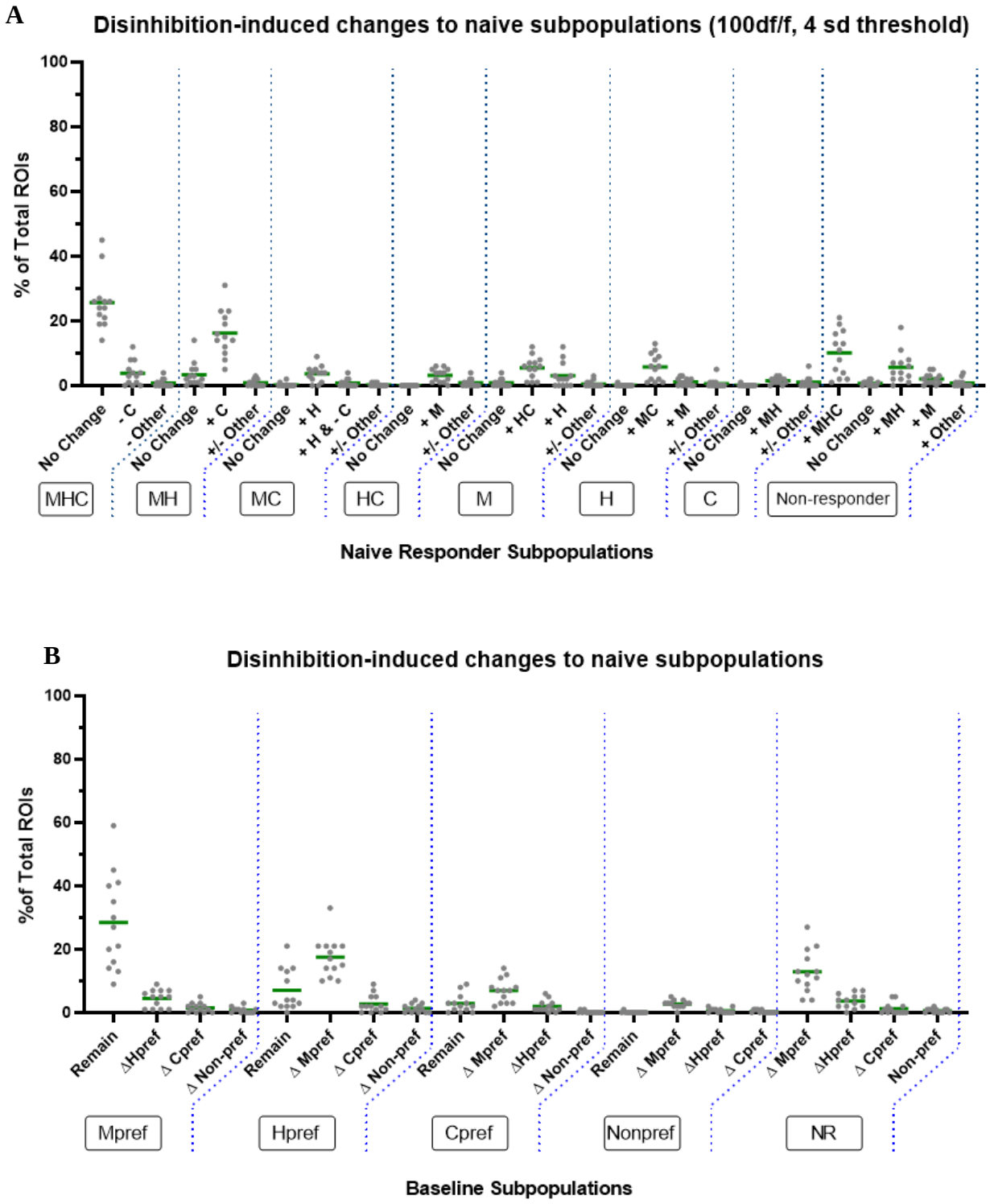

Supplemental Figure 6: Disinhbition-induced changes to naïve subpopulations

A: How individual naïve cutaneous modality responder subpopulations change during disinhibition. Note that the x-axis is percent of total naïve responders, but not the percent of each naïve subpopulation on the x-axis. The x-axis is divided into baseline subpopulations MHC, MH, MC, HC, M, H, C, and non-responders. Above these baseline subpopulations, on the x-axis, it showing whether the baseline subpopulation gained and/or loss a response to a modality during disinhibition. The number of neurons that gained and/or lost a response is expressed as a percent of total naïve responders.

B: How individual naïve primary preference responder subpopulations change during disinhibition. Note that the x-axis is percent of total naïve responders, but not the percent of each naïve subpopulation on the x-axis. The x-axis is divided into baseline subpopulations that had primary preferences to mechanical, heat, or cold. Above these baseline subpopulations, on the x-axis, it showing whether the baseline subpopulation gained and/or loss a primary preference to a modality during disinhibition. The number of neurons that gained and/or lost a primary preference is expressed as a percent of total naïve responders.

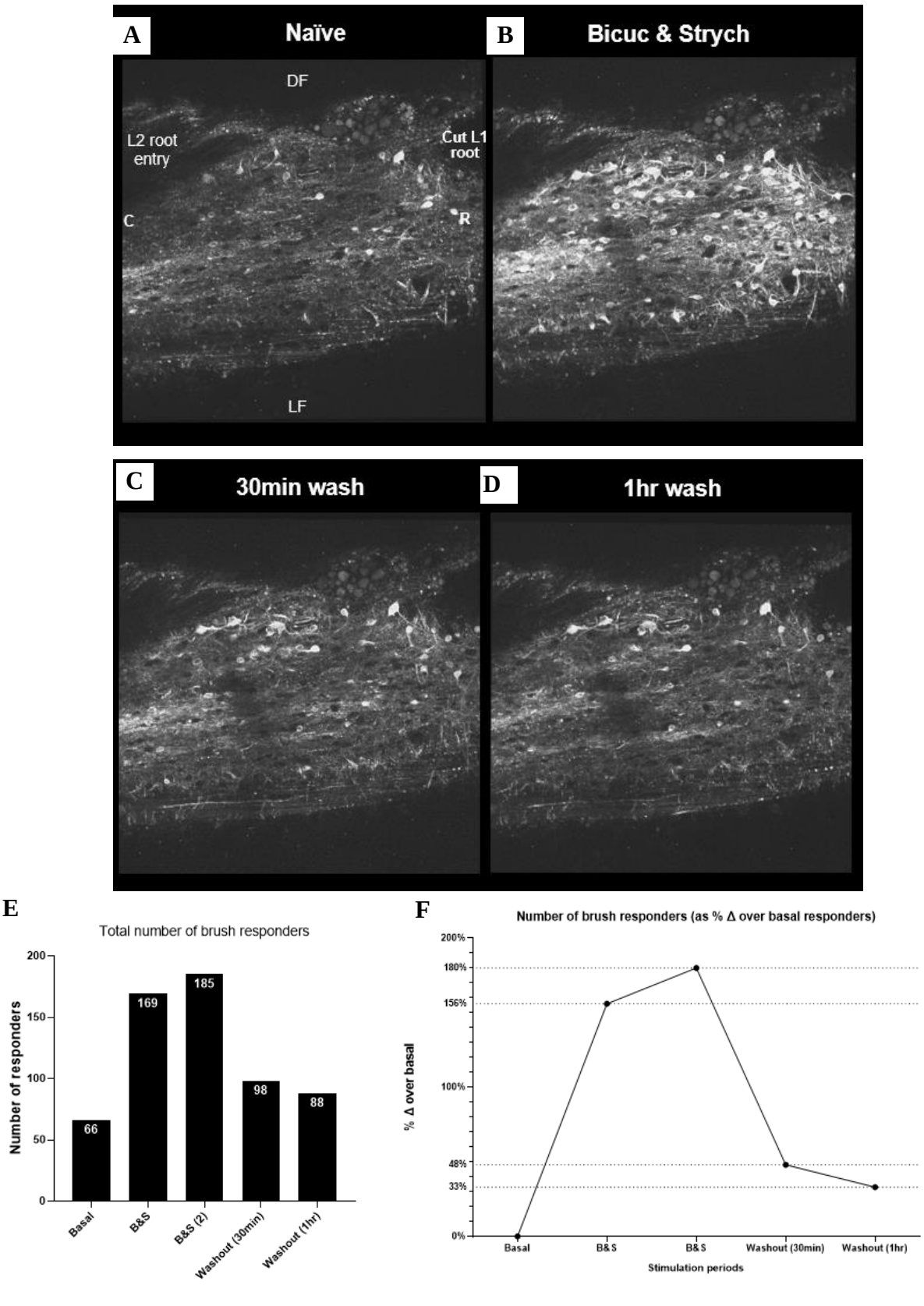

Supplemental Figure 7: Disinhibition Washouts

A-D: Early experiments not included in analysis. These are max stacked images of HT-mechanical brush responses during naïve, disinhibition, then wash outs of the bicuculline and strychnine.

E: Number of brush responders during naïve, disinhibition, and washouts

F: Number of brush responders normalized to naïve responders.

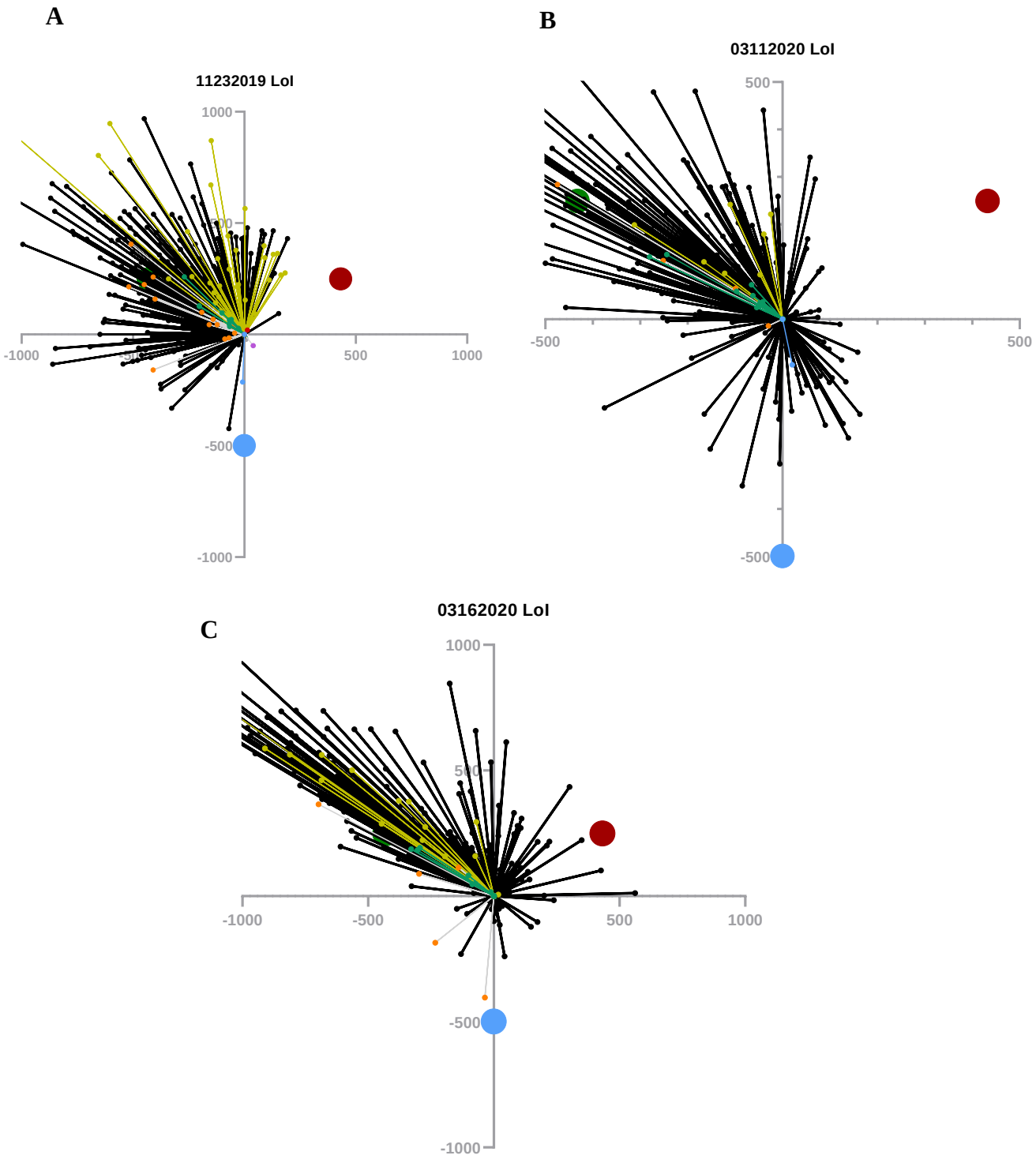

Individual animal examples of mechanical population tuning seen during disinhibition. Neurons are tuned to mechanical pointing to the top left. Heat is top right. Cold is bottom center.

Supplemental Figure 8: Disinhibition Mechanical Tuning in Individual Animals

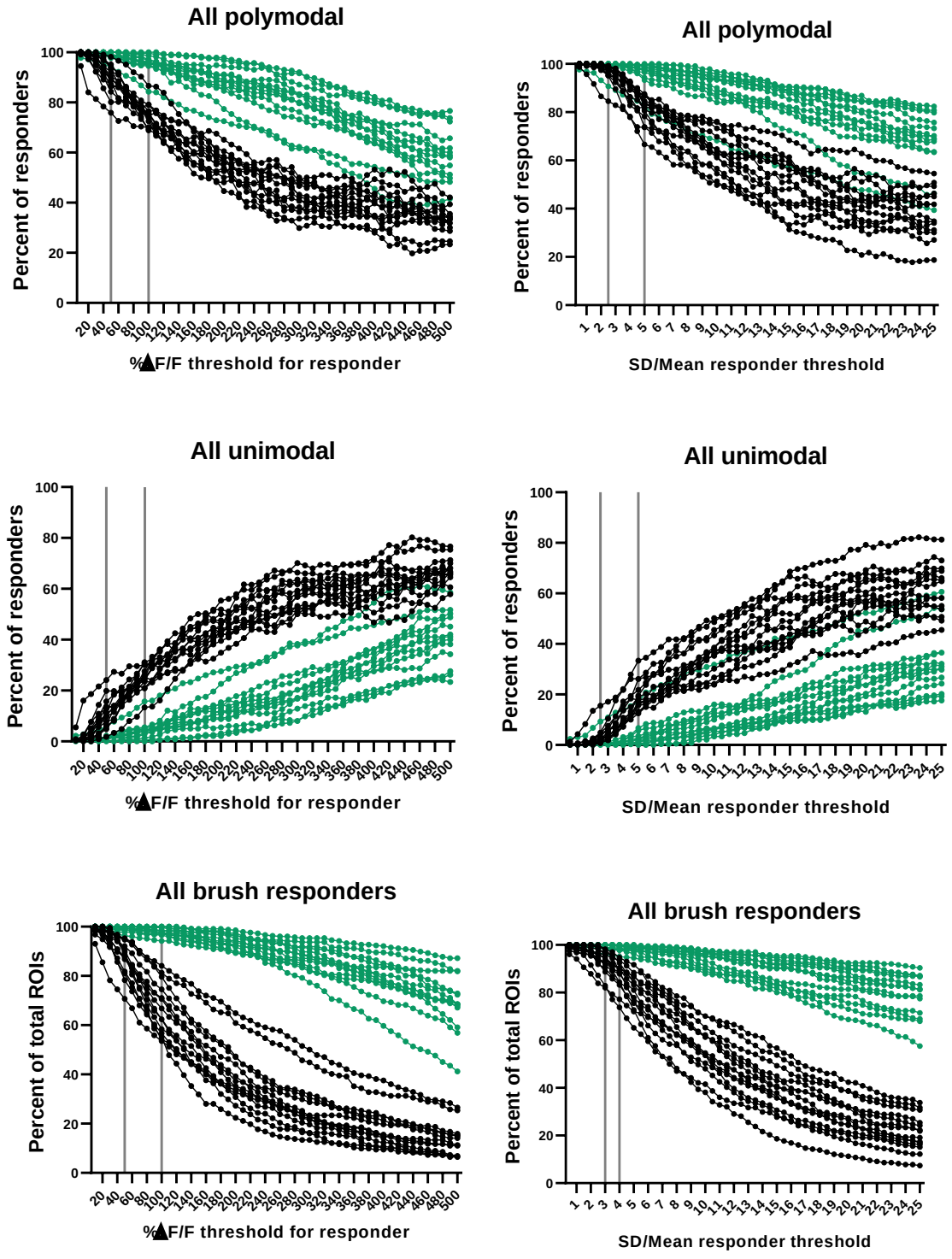

Black – Naïve; green – disinhibition (plotted as animals); SD/Mean should say z-score

Supplemental Figure 9: Number of Responders as a Function of Responder Threshold

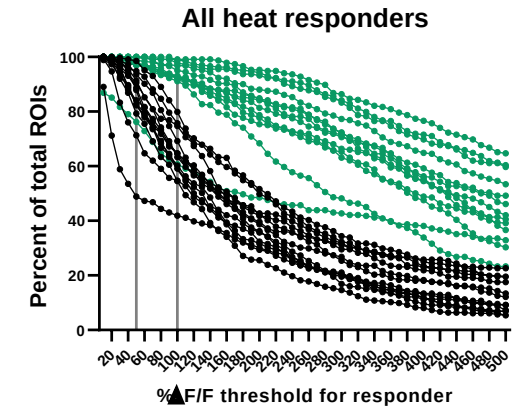

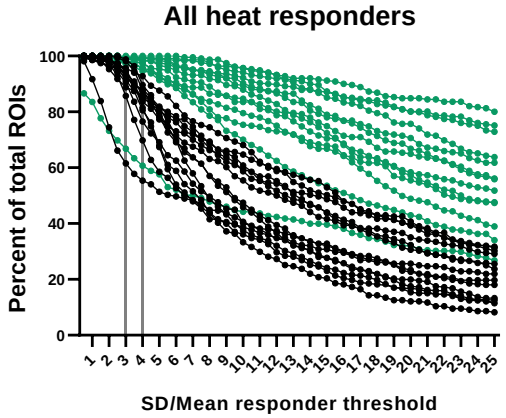

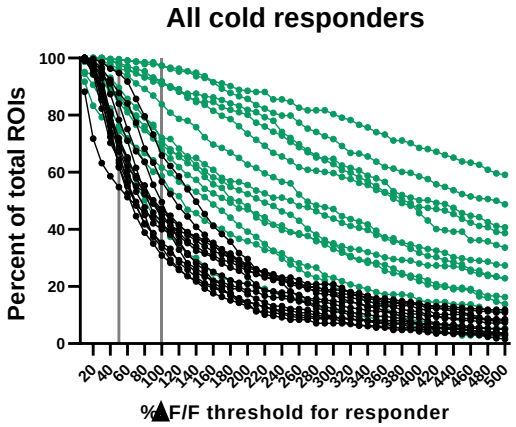

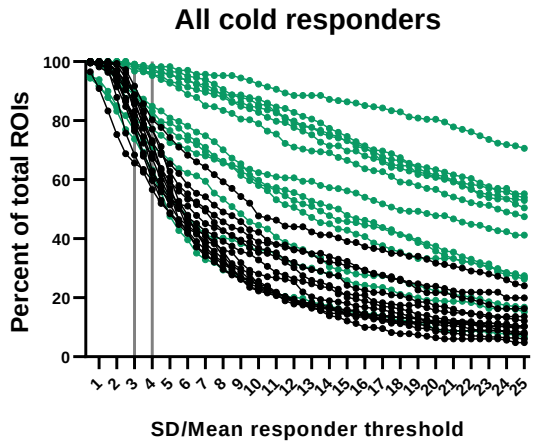

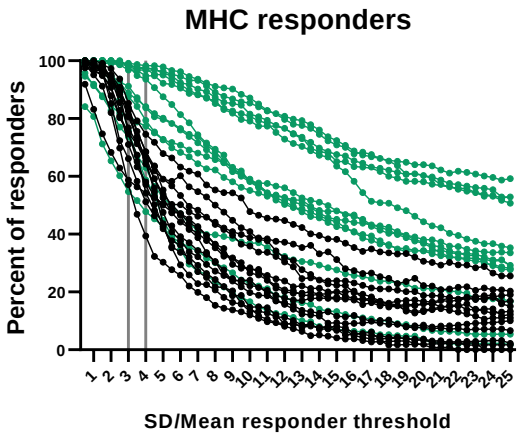

Black – Naïve; green – disinhibition (plotted as animals); SD/Mean should say z-score

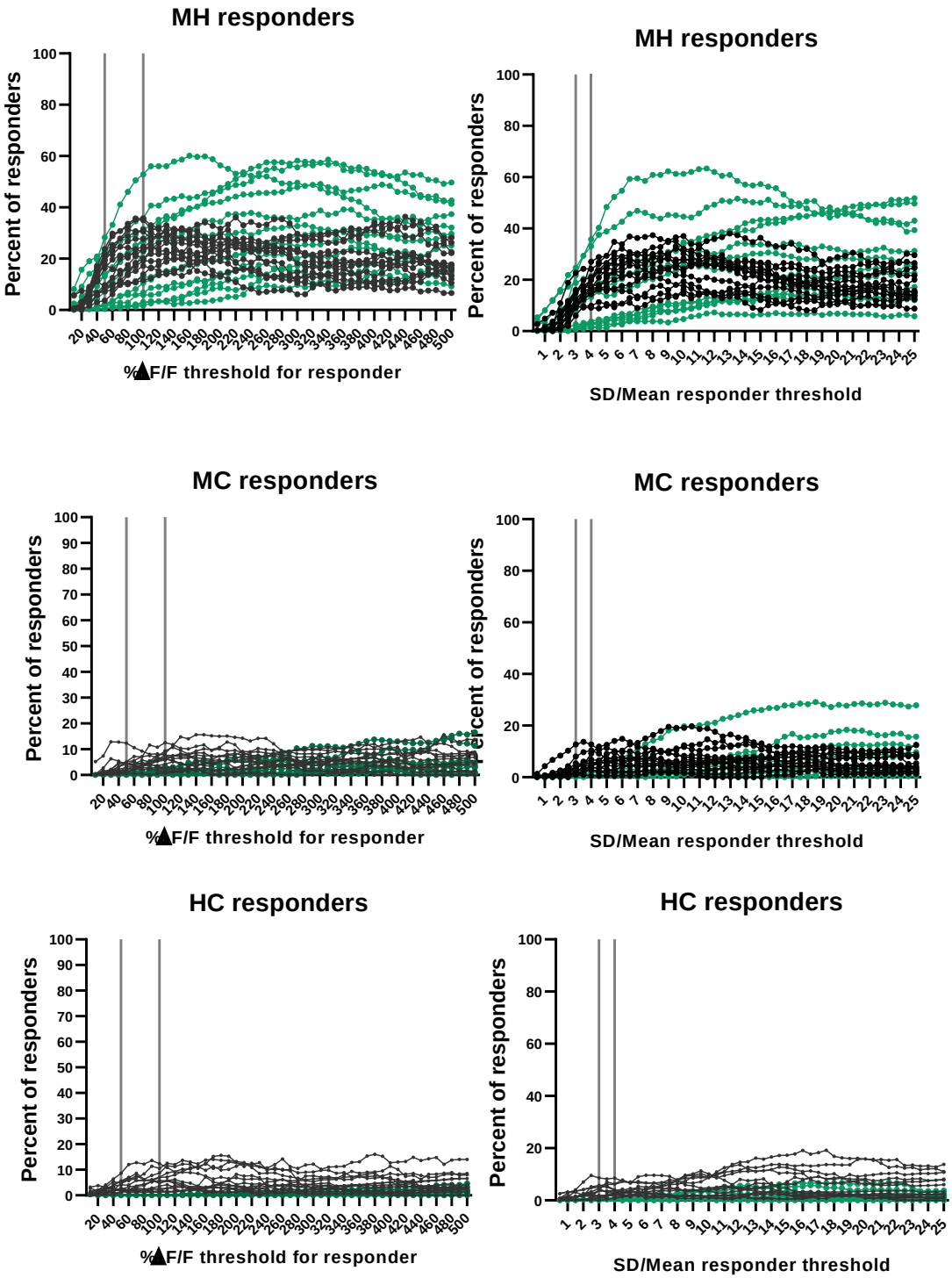

Black – Naïve; green – disinhibition (plotted as animals); SD/Mean should say z-score

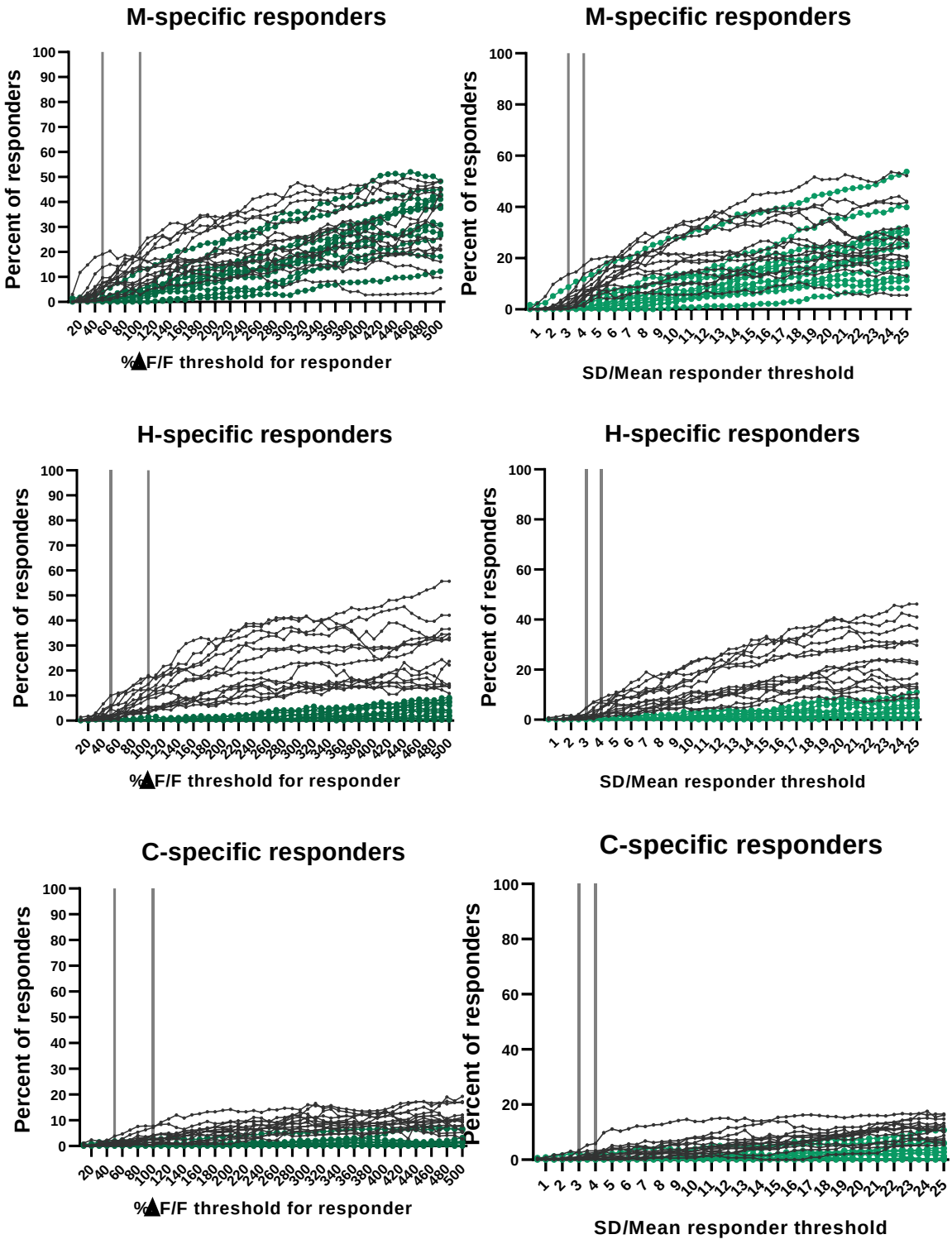

Black – Naïve; green – disinhibition (plotted as animals); SD/Mean should say z-score

Appendix B Supplemental Data Science

The next section shows the VBA tool that was developed to automate the generation of endpoints.

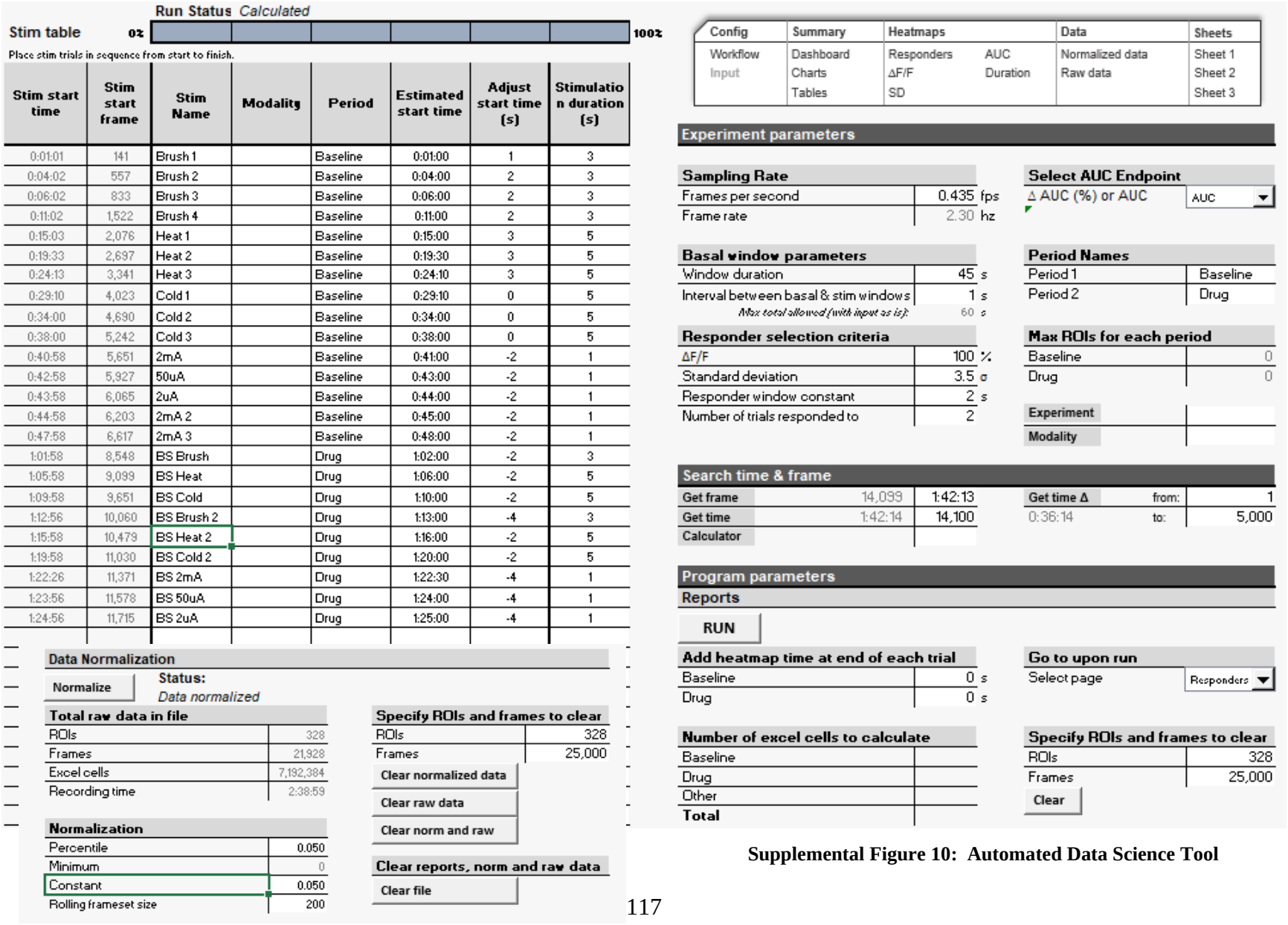

Supplemental Figure 10: Automated Data Science Tool

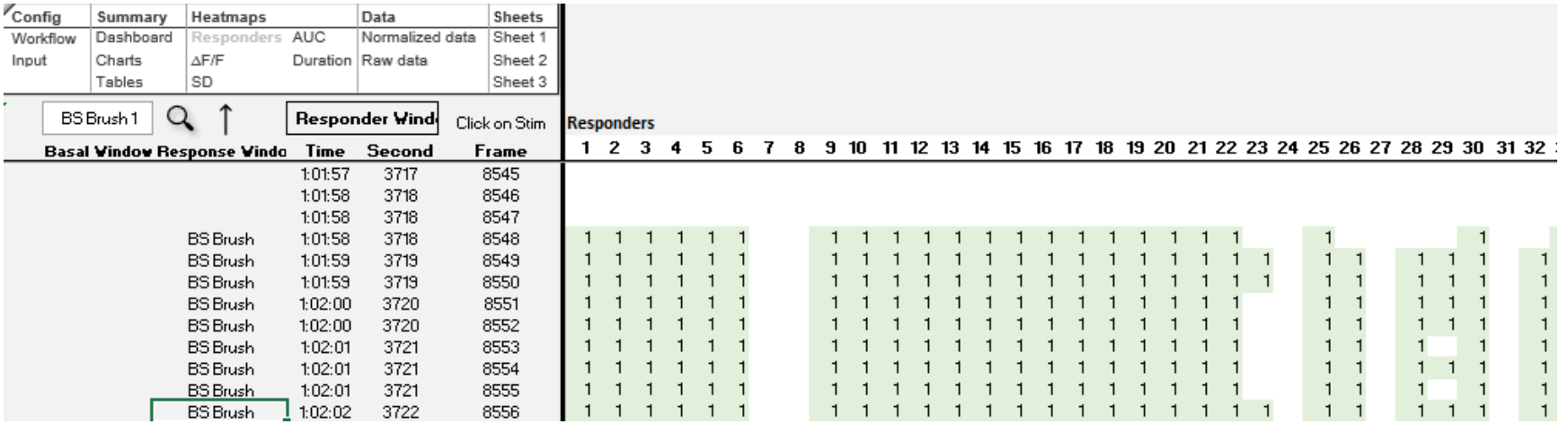

Config	Summary	Heatmaps		Data	Sheets
Workflow	Dashboard	Responders	AUC	Normalized data	Sheet 1
Input	Charts	ΔF/F	Duration	Raw data	Sheet 2
	Tables	SD			Sheet 3

BS Brush 1 | Responder Windo | Click on Stim

Basal Window	Response Windo	Time	Second	Frame	Responders 1	2	3	4	5	6	7	8	9	10	11	12	13	14	15	16	17	18	19	20	21	22	23	24	25	26	27	28	29	30	31	32
		1:01:57	3717	8545																																
		1:01:58	3718	8546																																
		1:01:58	3718	8547																																
	BS Brush	1:01:58	3718	8548	1	1	1	1	1	1			1	1	1	1	1	1	1	1	1	1	1	1	1			1						1		
	BS Brush	1:01:59	3719	8549	1	1	1	1	1	1			1	1	1	1	1	1	1	1	1	1	1	1	1	1	1	1	1	1		1	1	1	1	1	1
	BS Brush	1:01:59	3719	8550	1	1	1	1	1	1			1	1	1	1	1	1	1	1	1	1	1	1	1	1	1	1	1	1		1	1	1	1	1	1
	BS Brush	1:02:00	3720	8551	1	1	1	1	1	1			1	1	1	1	1	1	1	1	1	1	1	1	1	1	1	1		1	1		1	1	1	1	1
	BS Brush	1:02:00	3720	8552	1	1	1	1	1	1			1	1	1	1	1	1	1	1	1	1	1	1	1	1	1	1		1	1		1	1	1	1	1
	BS Brush	1:02:01	3721	8553	1	1	1	1	1	1			1	1	1	1	1	1	1	1	1	1	1	1	1	1	1	1		1	1		1		1	1	1
	BS Brush	1:02:01	3721	8554	1	1	1	1	1	1			1	1	1	1	1	1	1	1	1	1	1	1	1	1	1	1		1	1		1	1	1	1	1
	BS Brush	1:02:01	3721	8555	1	1	1	1	1	1			1	1	1	1	1	1	1	1	1	1	1	1	1	1	1	1		1	1		1		1	1	1
	BS Brush	1:02:02	3722	8556	1	1	1	1	1	1			1	1	1	1	1	1	1	1	1	1	1	1	1	1	1	1		1	1		1	1	1	1	1

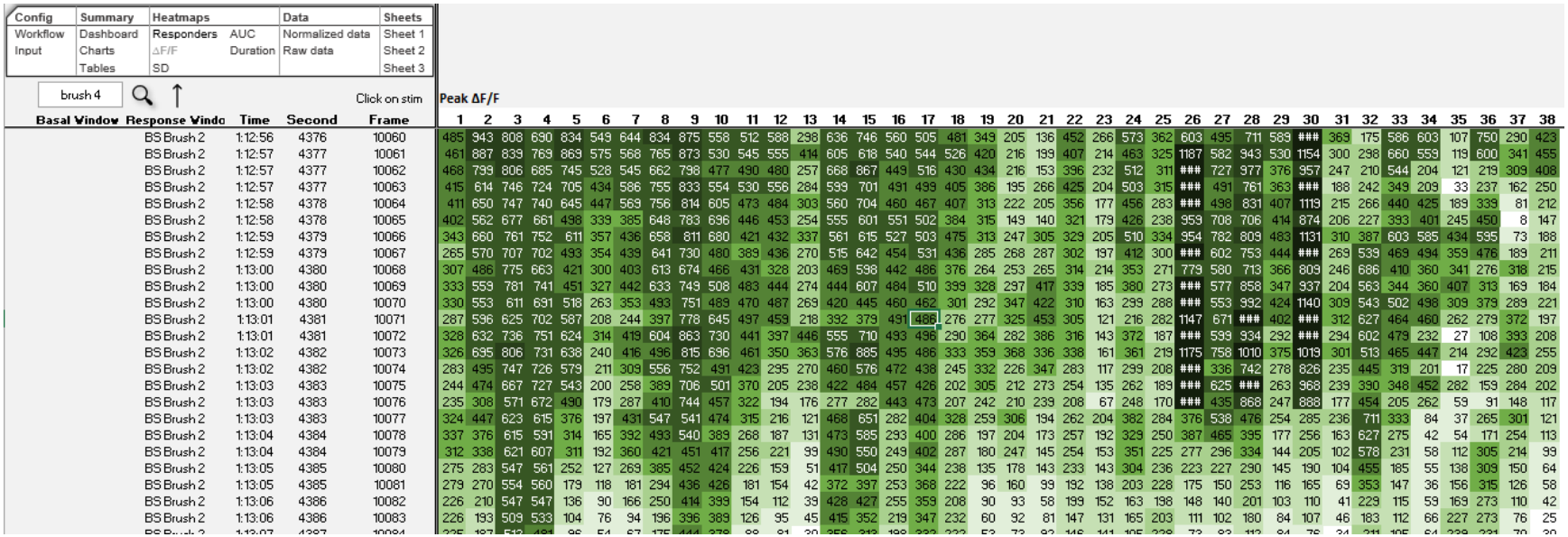

Config	Summary	Heatmaps		Data	Sheets
Workflow	Dashboard	Responders	AUC	Normalized data	Sheet 1
Input	Charts	ΔF/F	Duration	Raw data	Sheet 2
	Tables	SD			Sheet 3

brush 4 | Click on stim

Basal Window	Response Windo	Time	Second	Frame	Peak ΔF/F 1	2	3	4	5	6	7	8	9	10	11	12	13	14	15	16	17	18	19	20	21	22	23	24	25	26	27	28	29	30	31	32	33	34	35	36	37	38
	BS Brush 2	1:12:56	4376	10060	485	943	808	690	834	549	644	834	875	558	512	588	298	636	746	560	505	481	349	205	136	452	266	573	362	603	495	711	589	###	369	175	586	603	107	750	290	423
	BS Brush 2	1:12:57	4377	10061	461	887	839	769	869	575	568	765	873	530	545	555	414	605	618	540	544	526	420	216	199	407	214	463	325	1187	582	943	530	1154	300	298	660	559	119	600	341	455
	BS Brush 2	1:12:57	4377	10062	468	799	806	685	745	528	545	662	798	477	490	480	257	668	867	449	516	430	434	216	153	396	232	512	311	###	727	977	376	957	247	210	544	204	121	219	309	408
	BS Brush 2	1:12:57	4377	10063	415	614	746	724	705	434	586	755	833	554	530	556	284	599	701	491	493	405	386	195	266	425	204	503	315	###	491	761	363	###	188	242	349	209	33	237	162	250
	BS Brush 2	1:12:58	4378	10064	411	650	747	740	645	447	569	756	814	605	473	484	303	560	704	460	467	407	313	222	205	356	177	456	283	###	438	831	407	1119	215	266	440	425	189	339	81	212
	BS Brush 2	1:12:58	4378	10065	402	562	677	661	498	339	385	648	783	696	446	453	254	555	601	551	502	384	315	149	140	321	179	426	238	953	708	706	414	874	206	227	393	401	245	450	8	147
	BS Brush 2	1:12:59	4379	10066	343	660	761	752	611	357	436	658	811	680	421	432	337	561	615	527	503	475	313	247	305	329	205	510	334	954	782	809	483	1131	310	387	603	585	434	595	73	188
	BS Brush 2	1:12:59	4379	10067	265	570	707	702	493	354	439	641	730	480	389	436	270	515	642	454	531	436	285	268	287	302	197	412	300	###	602	753	444	###	269	539	469	494	359	476	189	211
	BS Brush 2	1:13:00	4380	10068	307	486	775	663	421	300	403	613	674	466	431	328	203	469	598	442	486	376	264	253	265	314	214	353	271	779	580	713	366	809	246	686	410	360	341	276	318	215
	BS Brush 2	1:13:00	4380	10069	333	559	781	741	451	327	442	633	749	508	483	444	274	444	607	484	510	399	328	297	417	339	185	380	273	###	577	858	347	937	204	563	344	360	407	313	169	184
	BS Brush 2	1:13:00	4380	10070	330	553	611	691	518	263	353	493	751	489	470	487	269	420	445	460	462	301	292	347	422	310	163	299	288	###	553	992	424	1140	309	543	502	498	309	379	289	221
	BS Brush 2	1:13:01	4381	10071	287	596	625	702	587	208	244	397	778	645	497	459	218	392	379	491	486	276	277	325	453	305	121	216	282	1147	671	###	402	###	312	627	464	460	262	279	372	197
	BS Brush 2	1:13:01	4381	10072	328	632	736	751	624	314	419	604	863	730	441	397	446	555	710	493	496	290	364	282	386	316	143	372	187	###	599	934	292	###	294	602	479	232	27	108	393	208
	BS Brush 2	1:13:02	4382	10073	326	695	806	731	638	240	416	496	815	696	461	350	363	576	885	495	486	333	359	368	336	338	161	361	219	1175	758	1010	375	1019	301	513	465	447	214	292	423	255
	BS Brush 2	1:13:02	4382	10074	283	495	747	726	579	211	309	556	752	491	423	295	270	460	576	472	438	245	332	226	347	283	117	299	208	###	336	742	278	826	235	445	319	201	17	225	280	209
	BS Brush 2	1:13:03	4383	10075	244	474	667	727	543	200	258	389	706	501	370	205	238	422	484	457	426	202	305	212	273	254	135	262	189	###	625	###	263	968	239	390	348	452	282	159	284	202
	BS Brush 2	1:13:03	4383	10076	235	308	571	672	490	179	287	410	744	457	322	194	176	277	282	443	473	207	242	210	239	208	67	248	170	###	435	868	247	888	177	454	205	262	59	91	148	117
	BS Brush 2	1:13:03	4383	10077	324	447	623	615	376	197	431	547	541	474	315	216	121	468	651	282	404	328	259	306	194	262	204	382	284	376	538	476	254	285	236	711	333	84	37	265	301	121
	BS Brush 2	1:13:04	4384	10078	337	376	615	591	314	165	392	493	540	389	268	187	131	473	585	293	400	286	197	204	173	257	192	329	250	387	465	395	177	256	163	627	275	42	54	171	254	113
	BS Brush 2	1:13:04	4384	10079	312	338	621	607	311	192	360	421	451	417	256	221	99	490	550	249	402	287	180	247	145	254	153	351	225	277	296	334	144	205	102	578	231	58	112	305	214	99
	BS Brush 2	1:13:05	4385	10080	275	283	547	561	252	127	269	385	452	424	226	159	51	417	504	250	344	238	135	178	143	233	143	304	236	223	227	290	145	190	104	455	185	55	138	309	150	64
	BS Brush 2	1:13:05	4385	10081	279	270	554	560	179	118	181	294	436	426	181	154	42	372	397	253	368	222	96	160	99	192	138	203	228	175	150	253	116	165	69	353	147	36	156	315	126	58
	BS Brush 2	1:13:06	4386	10082	226	210	547	547	136	90	166	250	414	399	154	112	39	428	427	255	359	208	90	93	58	199	152	163	198	148	140	201	103	110	41	229	115	59	169	273	110	42
	BS Brush 2	1:13:06	4386	10083	226	193	509	533	104	76	94	196	396	389	126	95	45	415	352	219	347	232	60	92	81	147	131	165	203	111	102	180	84	107	46	183	112	66	227	273	76	25

Supplemental Figure 10: Automated Data Science Tool Continued

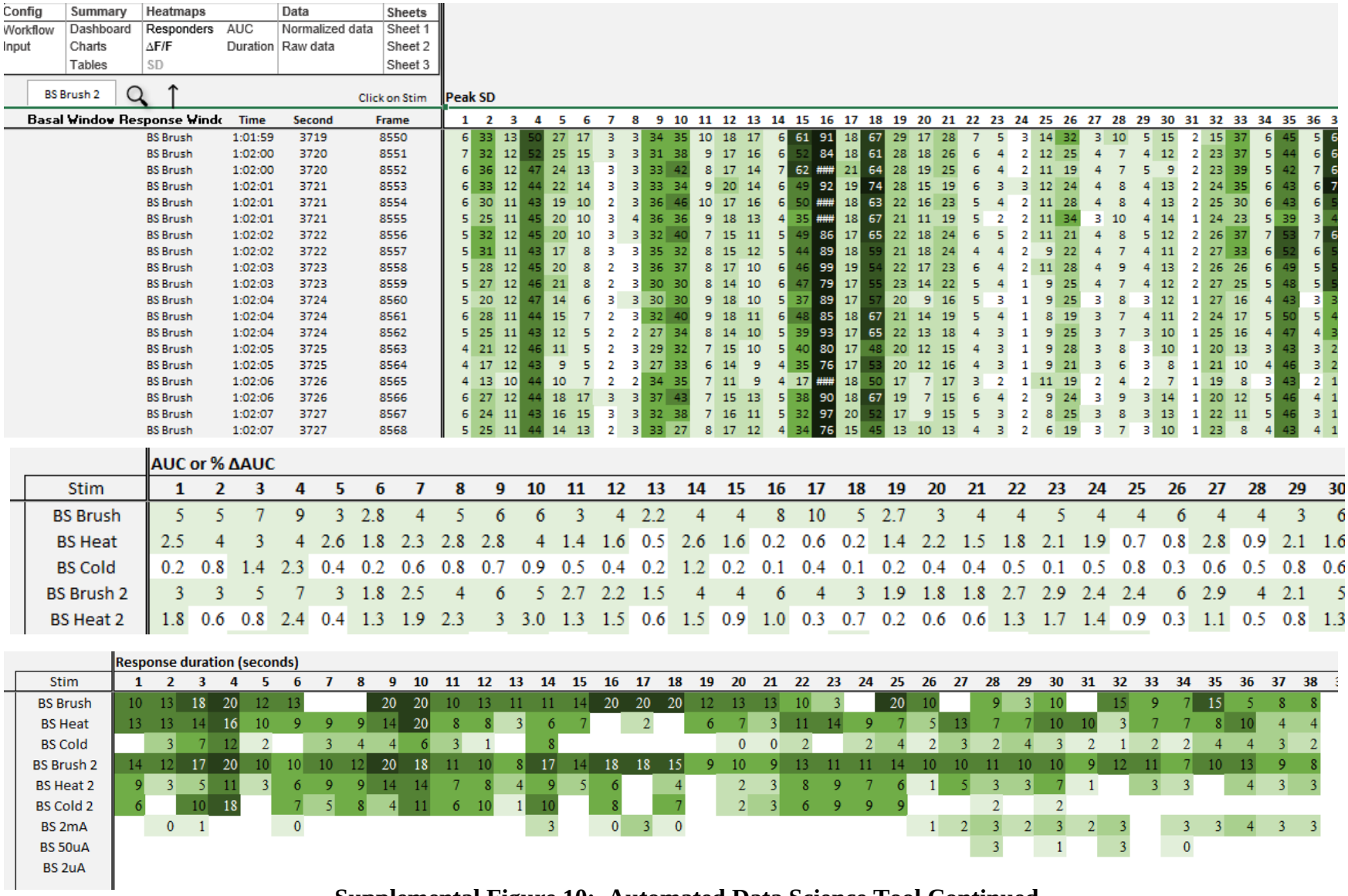

Config	Summary	Heatmaps		Data	Sheets
Workflow	Dashboard	Responders	AUC	Normalized data	Sheet 1
Input	Charts	ΔF/F	Duration	Raw data	Sheet 2
	Tables	SD			Sheet 3

BS Brush 2 — Click on Stim

Peak SD

Basal Window Response Windo	Time	Second	Frame	1	2	3	4	5	6	7	8	9	10	11	12	13	14	15	16	17	18	19	20	21	22	23	24	25	26	27	28	29	30	31	32	33	34	35	36	3
BS Brush	1:01:59	3719	8550	6	33	13	50	27	17	3	3	34	35	10	18	17	6	61	91	18	67	29	17	28	7	5	3	14	32	3	10	5	15	2	15	37	6	45	5	6
BS Brush	1:02:00	3720	8551	7	32	12	52	25	15	3	3	31	38	9	17	16	6	52	84	18	61	28	18	26	6	4	2	12	25	4	7	4	12	2	23	37	5	44	6	6
BS Brush	1:02:00	3720	8552	6	36	12	47	24	13	3	3	33	42	8	17	14	7	62	###	21	64	28	19	25	6	4	2	11	19	4	7	5	9	2	23	39	5	42	7	6
BS Brush	1:02:01	3721	8553	6	33	12	44	22	14	3	3	33	34	9	20	14	6	49	92	19	74	28	15	19	6	3	3	12	24	4	8	4	13	2	24	35	6	43	6	7
BS Brush	1:02:01	3721	8554	6	30	11	43	19	10	2	3	36	46	10	17	16	6	50	###	18	63	22	16	23	5	4	2	11	28	4	8	4	13	2	25	30	6	43	6	5
BS Brush	1:02:01	3721	8555	5	25	11	45	20	10	3	4	36	36	9	18	13	4	35	###	18	67	21	11	19	5	2	2	11	34	3	10	4	14	1	24	23	5	39	3	4
BS Brush	1:02:02	3722	8556	5	32	12	45	20	10	3	3	32	40	7	15	11	5	49	86	17	65	22	18	24	6	5	2	11	21	4	8	5	12	2	26	37	7	53	7	6
BS Brush	1:02:02	3722	8557	5	31	11	43	17	8	3	3	35	32	8	15	12	5	44	89	18	59	21	18	24	4	4	2	9	22	4	7	4	11	2	27	33	6	52	6	5
BS Brush	1:02:03	3723	8558	5	28	12	45	20	8	2	3	36	37	8	17	10	6	46	99	19	54	22	17	23	6	4	2	11	28	4	9	4	13	2	26	26	6	49	5	5
BS Brush	1:02:03	3723	8559	5	27	12	46	21	8	2	3	30	30	8	14	10	6	47	79	17	55	23	14	22	5	4	1	9	25	4	7	4	12	2	27	25	5	48	5	5
BS Brush	1:02:04	3724	8560	5	20	12	47	14	6	3	3	30	30	9	18	10	5	37	89	17	57	20	9	16	5	3	1	9	25	3	8	3	12	1	27	16	4	43	3	3
BS Brush	1:02:04	3724	8561	6	28	11	44	15	7	2	3	32	40	9	18	11	6	48	85	18	67	21	14	19	5	4	1	8	19	3	7	4	11	2	24	17	5	50	5	4
BS Brush	1:02:04	3724	8562	5	25	11	43	12	5	2	2	27	34	8	14	10	5	39	93	17	65	22	13	18	4	3	1	9	25	3	7	3	10	1	25	16	4	47	4	3
BS Brush	1:02:05	3725	8563	4	21	12	46	11	5	2	3	29	32	7	15	10	5	40	80	17	48	20	12	15	4	3	1	9	28	3	8	3	10	1	20	13	3	43	3	2
BS Brush	1:02:05	3725	8564	4	17	12	43	9	5	2	3	27	33	6	14	9	4	35	76	17	53	20	12	16	4	3	1	9	21	3	6	3	8	1	21	10	4	46	3	2
BS Brush	1:02:06	3726	8565	4	13	10	44	10	7	2	2	34	35	7	11	9	4	17	###	18	50	17	7	17	3	2	1	11	19	2	4	2	7	1	19	8	3	43	2	1
BS Brush	1:02:06	3726	8566	6	27	12	44	18	17	3	3	37	43	7	15	13	5	38	90	18	67	19	7	15	6	4	2	9	24	3	9	3	14	1	20	12	5	46	4	1
BS Brush	1:02:07	3727	8567	6	24	11	43	16	15	3	3	32	38	7	16	11	5	32	97	20	52	17	9	15	5	3	2	8	25	3	8	3	13	1	22	11	5	46	3	1
BS Brush	1:02:07	3727	8568	5	25	11	44	14	13	2	3	33	27	8	17	12	4	34	76	15	45	13	10	13	4	3	2	6	19	3	7	3	10	1	23	8	4	43	4	1

AUC or % ΔAUC

Stim	1	2	3	4	5	6	7	8	9	10	11	12	13	14	15	16	17	18	19	20	21	22	23	24	25	26	27	28	29	30
BS Brush	5	5	7	9	3	2.8	4	5	6	6	3	4	2.2	4	4	8	10	5	2.7	3	4	4	5	4	4	6	4	4	3	6
BS Heat	2.5	4	3	4	2.6	1.8	2.3	2.8	2.8	4	1.4	1.6	0.5	2.6	1.6	0.2	0.6	0.2	1.4	2.2	1.5	1.8	2.1	1.9	0.7	0.8	2.8	0.9	2.1	1.6
BS Cold	0.2	0.8	1.4	2.3	0.4	0.2	0.6	0.8	0.7	0.9	0.5	0.4	0.2	1.2	0.2	0.1	0.4	0.1	0.2	0.4	0.4	0.5	0.1	0.5	0.8	0.3	0.6	0.5	0.8	0.6
BS Brush 2	3	3	5	7	3	1.8	2.5	4	6	5	2.7	2.2	1.5	4	4	6	4	3	1.9	1.8	1.8	2.7	2.9	2.4	2.4	6	2.9	4	2.1	5
BS Heat 2	1.8	0.6	0.8	2.4	0.4	1.3	1.9	2.3	3	3.0	1.3	1.5	0.6	1.5	0.9	1.0	0.3	0.7	0.2	0.6	0.6	1.3	1.7	1.4	0.9	0.3	1.1	0.5	0.8	1.3

Response duration (seconds)

Stim	1	2	3	4	5	6	7	8	9	10	11	12	13	14	15	16	17	18	19	20	21	22	23	24	25	26	27	28	29	30	31	32	33	34	35	36	37	38
BS Brush	10	13	18	20	12	13			20	20	10	13	11	11	14	20	20	20	12	13	13	10	3		20	10		9	3	10		15	9	7	15	5	8	8
BS Heat	13	13	14	16	10	9	9	9	14	20	8	8	3	6	7		2		6	7	3	11	14	9	7	5	13	7	7	10	10	3	7	7	8	10	4	4
BS Cold		3	7	12	2		3	4	4	6	3	1		8							0	0	2		2	4	2	3	2	4	3	2	1	2	2	4	4	3	2
BS Brush 2	14	12	17	20	10	10	10	12	20	18	11	10	8	17	14	18	18	15	9	10	9	13	11	11	14	10	10	11	10	10	9	12	11	7	10	13	9	8
BS Heat 2	9	3	5	11	3	6	9	9	14	14	7	8	4	9	5	6		4		2	3	8	9	7	6	1	5	3	3	7	1		3	3		4	3	3
BS Cold 2	6		10	18		7	5	8	4	11	6	10	1	10		8		7		2	3	6	9	9	9			2		2								
BS 2mA		0	1			0								3		0	3	0								1	2	3	2	3	2	3		3	3	4	3	3	
BS 50uA																												3		1		3		0				
BS 2uA																																						

Supplemental Figure 10: Automated Data Science Tool Continued

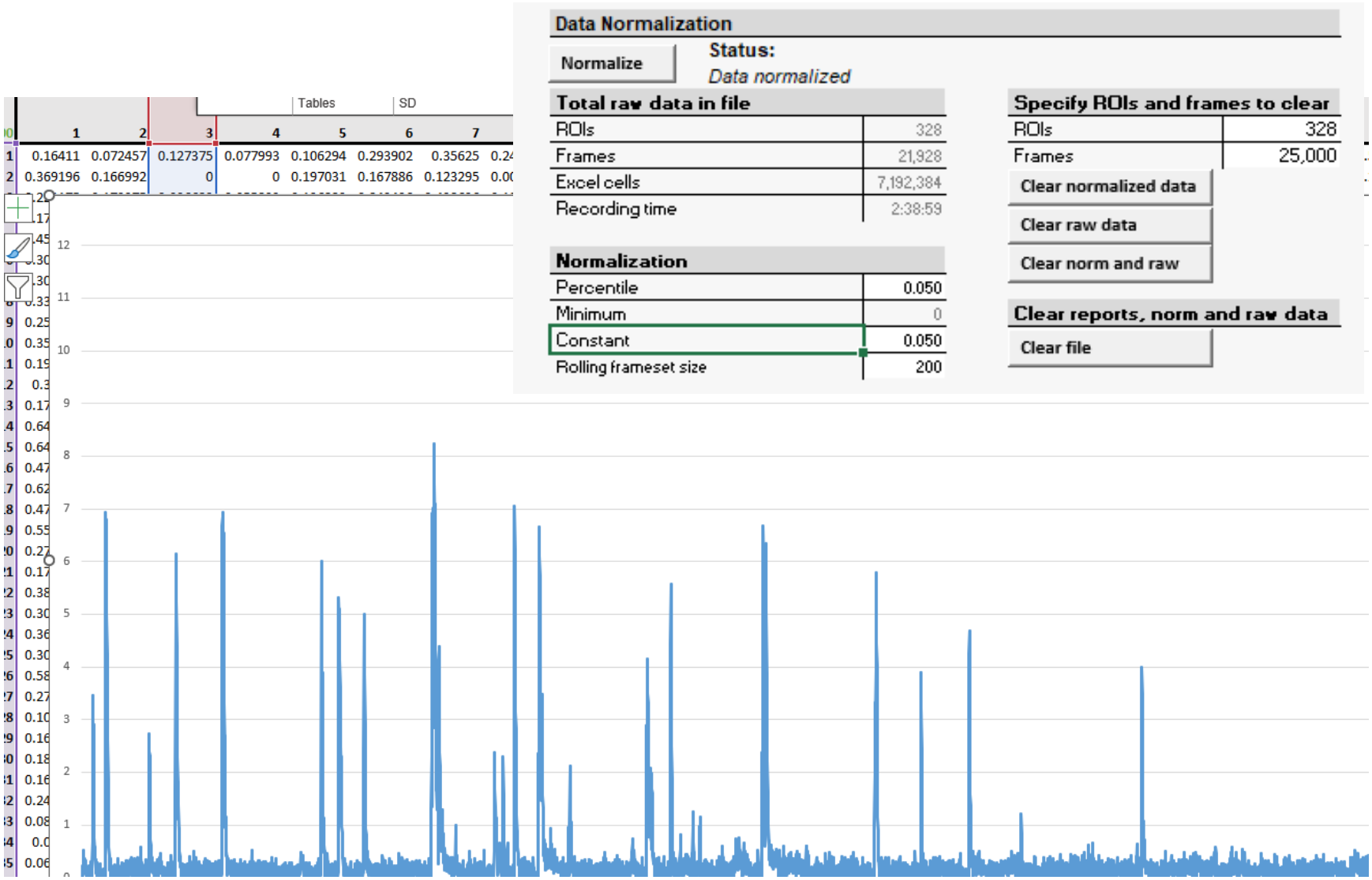

Supplemental Figure 10: Automated Data Science Tool Continued

Appendix C Data Science Code

```
'Pre-stimulus window validation. The prestim window frames should not overlap with the frames of the response window of the prior stim.
'
 Dim row1 As Integer, row2 As Integer, frame_col As String, responder_col As String, colrow1 As String
 Dim colrow2 As String, colrow1_responder As String
 Dim basal_duration As Integer, basal_constant As Integer, FR As Variant, FPS As Variant
 Dim colrow1_value As Integer, colrow2_value As Integer, colrow_responder_value As Integer
 frame_col = "E"
 responder_col = "M"
 FR = Sheets("Input").Range("P11").Value
 FPS = Sheets("Input").Range("P10").Value
 basal_duration = Sheets("Input").Range("P14").Value * FR
 basal_constant = Sheets("Input").Range("P15").Value * FR

    If Sheets("input").Range("E8") > 0 Then

        For row1 = 8 To 107

            row2 = row1 + 1
            colrow1 = frame_col + CStr(row1)
            colrow2 = frame_col + CStr(row2)
            colrow1_responder = responder_col + CStr(row1)

            colrow1_value = Sheets("Input").Range(colrow1).Value
            colrow2_value = Sheets("Input").Range(colrow2).Value
            colrow1_responder_value = Sheets("Input").Range(colrow1_responder).Value * FR

            If colrow2_value < 1 Or IsEmpty(Sheets("input").Range(colrow2)) Then Exit For
            '
            If colrow2_value - basal_duration - basal_constant < colrow1_value + colrow1_responder_value Then
                Call Basal_window_error
                Exit Sub
            End If
            '
        Next row1

    End If
```

```
Sub protect()

Dim ws As Worksheet
    For Each ws In ThisWorkbook.Worksheets
        If ws.Name = "Input" Or ws.Name = "Responders" Or ws.Name = "Percent" Or ws.Name = "SD"
            ws.protect Password:="vba", UserInterfaceOnly:=True
        End If
Next ws

End Sub
```

```
Sub Run()
'
Call protect
Sheets("input").Select

'DATA VALIDATION
    'Main table should be filled out with at least one stimulation
    If Sheets("Input").Range("D8").Value = 0 Or IsEmpty(Sheets("Input").Range("E8")) Then
        Call Run_error
        Exit Sub
    End If
    '
    'Number of ROIs should be between 1 and 328

        If Sheets("input").Range("AL9") < 1 Or Sheets("input").Range("AL10") > 328 Then
            Call ROI_error
            Exit Sub
        End If

    'Any stim trial's ROIs should be equal to or less than total ROIs in file
    'Dim cells As Range
   ' For Each cells In Sheets("input").Range("G8:G107")
        'If cells.Value > Sheets("input").Range("P57") Then
            'Call maxROI_error
            'Exit Sub
       ' End If
   ' Next cells


    'Number of frames should be less than 25000
    If Sheets("Input").Range("AL8").Value > 25000 Then
        Call maxframes_error
        Exit Sub
    End If


    'Basal window should start after time 0
        If Sheets("input").Range("E8") > 0 Then
            If Sheets("Input").Range("AH8").Value < 0 Then
                Call Basal_window_error2
                Exit Sub
            End If
        End If
```

```
    '
    'Stim trials cannot have the same name
    'Dim dup As Integer
    'Dim tname As String
    'Dim dup_tname As String
    'Dim dup_value As String
    'tname = "F"
        'For dup = 8 To 107
            'dup_tname = tname + CStr(dup)
            'dup_value = Sheets("input").Range(dup_tname).Value
        'Next dup
        'For Each cell In Sheets("input").Range("F8:F107")

    Dim Cell As Variant
    Dim Source As Range
    Set Source = Sheets("input").Range("F8:F107")
    For Each Cell In Source
     If Application.WorksheetFunction.CountIf(Source, Cell) > 1 Then
        Call duptrial_error
        Exit Sub
     End If
    Next Cell



    'Period 1 should end before period 2
    If Sheets("Input").Range("AP10").Value > 0 And Sheets("Input").Range("AP15").Value > 0 Then
        If Sheets("Input").Range("AP10").Value >= Sheets("Input").Range("AP15").Value Then
            Call period_frame_error
            Exit Sub
        End If
    End If

    'If there's only 1 period, it should be placed in period 1 not period 2
    If IsEmpty(Sheets("input").Range("U14")) And Not IsEmpty(Sheets("input").Range("U15")) Then
        Call period_frame_error2
        Exit Sub
    End If
    '
    'Period 1 and period 2 cannot have the same name
    If Sheets("input").Range("U14").Value = Sheets("input").Range("U15").Value Then
        Call period_frame_error3
        Exit Sub
    End If
    '
    'Data should be normalized before run
    If Sheets("input").Range("O45").Value <> CStr(" Data normalized") Then
        Call datanotnorm
        Exit Sub
    End If


'Reset previously calculated data
'
'
    If Not IsEmpty(Sheets("Input").Range("G3")) Then
        Sheets("Input").Range("G3").FormulaR1C1 = " Clearing Data..."
    Call reset_new
    End If

''
'Run Status start
'
'
    Sheets("Input").Range("G3").FormulaR1C1 = " In Progress"
    Sheets("Input").Range("G3").FormulaR1C1 = " In Progress."
    Sheets("Input").Range("G3").FormulaR1C1 = " In Progress.."
    Sheets("Input").Range("G3").FormulaR1C1 = " In Progress..."

'''
```

```
'GLOBAL DEFINITIONS
'
'
        Dim r As Integer, c As String, c2 As String, cr As String, max As Integer, max2 As Integer
        Dim Beg_st As Integer, Beg_end As Integer, Btwn_st As Integer, Btwn_end As Integer, Beg As String
        Dim Btwn As String
        Dim trial_st As String, trial_end As String, trial_st_v As String, trial_end_v As String, col2_st As String
        Dim col2_end As String, trial_CR As String
        Dim trial_st2 As String, trial_end2 As String, trial_st_v2 As String, trial_end_v2 As String, col3_st As String
        Dim col3_end As String, trial_CR2 As String, trial_RR_done As String
        Dim hrow As Integer, hCR As String
        Dim trial_CR3 As String
        Dim master As Integer, master_rng As String
        Dim hCR_st As String, hCR_stf As String
        '
        '
        '
        Beg_st = 111
        Beg_end = 109 + Sheets("input").Range("AH8").Value
        'Btwn_st = 114 + Sheets("input").Range("P35").Value
        'Btwn_end = 109 + Sheets("input").Range("P40").Value
        Beg = CStr(Beg_st) + ":" + CStr(Beg_end)
        'Btwn = CStr(Btwn_st) + ":" + CStr(Btwn_end)
        col_st = "B"
        col_end = "N"
        '
        col2_st = "AH"
        col2_end = "AI"
        '
        col3_st = "E"
        col3_end = "AJ"
        '
        '
        '
        c = "C"
        c2 = "D"
        max = Sheets("Input").Range("A6").Value + 4
        max2 = Sheets("Input").Range("P26").Value
        '
'
```

```
PERCENT CHANGE

    '
    'LEFT PANEL
    '

    'Sheets("percent").Range(Sheets("input").Range("AM10")) = Sheets("AUC").Range(Sheets("input").Range("AM10")).Value
    'Sheets("percent").Range(Sheets("input").Range("AM10")).Value = Sheets("percent").Range(Sheets("input").Range("AM10")).Value

    Sheets("Percent").Range("H111").Value = "=1"
    Sheets("Percent").Range(Sheets("input").Range("AM11")).FormulaR1C1 = "=R[-1]C + 1"
    Sheets("Percent").Range(Sheets("input").Range("AM11")).Value = Sheets("Percent").Range(Sheets("input").Range("AM11")).Value

    'For hrow = 8 To 107
        'hCR = "AN" + CStr(hrow)
       'hCR_st = "AT" + CStr(hrow)
        'hCR_stf = "E" + CStr(hrow)
        'If Len(Sheets("input").Range(hCR)) = 0 Then Exit For
        'Sheets("Percent").Range(Sheets("input").Range(hCR_st)).Value = Sheets("input").Range(hCR_stf).Value
        ''Sheets("Percent").Range(Sheets("input").Range(hCR)).FormulaR1C1 = "=R[-1]C + 1"
        'Sheets("Percent").Range(Sheets("input").Range(hCR)).Value = Sheets("Percent").Range(Sheets("input").Range(hCR)).Value
    'Next hrow


    Sheets("percent").Range(Sheets("Input").Range("A7")).FormulaR1C1 = "=RC[1]*Input!R10C16"
    Sheets("percent").Range(Sheets("Input").Range("A7")).Value = Sheets("percent").Range(Sheets("Input").Range("A7")).Value
    '
    Sheets("percent").Range(Sheets("Input").Range("A8")).FormulaR1C1 = "=RC[1]/86400"
    Sheets("percent").Range(Sheets("Input").Range("A8")).Value = Sheets("percent").Range(Sheets("Input").Range("A8")).Value
    '
    Sheets("percent").Range(Sheets("Input").Range("A9")).FormulaR1C1 = "=VLOOKUP(RC[5],INDIRECT(""Input!$E$8:$F$""&Input!R18C1),2,1)"
    Sheets("percent").Range(Sheets("Input").Range("A9")).Value = Sheets("percent").Range(Sheets("Input").Range("A9")).Value
    '
    Sheets("percent").Range(Sheets("Input").Range("A10")).FormulaR1C1 = "=INDIRECT(""C""&SUM(ROW(RC),ROUNDUP(Input!R14C16/Input!R10C16,0)
    Sheets("percent").Range(Sheets("Input").Range("A10")).Value = Sheets("percent").Range(Sheets("Input").Range("A10")).Value
    '
    'TOP PANEL
    '
    'Sheets("percent").Range("I5:IA104").FormulaR1C1 = "=AVERAGE(INDIRECT(""raw!""&R107C&""""&RC6&"":""&R107C&""""&RC7))"
    'Sheets("percent").Range("J5:IA5").Value = Sheets("percent").Range("J5:IA5").Value
    'Sheets("percent").Range("I6:IA104").Value = Sheets("percent").Range("I6:IA104").Value
    '
    '
    '
        For r = 5 To 104
            cr = c + CStr(r)
            If r > max Then Exit For
            Sheets("Percent").Range(Sheets("Percent").Range(cr)).FormulaR1C1 = "=AVERAGE(INDIRECT(""raw!""&R107C&""""&RC6&"":""&R107C&""'
        Next r
```

```
'HEAT MAP
'
'
'Sheets("percent").Range(Sheets("Input").Range("A4")).FormulaR1C1 = "=((raw!RC-(VLOOKUP(RC2,R5C8:R104C336,R108C,0)))/(VLOOKUP(RC2,R5
'Sheets("percent").Range(Sheets("Input").Range("A5")).FormulaR1C1 = "=((raw!RC-(VLOOKUP(RC2,R5C8:R104C336,R108C,0)))/(VLOOKUP(RC2,R5

For hrow = 8 To 107
hCR = "AF" + CStr(hrow)
    If Len(Sheets("input").Range(hCR)) = 0 Then Exit For
    'If mean basal fluorescence is 0, make the percent change 0 as you can't divide by 0.
Sheets("percent").Range(Sheets("Input").Range(hCR)).FormulaR1C1 = "=IF(VLOOKUP(RC2,R5C8:R104C336,R108C,0)=0,0,"
((raw!RC-(VLOOKUP(RC2,R5C8:R104C336,R108C,0)))/(VLOOKUP(RC2,R5C8:R104C336,R108C,0)))*100)"
Sheets("percent").Range(Sheets("Input").Range(hCR)).Value = Sheets("percent").Range(Sheets("Input").Range(hCR)).Value
Next hrow

'
'Run Status 1
 Sheets("Input").Range("G3").FormulaR1C1 = " In Progress"
 Sheets("Input").Range("G3").FormulaR1C1 = " In Progress."
 Sheets("Input").Range("G3").FormulaR1C1 = " In Progress.."
 Sheets("Input").Range("G3").FormulaR1C1 = " In Progress..."
'
With Sheets("Input").Range("F4").Interior
    .Pattern = xlSolid
    .PatternColorIndex = xlAutomatic
    .Color = 12626844
    .TintAndShade = 0
    .PatternTintAndShade = 0
End With
'
'Change formula to value
'Sheets("percent").Range(Sheets("Input").Range("A4")).Value = Sheets("percent").Range(Sheets("Input").Range("A4")).Value
'Sheets("percent").Range(Sheets("Input").Range("A5")).Value = Sheets("percent").Range(Sheets("Input").Range("A5")).Value
'
'
'
'For heatmap, hide rows between stim trials
'
'Sheets("Percent").Rows(Beg).group
'Sheets("Percent").Rows(Beg_st).ShowDetail = False
Sheets("Percent").Rows(Beg).entirerow.Hidden = True
'Sheets("Percent").Rows(Btwn).group
'Sheets("Percent").Rows(Btwn_st).ShowDetail = False
'
```

```
'For heatmaps, on left panel, specify which rows are basal and stim
'
Sheets("Percent").Range("B111:B25000").ClearContents
Sheets("Percent").Range("C111:C25000").ClearContents


For trial_row = 8 To 107
    '
    trial_st = col2_st + CStr(trial_row)
    trial_end = col2_end + CStr(trial_row)
    trial_st_v = 110 + Sheets("input").Range(trial_st).Value
    trial_end_v = 110 + Sheets("input").Range(trial_end).Value
    '
            If trial_end_v = 110 Then Exit For
    '
    trial_st2 = col3_st + CStr(trial_row)
    trial_end2 = col3_end + CStr(trial_row)
    trial_st_v2 = 110 + Sheets("input").Range(trial_st2).Value
    trial_end_v2 = 110 + Sheets("input").Range(trial_end2).Value
    '
            If trial_end_v2 = 110 Then Exit For
    '
    trial_CR = "B" + CStr(trial_st_v) + ":" + "B" + CStr(trial_end_v)
    trial_CR2 = "C" + CStr(trial_st_v2) + ":" + "C" + CStr(trial_end_v2)
    '
    Sheets("percent").Range(trial_CR) = Sheets("input").Range("F" + CStr(trial_row)).Value
    Sheets("percent").Range(trial_CR2) = Sheets("input").Range("F" + CStr(trial_row)).Value
    '
    '
    '
    trial_CR3 = "A" + CStr(trial_st_v) + ":" + "H" + CStr(trial_st_v)
    '
    With Sheets("percent").Range(trial_CR3).Interior
    .Pattern = xlSolid
    .PatternColorIndex = xlAutomatic
    .ThemeColor = xlThemeColorLight1
    .TintAndShade = 4.99893185216834E-02
    .PatternTintAndShade = 0
    End With
    With Sheets("percent").Range(trial_CR3).Font
    .ThemeColor = xlThemeColorDark1
    .TintAndShade = 0
    End With
    '
    '
Next trial_row
```

```
STANDARD DEVIATION

    '
    'LEFT PANEL
    '
    'Sheets("SD").Range(Sheets("input").Range("AM10")) = Sheets("AUC").Range(Sheets("input").Range("AM10")).Value
    'Sheets("SD").Range(Sheets("input").Range("AM10")).Value = Sheets("SD").Range(Sheets("input").Range("AM10")).Value
    '
    Sheets("SD").Range("H111").Value = "=1"
    Sheets("SD").Range(Sheets("input").Range("AM11")).FormulaR1C1 = "=R[-1]C + 1"
    Sheets("SD").Range(Sheets("input").Range("AM11")).Value = Sheets("SD").Range(Sheets("input").Range("AM11")).Value
    '
    Sheets("SD").Range(Sheets("Input").Range("A7")).FormulaR1C1 = "=RC[1]*Input!R10C16"
    Sheets("SD").Range(Sheets("Input").Range("A7")).Value = Sheets("SD").Range(Sheets("Input").Range("A7")).Value
    '
    Sheets("SD").Range(Sheets("Input").Range("A8")).FormulaR1C1 = "=RC[1]/86400"
    Sheets("SD").Range(Sheets("Input").Range("A8")).Value = Sheets("SD").Range(Sheets("Input").Range("A8")).Value
    '
    Sheets("SD").Range(Sheets("Input").Range("A9")).FormulaR1C1 = "=VLOOKUP(RC[5],INDIRECT(""Input!$E$8:$F$""&Input!R18C1),2,1)"
    Sheets("SD").Range(Sheets("Input").Range("A9")).Value = Sheets("SD").Range(Sheets("Input").Range("A9")).Value
    '
    'For Each cell In Sheets("SD").Range(Sheets("Input").Range("A9"))
        'If IsError(cell.Value) Then
        'cell.ClearContents
    'End If
    'Next cell
    '
    '
    '
    Sheets("SD").Range(Sheets("Input").Range("A10")).FormulaR1C1 = "=INDIRECT(""C""&SUM(ROW(RC),ROUNDUP(Input!R14C16/Input!R10C16,
    Sheets("SD").Range(Sheets("Input").Range("A10")).Value = Sheets("SD").Range(Sheets("Input").Range("A10")).Value
    '
    'For Each cell In Sheets("SD").Range(Sheets("Input").Range("A10"))
        'If IsError(cell.Value) Then
        'cell.ClearContents
    'End If
    'Next cell
    '
    '
    '
    'For Each cell In Sheets("SD").Range(Sheets("Input").Range("A10"))
        'If IsError(cell.Value) Then
        'cell.ClearContents
    'End If
    'Next cell
    '
    .
```

```
'TOP PANEL
'
'Sheets("SD").Range("I5:IA104").FormulaR1C1 = "=STDEV.S(INDIRECT(""raw!""&R107C&""""&RC6&"":""&R107C&""""&RC7))"
'Sheets("SD").Range("J5:IA5").Value = Sheets("SD").Range("J5:IA5").Value
'Sheets("SD").Range("I6:IA104").Value = Sheets("SD").Range("I6:IA104").Value
'
'
    For r = 5 To 104
        cr = c + CStr(r)
        If r > max Then Exit For
        Sheets("SD").Range(Sheets("SD").Range(cr)).FormulaR1C1 = "=STDEV.S(INDIRECT(""raw!""&R107C&""""&RC6&"":"'
    Next r


    'Count how many instances in which an ROI has a basal period that flat-lined and therefore have a SD of 0.
    Set Source2 = Sheets("SD").Range("I5:LX107")
    Dim SDzero As Integer
    SDzero = Application.WorksheetFunction.CountIf(Source2, 0)

'
'
'HEAT MAP
'
'
'
'Sheets("SD").Range(Sheets("Input").Range("A4")).FormulaR1C1 = "=((raw!RC-(VLOOKUP(RC2,Percent!R5C8:R104C336,R108
'Sheets("SD").Range(Sheets("Input").Range("A5")).FormulaR1C1 = "=((raw!RC-(VLOOKUP(RC2,Percent!R5C8:R104C336,R108
'


For hrow = 8 To 107
hCR = "AF" + CStr(hrow)
    If Len(Sheets("input").Range(hCR)) = 0 Then Exit For
'If SD of basal fluorescence is 0, make the number of SD over mean basal 0 as you can't divide by 0.
Sheets("SD").Range(Sheets("Input").Range(hCR)).FormulaR1C1 = "=IF(VLOOKUP(RC2,R5C8:R104C336,R108C,0)=0,0,((raw!RC
Sheets("SD").Range(Sheets("Input").Range(hCR)).Value = Sheets("SD").Range(Sheets("Input").Range(hCR)).Value
Next hrow




'Run Status 3
 Sheets("Input").Range("G3").FormulaR1C1 = " In Progress"
 Sheets("Input").Range("G3").FormulaR1C1 = " In Progress."
 Sheets("Input").Range("G3").FormulaR1C1 = " In Progress.."
 Sheets("Input").Range("G3").FormulaR1C1 = " In Progress..."
'
With Sheets("Input").Range("H4").Interior
    .Pattern = xlSolid
    .PatternColorIndex = xlAutomatic
    .Color = 12626844
    .TintAndShade = 0
    .PatternTintAndShade = 0
End With
'
```

```
'For heatmap, hide rows between stim trials
'
'Sheets("SD").Rows(Beg).group
'Sheets("SD").Rows(Beg_st).ShowDetail = False
Sheets("SD").Rows(Beg).entirerow.Hidden = True
    'Sheets("SD").Rows(Btwn).group
    'Sheets("SD").Rows(Btwn_st).ShowDetail = False
'
For trial_row = 8 To 107
'
    trial_st = col_st + CStr(trial_row)
    trial_end = col_end + CStr(trial_row)
    trial_st_v = 109 + Sheets("input").Range(trial_st).Value
    trial_end_v = 109 + Sheets("input").Range(trial_end).Value
    trial_RR_done = CStr(trial_st_v) + ":" + CStr(Sheets("input").Range("AM8"))
            If trial_end_v = 109 Then
                'Sheets("SD").Rows(trial_RR_done).group
                'Sheets("SD").Rows(trial_st_v).ShowDetail = False
                Sheets("SD").Rows(trial_RR_done).entirerow.Hidden = True
                Exit For
            End If
    trial_RR = CStr(trial_st_v) + ":" + CStr(trial_end_v)
    'Sheets("SD").Rows(trial_RR).group
    'Sheets("SD").Rows(trial_st_v).ShowDetail = False
    Sheets("SD").Rows(trial_RR).entirerow.Hidden = True

Next trial_row
'
'
'
'For heatmaps, on left panel, specify which rows are basal and stim
'
Sheets("SD").Range("B111:B25000").ClearContents
Sheets("SD").Range("C111:C25000").ClearContents


For trial_row = 8 To 107
    '
    trial_st = col2_st + CStr(trial_row)
    trial_end = col2_end + CStr(trial_row)
    trial_st_v = 110 + Sheets("input").Range(trial_st).Value
    trial_end_v = 110 + Sheets("input").Range(trial_end).Value
    '
            If trial_end_v = 110 Then Exit For
    '
    trial_st2 = col3_st + CStr(trial_row)
    trial_end2 = col3_end + CStr(trial_row)
    trial_st_v2 = 110 + Sheets("input").Range(trial_st2).Value
    trial_end_v2 = 110 + Sheets("input").Range(trial_end2).Value
    '
            If trial_end_v2 = 110 Then Exit For
    '
    trial_CR = "B" + CStr(trial_st_v) + ":" + "B" + CStr(trial_end_v)
    trial_CR2 = "C" + CStr(trial_st_v2) + ":" + "C" + CStr(trial_end_v2)
    '
```

```
    trial_CR = "B" + CStr(trial_st_v) + ":" + "B" + CStr(trial_end_v)
    trial_CR2 = "C" + CStr(trial_st_v2) + ":" + "C" + CStr(trial_end_v2)
    '
    Sheets("SD").Range(trial_CR) = Sheets("input").Range("F" + CStr(trial_row)).Value
    Sheets("SD").Range(trial_CR2) = Sheets("input").Range("F" + CStr(trial_row)).Value
    '
    '
    '
    trial_CR3 = "A" + CStr(trial_st_v) + ":" + "H" + CStr(trial_st_v)
    '
    With Sheets("SD").Range(trial_CR3).Interior
    .Pattern = xlSolid
    .PatternColorIndex = xlAutomatic
    .ThemeColor = xlThemeColorLight1
    .TintAndShade = 4.99893185216834E-02
    .PatternTintAndShade = 0
    End With
    With Sheets("SD").Range(trial_CR3).Font
    .ThemeColor = xlThemeColorDark1
    .TintAndShade = 0
    End With
    '
Next trial_row
'
'
'
'Run Status 4
 Sheets("Input").Range("G3").FormulaR1C1 = " In Progress"
 Sheets("Input").Range("G3").FormulaR1C1 = " In Progress."
 Sheets("Input").Range("G3").FormulaR1C1 = " In Progress.."
 Sheets("Input").Range("G3").FormulaR1C1 = " In Progress..."

    With Sheets("Input").Range("I4").Interior
    .Pattern = xlSolid
    .PatternColorIndex = xlAutomatic
    .Color = 12626844
    .TintAndShade = 0
    .PatternTintAndShade = 0
    End With
```

```
'RESPONDERS
'
'
'
    '
    'LEFT PANEL
    '
    'Sheets("Responders").Range(Sheets("input").Range("AM10")) = Sheets("AUC").Range(Sheets("input").Range("AM10")).Value
    'Sheets("Responders").Range(Sheets("input").Range("AM10")).Value = Sheets("Responders").Range(Sheets("input").Range("AM10")).Value
    '

    Sheets("Responders").Range("H111").Value = "=1"
    Sheets("Responders").Range(Sheets("input").Range("AM11")).FormulaR1C1 = "=R[-1]C + 1"
    Sheets("Responders").Range(Sheets("input").Range("AM11")).Value = Sheets("Responders").Range(Sheets("input").Range("AM11")).Value
    '
    Sheets("Responders").Range(Sheets("Input").Range("A7")).FormulaR1C1 = "=RC[1]*Input!R10C16"
    Sheets("Responders").Range(Sheets("Input").Range("A7")).Value = Sheets("Responders").Range(Sheets("Input").Range("A7")).Value
    '
    Sheets("Responders").Range(Sheets("Input").Range("A8")).FormulaR1C1 = "=RC[1]/86400"
    Sheets("Responders").Range(Sheets("Input").Range("A8")).Value = Sheets("Responders").Range(Sheets("Input").Range("A8")).Value
    '
    Sheets("Responders").Range(Sheets("Input").Range("A9")).FormulaR1C1 = "=VLOOKUP(RC[5],INDIRECT(""Input!$E$8:$F$""&Input!R18C1),2,1)"
    Sheets("Responders").Range(Sheets("Input").Range("A9")).Value = Sheets("Responders").Range(Sheets("Input").Range("A9")).Value
    '
    'For Each cell In Sheets("Responders").Range(Sheets("Input").Range("A9"))
        'If IsError(cell.Value) Then
        'cell.ClearContents
    'End If
    'Next cell
    '
    '
    '
    Sheets("Responders").Range(Sheets("Input").Range("A10")).FormulaR1C1 = "=INDIRECT(""C""&SUM(ROW(RC),ROUNDUP(Input!R14C16/Input!R10C16,(
    '
    'For Each cell In Sheets("Responders").Range(Sheets("Input").Range("A10"))
            'If IsError(cell.Value) Then
            'cell.ClearContents
       ' End If
    'Next cell
    '
    '
    'HEAT MAP
    '
    'Sheets("Responders").Range(Sheets("Input").Range("A4")).FormulaR1C1 = "=IF(AND(Percent!RC>Input!R18C16,SD!RC>Input!R19C16),1,"""")"
    'Sheets("Responders").Range(Sheets("Input").Range("A5")).FormulaR1C1 = "=IF(AND(Percent!RC>Input!R18C16,SD!RC>Input!R19C16),1,"""")"

    For hrow = 8 To 107
    hCR = "AF" + CStr(hrow)
        If Len(Sheets("input").Range(hCR)) = 0 Then Exit For
    Sheets("Responders").Range(Sheets("Input").Range(hCR)).FormulaR1C1 = "=IF(AND(Percent!RC>Input!R18C16,SD!RC>Input!R19C16),1,"""")"
    Sheets("Responders").Range(Sheets("Input").Range(hCR)).Value = Sheets("Responders").Range(Sheets("Input").Range(hCR)).Value
    Next hrow
```

```
'
'Too slow:
'For r = 111 To 25000
    'c2r = c2 + CStr(r)
    'If r > max2 Then Exit For
    'Sheets("Responders").Range(Sheets("Responders").Range(c2r)).FormulaR1C1 = "=IF(AND(Percent!RC>Input!R18C16,SD!RC>Input!R19C16),1,0)"
'Next r
'
'Run Status 5
 Sheets("Input").Range("G3").FormulaR1C1 = " In Progress"
 Sheets("Input").Range("G3").FormulaR1C1 = " In Progress."
 Sheets("Input").Range("G3").FormulaR1C1 = " In Progress.."
 Sheets("Input").Range("G3").FormulaR1C1 = " In Progress..."
'
With Sheets("Input").Range("J4").Interior
    .Pattern = xlSolid
    .PatternColorIndex = xlAutomatic
    .Color = 12626844
    .TintAndShade = 0
    .PatternTintAndShade = 0
End With
'
'Change formula to value
'Sheets("Responders").Range(Sheets("Input").Range("A4")).Value = Sheets("Responders").Range(Sheets("Input").Range("A4")).Value
'Sheets("Responders").Range(Sheets("Input").Range("A5")).Value = Sheets("Responders").Range(Sheets("Input").Range("A5")).Value
'
'
'TOP PANEL
'
    For r = 5 To 104
        cr = c + CStr(r)
        If r > max Then Exit For
        Sheets("Responders").Range(Sheets("Responders").Range(cr)).FormulaR1C1 = "=IF(R4C<=RC1,IF(SUM(INDIRECT(""""&R107C&""""&RC4&"":""&R1(
    Next r

    'Group top panel stim rows that are empty
    Dim start_group As Integer
    start_group = Sheets("input").Range("A6").Value + 5
    'Sheets("responders").Rows(CStr(start_group) + ":" + "108").group
    'Sheets("responders").Rows(start_group).ShowDetail = False
    Sheets("responders").Rows(CStr(start_group) + ":" + "108").entirerow.Hidden = True
'
'
'
```

```
'
'Run Status 6
 Sheets("Input").Range("G3").FormulaR1C1 = " In Progress"
 Sheets("Input").Range("G3").FormulaR1C1 = " In Progress."
 Sheets("Input").Range("G3").FormulaR1C1 = " In Progress.."
 Sheets("Input").Range("G3").FormulaR1C1 = " In Progress..."
'
With Sheets("Input").Range("K4").Interior
    .Pattern = xlSolid
    .PatternColorIndex = xlAutomatic
    .Color = 12626844
    .TintAndShade = 0
    .PatternTintAndShade = 0
End With
'
'
'For heatmap, hide rows between stim trials
'
'Sheets("responders").Rows(Beg).group
'Sheets("responders").Rows(Beg_st).ShowDetail = False
Sheets("responders").Rows(Beg).entirerow.Hidden = True
'Sheets("responders").Rows(Btwn).group
'Sheets("responders").Rows(Btwn_st).ShowDetail = False


For trial_row = 8 To 107
'
    trial_st = col_st + CStr(trial_row)
    trial_end = col_end + CStr(trial_row)
    trial_st_v = 109 + Sheets("input").Range(trial_st).Value
    trial_end_v = 109 + Sheets("input").Range(trial_end).Value
    trial_RR_done = CStr(trial_st_v) + ":" + CStr(Sheets("input").Range("AM8"))
            If trial_end_v = 109 Then
                'Sheets("Responders").Rows(trial_RR_done).group
                'Sheets("Responders").Rows(trial_st_v).ShowDetail = False
                Sheets("responders").Rows(trial_RR_done).entirerow.Hidden = True
                Exit For
            End If
    trial_RR = CStr(trial_st_v) + ":" + CStr(trial_end_v)
    'Sheets("Responders").Rows(trial_RR).group
    'Sheets("Responders").Rows(trial_st_v).ShowDetail = False
    Sheets("responders").Rows(trial_RR).entirerow.Hidden = True
'
Next trial_row
'
'For heatmaps, on left panel, specify which rows are basal and stim
'
Sheets("Responders").Range("B111:B25000").ClearContents
Sheets("Responders").Range("C111:C25000").ClearContents
```

```
For trial_row = 8 To 107
    '
    trial_st = col2_st + CStr(trial_row)
    trial_end = col2_end + CStr(trial_row)
    trial_st_v = 110 + Sheets("input").Range(trial_st).Value
    trial_end_v = 110 + Sheets("input").Range(trial_end).Value
    '
            If trial_end_v = 110 Then Exit For
    '
    trial_st2 = col3_st + CStr(trial_row)
    trial_end2 = col3_end + CStr(trial_row)
    trial_st_v2 = 110 + Sheets("input").Range(trial_st2).Value
    trial_end_v2 = 110 + Sheets("input").Range(trial_end2).Value
    '
            If trial_end_v2 = 110 Then Exit For
    '
    trial_CR = "B" + CStr(trial_st_v) + ":" + "B" + CStr(trial_end_v)
    trial_CR2 = "C" + CStr(trial_st_v2) + ":" + "C" + CStr(trial_end_v2)
    '
    Sheets("Responders").Range(trial_CR) = Sheets("input").Range("F" + CStr(trial_row)).Value
    Sheets("Responders").Range(trial_CR2) = Sheets("input").Range("F" + CStr(trial_row)).Value
    '
    '
    '
    trial_CR3 = "A" + CStr(trial_st_v) + ":" + "H" + CStr(trial_st_v)
    '
    With Sheets("Responders").Range(trial_CR3).Interior
    .Pattern = xlSolid
    .PatternColorIndex = xlAutomatic
    .ThemeColor = xlThemeColorLight1
    .TintAndShade = 4.998931852168346E-02
    .PatternTintAndShade = 0
    End With
    With Sheets("Responders").Range(trial_CR3).Font
    .ThemeColor = xlThemeColorDark1
    .TintAndShade = 0
    End With
    '
Next trial_row
'
'Run Status 7
 Sheets("Input").Range("G3").FormulaR1C1 = " In Progress"
 Sheets("Input").Range("G3").FormulaR1C1 = " In Progress."
 Sheets("Input").Range("G3").FormulaR1C1 = " In Progress.."
 Sheets("Input").Range("G3").FormulaR1C1 = " In Progress..."
'
 With Sheets("Input").Range("L4").Interior
    .Pattern = xlSolid
    .PatternColorIndex = xlAutomatic
    .Color = 12626844
    .TintAndShade = 0
    .PatternTintAndShade = 0
End With
```

AUC

```
'
'LEFT PANEL
'
Sheets("AUC").Range("H111").Value = "=1"
Sheets("AUC").Range(Sheets("input").Range("AM11")).FormulaR1C1 = "=R[-1]C + 1"
Sheets("AUC").Range(Sheets("input").Range("AM11")).Value = Sheets("AUC").Range(Sheets("input").Range("AM11")).Value
'
Sheets("AUC").Range(Sheets("Input").Range("A7")).FormulaR1C1 = "=RC[1]*Input!R10C16"
Sheets("AUC").Range(Sheets("Input").Range("A7")).Value = Sheets("AUC").Range(Sheets("Input").Range("A7")).Value
'
Sheets("AUC").Range(Sheets("Input").Range("A8")).FormulaR1C1 = "=RC[1]/86400"
Sheets("AUC").Range(Sheets("Input").Range("A8")).Value = Sheets("AUC").Range(Sheets("Input").Range("A8")).Value
'
Sheets("AUC").Range(Sheets("Input").Range("A9")).FormulaR1C1 = "=VLOOKUP(RC[5],INDIRECT(""Input!$E$8:$F$""&Input!R18C1),2,1)"
Sheets("AUC").Range(Sheets("Input").Range("A9")).Value = Sheets("AUC").Range(Sheets("Input").Range("A9")).Value
'
Sheets("AUC").Range(Sheets("Input").Range("A10")).FormulaR1C1 = "=INDIRECT(""C""&SUM(ROW(RC),ROUNDUP(Input!R14C16/Input!R10C16,0),ROUNDUP((Input!R15C
Sheets("AUC").Range(Sheets("Input").Range("A10")).Value = Sheets("AUC").Range(Sheets("Input").Range("A10")).Value
'
'HEAT MAP
'

    For hrow = 8 To 107
    hCR = "AF" + CStr(hrow)
        If Len(Sheets("input").Range(hCR)) = 0 Then Exit For
        '
        If Sheets("input").Range("AR5").Value = 1 Then
            Sheets("AUC").Range(Sheets("Input").Range(hCR)).FormulaR1C1 = "=((raw!RC)+(raw!R[1]C))/2"
            Sheets("AUC").Range(Sheets("Input").Range(hCR)).Value = Sheets("AUC").Range(Sheets("Input").Range(hCR)).Value
        End If
        '
        If Sheets("input").Range("AR5").Value = 0 Then
            Sheets("AUC").Range(Sheets("Input").Range(hCR)).FormulaR1C1 = "=((raw!RC)+(raw!R[1]C)-2)/2"
            Sheets("AUC").Range(Sheets("Input").Range(hCR)).Value = Sheets("AUC").Range(Sheets("Input").Range(hCR)).Value
        End If
    '
    Next hrow
```

```
'Change formula to value
'Sheets("AUC").Range(Sheets("Input").Range("A4")).Value = Sheets("AUC").Range(Sheets("Input").Range("A4")).Value
'Sheets("AUC").Range(Sheets("Input").Range("A5")).Value = Sheets("AUC").Range(Sheets("Input").Range("A5")).Value
'
'
'Sheets("AUC").Range("I112:IA12040").Value = Sheets("AUC").Range("I112:IA12040").Value
'
'TOP PANEL
'
'Sheets("AUC").Range("I5:IA104").FormulaR1C1 = "=IF(R4C<=RC1, IF((((((SUM(INDIRECT(R107C&""""&RC4&"":""&R107C&""""&RC5)))/(RC5-RC4))-((SUM
    "IRECT(R107C&""""&RC6&"":""&R107C&""""&RC7)))/(RC7-RC6)))*100),0)"
    '


    Dim AUCr As Integer, AUCcr As String, AUCcr2 As String, inputcr As String, inputcr2 As String
    For AUCr = 5 To 105
        AUCcr = "D" + CStr(AUCr)
        AUCcr2 = "E" + CStr(AUCr)
        inputcr = "AX" + CStr(AUCr + 3)
        inputcr2 = "AY" + CStr(AUCr + 3)
            If Sheets("input").Range(inputcr).Value = 0 Then Exit For
        Sheets("AUC").Range(AUCcr).Value = Sheets("input").Range(inputcr).Value
        Sheets("AUC").Range(AUCcr2).Value = Sheets("input").Range(inputcr2).Value
    Next AUCr
    '
    For r = 5 To 104
        cr = c + CStr(r)
        If r > max Then Exit For
        '
        If Sheets("input").Range("AR5").Value = 1 Then
            Sheets("AUC").Range(Sheets("AUC").Range(cr)).FormulaR1C1 = "=IF((SUM(INDIRECT(R107C&""""&RC6&"":""&R107C&""""&RC7))/(RC7-RC6))
        End If
        '
        If Sheets("input").Range("AR5").Value = 0 Then
            Sheets("AUC").Range(Sheets("AUC").Range(cr)).FormulaR1C1 = "=IF(Responders!RC>=0,IF(R4C<=RC1, SUM(INDIRECT(R107C&""""&RC4&"":"
        End If
    Next r
```

```
'
' PEAK PERCENT
'
    '
    'TOP PANEL
    '
    'Sheets("Peak Percent").Range("I5:IA104").FormulaR1C1 = "=IF(R4C<=RC1,(MAX(INDIRECT(""percent!""&R107C&""""&RC4&"":""&R107C&""""&RC5))),0)"
    '
    For r = 5 To 104
            cr = c + CStr(r)
            If r > max Then Exit For
            Sheets("Percent").Range(Sheets("Percent").Range(cr)).FormulaR1C1 = "=IF(Responders!RC>=0,IF(R4C<=RC1,(MAX(INDIRECT(""percent!""&R107C&
            Sheets("Percent").Range(Sheets("Percent").Range(cr)).Value = Sheets("Percent").Range(Sheets("Percent").Range(cr)).Value
    Next r

        'Group top panel stim rows that are empty
        start_group = Sheets("input").Range("A6").Value + 5
        'Sheets("Percent").Rows(CStr(start_group) + ":" + "108").group
        'Sheets("Percent").Rows(start_group).ShowDetail = False
        Sheets("percent").Rows(CStr(start_group) + ":" + "108").entirerow.Hidden = True

'
' PEAK SD
'
'
    '
    'TOP PANEL
    '
    'Sheets("Peak SD").Range("I5:IA104").FormulaR1C1 = "=IF(R4C<=RC1,(MAX(INDIRECT(""sd!""&R107C&""""&RC4&"":""&R107C&""""&RC5))),0)"
    '
    For r = 5 To 104
            cr = c + CStr(r)
            If r > max Then Exit For
            Sheets("SD").Range(Sheets("SD").Range(cr)).FormulaR1C1 = "=IF(Responders!RC>=0,IF(R4C<=RC1,(MAX(INDIRECT(""sd!""&R107C&""""&AUC!RC4&""
            Sheets("SD").Range(Sheets("SD").Range(cr)).Value = Sheets("SD").Range(Sheets("SD").Range(cr)).Value
    Next r

        'Group top panel stim rows that are empty
        start_group = Sheets("input").Range("A6").Value + 5
        'Sheets("SD").Rows(CStr(start_group) + ":" + "108").group
        'Sheets("SD").Rows(start_group).ShowDetail = False
        Sheets("SD").Rows(CStr(start_group) + ":" + "108").entirerow.Hidden = True
'
'
```

```
' DURATION
'
    '
    'TOP PANEL
    '
    'Sheets("Duration").Range("I5:IA104").FormulaR1C1 = "=IF(R4C<=RC1,IF((SUM(INDIRECT(""responders!""&R107C&""""&RC4&"":""&R107C&""""&RC5)))*Input!R10C
    '
    For r = 5 To 104
            cr = c + CStr(r)
            If r > max Then Exit For
            Sheets("Duration").Range(Sheets("Duration").Range(cr)).FormulaR1C1 = "=IF(R4C<=RC1,IF(Responders!RC>=0,(SUM(INDIRECT(""responders!""&R107C&"
            Sheets("Duration").Range(Sheets("Duration").Range(cr)).Value = Sheets("Duration").Range(Sheets("Duration").Range(cr)).Value
    Next r
'
'
'Progress complete
'
'   Run Status 8
        With Sheets("Input").Range("M4").Interior
        .Pattern = xlSolid
        .PatternColorIndex = xlAutomatic
        .Color = 12626844
        .TintAndShade = 0
        .PatternTintAndShade = 0
        End With
    '
     Sheets("Input").Range("G3").FormulaR1C1 = " In Progress"
     Sheets("Input").Range("G3").FormulaR1C1 = " In Progress."
     Sheets("Input").Range("G3").FormulaR1C1 = " In Progress.."
     Sheets("Input").Range("G3").FormulaR1C1 = " In Progress..."
     Sheets("Input").Range("G3").FormulaR1C1 = " In Progress"
     Sheets("Input").Range("G3").FormulaR1C1 = " In Progress."
     Sheets("Input").Range("G3").FormulaR1C1 = " In Progress.."
     Sheets("Input").Range("G3").FormulaR1C1 = " In Progress..."
     Sheets("Input").Range("G3").FormulaR1C1 = " Calculated"
    '
```

```
Sheets("dashboard").Range("AN3") = CStr(Sheets("input").Range("P14").Value) + "s"
Sheets("dashboard").Range("AN4") = CStr(Sheets("input").Range("P15").Value) + "s"
Sheets("dashboard").Range("AQ3") = CStr(Sheets("input").Range("P18").Value) + "%"
Sheets("dashboard").Range("AQ4") = CStr(Sheets("input").Range("P19").Value)
Sheets("dashboard").Range("AQ5") = CStr(Sheets("input").Range("P20").Value) + "s"
Sheets("dashboard").Range("AT3") = CStr(Sheets("input").Range("P22").Value) + "s"
Sheets("dashboard").Range("AU3") = CStr(Sheets("input").Range("U10").Value)
Sheets("dashboard").Range("AH9") = CStr(Sheets("input").Range("U10").Value)
Sheets("dashboard").Range("BL8") = CStr(Sheets("input").Range("U10").Value)
Sheets("dashboard").Range("BL13") = CStr(Sheets("input").Range("U10").Value)
Sheets("dashboard").Range("BL14") = CStr(Sheets("input").Range("U10").Value)
Sheets("dashboard").Range("BL26") = CStr(Sheets("input").Range("U10").Value)
Sheets("charts").Range("U6") = CStr(Sheets("input").Range("P14").Value) + "s"
Sheets("charts").Range("U7") = CStr(Sheets("input").Range("P15").Value) + "s"
Sheets("charts").Range("W6") = CStr(Sheets("input").Range("P18").Value) + "%"
Sheets("charts").Range("W7") = CStr(Sheets("input").Range("P19").Value)
Sheets("charts").Range("W8") = CStr(Sheets("input").Range("P20").Value) + "s"
Sheets("charts").Range("Y6") = CStr(Sheets("input").Range("P22").Value) + "s"
Sheets("charts").Range("Z6") = CStr(Sheets("input").Range("U10").Value)

If Sheets("input").Range("U34").Value = "Dashboard" Then
    Sheets("Dashboard").Select
End If

If Sheets("input").Range("U34").Value = "Charts" Then
    Sheets("Charts").Select
End If

If Sheets("input").Range("U34").Value = "Responders" Then
    Sheets("Responders").Select
End If


'Let user know how many times ROIs have a basal SD of 0
If SDzero = 1 Then
    MsgBox "A basal fluorescence SD of 0 has occured " + CStr(SDzero) + " time across all trials. If an ROI has a basal SD of 0 for a trial,
End If

If SDzero > 1 Then
    MsgBox "A basal fluorescence SD of 0 has occured " + CStr(SDzero) + " times across all trials. If an ROI has a basal SD of 0 for a trial
End If
```

```
Sub reset_new()


Call protect

'
'Top Panel
Sheets("AUC").Range("I5:LX104").ClearContents
Sheets("Percent").Range("I5:LX104").ClearContents
Sheets("Responders").Range("I5:LX104").ClearContents
Sheets("SD").Range("I5:LX104").ClearContents
Sheets("Duration").Range("I5:LX104").ClearContents
'
'
'Left panel
Sheets("AUC").Range("H111:B25110").ClearContents
Sheets("Percent").Range("H111:B25110").ClearContents
Sheets("Responders").Range("H111:B25110").ClearContents
Sheets("SD").Range("H111:B25110").ClearContents
'
'Heat maps
Sheets("AUC").Range("I111:LX25110").ClearContents
Sheets("Percent").Range("I111:LX25110").ClearContents
Sheets("Responders").Range("I111:LX25110").ClearContents
Sheets("SD").Range("I111:LX25110").ClearContents
'

'Clears groupings
Sheets("Responders").Rows("111:25110").entirerow.Hidden = False
Sheets("Percent").Rows("111:25110").entirerow.Hidden = False
Sheets("SD").Rows("111:25110").entirerow.Hidden = False
Sheets("responders").Rows("1:108").entirerow.Hidden = False
Sheets("percent").Rows("1:108").entirerow.Hidden = False
Sheets("SD").Rows("1:108").entirerow.Hidden = False
'
'

'Clear left panel trial start formatting
        With Sheets("Responders").Range("A111:H25110").Font
            .ColorIndex = xlAutomatic
            .TintAndShade = 0
        End With
        With Sheets("Responders").Range("A111:H25110").Interior
        .Pattern = xlSolid
        .PatternColorIndex = xlAutomatic
        .ThemeColor = xlThemeColorDark1
        .TintAndShade = -4.99893185216834E-02
        .PatternTintAndShade = 0
        End With
        '
```

```
        With Sheets("SD").Range("A111:H25110").Font
            .ColorIndex = xlAutomatic
            .TintAndShade = 0
        End With
        With Sheets("SD").Range("A111:H25110").Interior
        .Pattern = xlSolid
        .PatternColorIndex = xlAutomatic
        .ThemeColor = xlThemeColorDark1
        .TintAndShade = -4.99893185216834E-02
        .PatternTintAndShade = 0
        End With
'Clear status progress on input tab
With Sheets("Input").Range("F4:M4").Interior
        .Pattern = xlNone
        .TintAndShade = 0
        .PatternTintAndShade = 0
    End With

     Sheets("Input").Range("G3").FormulaR1C1 = " Cleared"

    With Sheets("Input").Range("G3").Interior
        .Pattern = xlNone
        .TintAndShade = 0
        .PatternTintAndShade = 0
        .Color = 16250871
    End With
    Sheets("dashboard").Range("AN3").ClearContents
    Sheets("dashboard").Range("AN4").ClearContents
    Sheets("dashboard").Range("AQ3").ClearContents
    Sheets("dashboard").Range("AQ4").ClearContents
    Sheets("dashboard").Range("AQ5").ClearContents
    Sheets("dashboard").Range("AT3").ClearContents
    Sheets("dashboard").Range("AU3").ClearContents
    Sheets("charts").Range("U6").ClearContents
    Sheets("charts").Range("U7").ClearContents
    Sheets("charts").Range("W6").ClearContents
    Sheets("charts").Range("W7").ClearContents
    Sheets("charts").Range("W8").ClearContents
    Sheets("charts").Range("Y6").ClearContents
    Sheets("charts").Range("Z6").ClearContents

End Sub
```

```
Sub Reset_2()
Call protect

''
'Data Validation for user-defined clearing
'
    'Number of ROIs should be between 1 and 328

        If Sheets("input").Range("U38") < 1 Or Sheets("input").Range("U38") > 328 Then
            Call ROI_error
            Exit Sub
        End If

    'Number of frames should be less than 25000
    If Sheets("Input").Range("U39").Value > 25000 Then
        Call maxframes_error
        Exit Sub
    End If

Sheets("Input").Range("G3").FormulaR1C1 = " Clearing Data..."
'
'
'Top Panel
Sheets("AUC").Range("I5:LX104").ClearContents
Sheets("Percent").Range("I5:LX104").ClearContents
Sheets("Responders").Range("I5:LX104").ClearContents
Sheets("SD").Range("I5:LX104").ClearContents
Sheets("Duration").Range("I5:LX104").ClearContents
'
'
'Left panel
Sheets("AUC").Range(Sheets("Input").Range("A12")).ClearContents
Sheets("Percent").Range(Sheets("Input").Range("A12")).ClearContents
Sheets("Responders").Range(Sheets("Input").Range("A12")).ClearContents
Sheets("SD").Range(Sheets("Input").Range("A12")).ClearContents
'
'Heat maps
Sheets("AUC").Range(Sheets("Input").Range("A3")).ClearContents
Sheets("Percent").Range(Sheets("Input").Range("A3")).ClearContents
Sheets("Responders").Range(Sheets("Input").Range("A3")).ClearContents
Sheets("SD").Range(Sheets("Input").Range("A3")).ClearContents
'
'
'
Dim endrow As Integer, startrow As Integer, startend As String
endrow = Sheets("Input").Range("U39").Value
startrow = 111
startend = CStr(startrow) + ":" + CStr(endrow)
```

```
'Clears groupings
Sheets("Responders").Rows(startend).entirerow.Hidden = False
Sheets("Percent").Rows(startend).entirerow.Hidden = False
Sheets("SD").Rows(startend).entirerow.Hidden = False
Sheets("responders").Rows("1:108").entirerow.Hidden = False
Sheets("percent").Rows("1:108").entirerow.Hidden = False
Sheets("sd").Rows("1:108").entirerow.Hidden = False
'
'
'Clear left panel trial start formatting
        With Sheets("Responders").Range(Sheets("input").Range("A13")).Font
            .ColorIndex = xlAutomatic
            .TintAndShade = 0
        End With
        With Sheets("Responders").Range(Sheets("input").Range("A13")).Interior
        .Pattern = xlSolid
        .PatternColorIndex = xlAutomatic
        .ThemeColor = xlThemeColorDark1
        .TintAndShade = -4.99893185216834E-02
        .PatternTintAndShade = 0
        End With
        '
        With Sheets("percent").Range(Sheets("input").Range("A13")).Font
            .ColorIndex = xlAutomatic
            .TintAndShade = 0
        End With
        With Sheets("percent").Range(Sheets("input").Range("A13")).Interior
        .Pattern = xlSolid
        .PatternColorIndex = xlAutomatic
        .ThemeColor = xlThemeColorDark1
        .TintAndShade = -4.99893185216834E-02
        .PatternTintAndShade = 0
        End With
        'Sheets("percent").Rows("112:25110").Borders(xlInsideHorizontal).LineStyle = xlNone
        '
        With Sheets("SD").Range(Sheets("input").Range("A13")).Font
            .ColorIndex = xlAutomatic
            .TintAndShade = 0
        End With
        With Sheets("SD").Range(Sheets("input").Range("A13")).Interior
        .Pattern = xlSolid
        .PatternColorIndex = xlAutomatic
        .ThemeColor = xlThemeColorDark1
        .TintAndShade = -4.99893185216834E-02
        .PatternTintAndShade = 0
        End With
'
'Clear status progress on input tab
With Sheets("Input").Range("F4:M4").Interior
        .Pattern = xlNone
        .TintAndShade = 0
        .PatternTintAndShade = 0
    End With
```

```
Sub Normalize_raw_data1()

ActiveSheet.protect Password:="vba", UserInterfaceOnly:=True
Sheets("input").Select
Sheets("Input").Range("O45").FormulaR1C1 = " Normalizing data..."

If Sheets("Input").Range("P47").Value = 0 Or Sheets("Input").Range("P48").Value = 0 Or IsEmpty(Sheets("Input").Range("P47")) Or
    Call normalization_error
    Exit Sub
End If


If Sheets("Input").Range("P47").Value > 328 Then
    Call ROI_error
    Exit Sub
End If



Call Reset_normalize5


Dim endrow As Integer
Dim frameset As Integer
endrow = 111 + Sheets("input").Range("P56").Value
frameset = Sheets("input").Range("P56").Value

Sheets("Input").Range("O45").FormulaR1C1 = " Normalizing"
'
Sheets("raw").Range(Sheets("input").Range("A20")) = "=IF(((rawOG!RC/PERCENTILE(rawOG!R111C:R" & endrow & "C,R107C8))-R109C8)<1,1
Sheets("raw").Range(Sheets("input").Range("A20")).Value = Sheets("raw").Range(Sheets("input").Range("A20")).Value
Sheets("raw0").Range(Sheets("input").Range("A20")).Value = "=raw!RC-1"
Sheets("raw0").Range(Sheets("input").Range("A20")).Value = Sheets("raw0").Range(Sheets("input").Range("A20")).Value
'
Sheets("raw").Range(Sheets("input").Range("A21")) = "=IF(((rawOG!RC/PERCENTILE(rawOG!R[-" & frameset & "]C:R[" & frameset & "]C,
Sheets("raw").Range(Sheets("input").Range("A21")).Value = Sheets("raw").Range(Sheets("input").Range("A21")).Value
Sheets("raw0").Range(Sheets("input").Range("A21")).Value = "=raw!RC-1"
Sheets("raw0").Range(Sheets("input").Range("A21")).Value = Sheets("raw0").Range(Sheets("input").Range("A21")).Value
'
'
Sheets("input").Range("A50").Value = "=1"
Sheets("Input").Range("O45").FormulaR1C1 = " Data normalized"
Sheets("raw0").Select

End Sub
```

```
Sub Normalize_raw_data0()

ActiveSheet.protect Password:="vba", UserInterfaceOnly:=True
Sheets("input").Select
Sheets("Input").Range("O45").FormulaR1C1 = " Normalizing data..."

If Sheets("Input").Range("P47").Value = 0 Or Sheets("Input").Range("P48").Value = 0 Or IsEmpty(Sheets("Input").Range("P47")) Or IsEmpty(
    Call normalization_error
    Exit Sub
End If


If Sheets("Input").Range("P47").Value > 328 Then
    Call ROI_error
    Exit Sub
End If


Call Reset_normalize5

Dim endrow As Integer
Dim frameset As Integer
endrow = 111 + Sheets("input").Range("P56").Value
frameset = Sheets("input").Range("P56").Value

Sheets("Input").Range("O45").FormulaR1C1 = " Normalizing"
'
Sheets("raw").Range(Sheets("input").Range("A20")) = "=IF(((rawOG!RC/PERCENTILE(rawOG!R111C:R" & endrow & "C,R107C8))-R109C8)<1,1,(rawOG!
Sheets("raw").Range(Sheets("input").Range("A20")).Value = Sheets("raw").Range(Sheets("input").Range("A20")).Value
'
Sheets("raw").Range(Sheets("input").Range("A21")) = "=IF(((rawOG!RC/PERCENTILE(rawOG!R[-" & frameset & "]C:R[" & frameset & "]C,R107C8))
Sheets("raw").Range(Sheets("input").Range("A21")).Value = Sheets("raw").Range(Sheets("input").Range("A21")).Value
'
Sheets("input").Range("A50").Value = "=1"
Sheets("Input").Range("O45").FormulaR1C1 = " Data normalized"
Sheets("raw").Select

If Sheets("raw").Range("H110") <> 0 Then
    Call not_normal2
End If

End Sub
```

```
Sub Reset_normalize2()

ActiveSheet.protect Password:="vba", UserInterfaceOnly:=True
Sheets("Input").Range("O45").FormulaR1C1 = " Clearing Data"

If Sheets("Input").Range("U47").Value = 0 Or Sheets("Input").Range("U48").Value = 0 Or IsEmpty(Sheets("Input").Range("U47")) Or IsE
    Call Reset2_error
    Exit Sub
End If


If Sheets("Input").Range("U47").Value > 328 Then
    Call ROI_error
    Exit Sub
End If

Sheets("raw").Range(Sheets("input").Range("A16")).ClearContents
Sheets("raw0").Range(Sheets("input").Range("A16")).ClearContents
Sheets("Input").Range("O45").FormulaR1C1 = " Not normalized"
End Sub
```

```
Sub Reset_normalize3()

ActiveSheet.protect Password:="vba", UserInterfaceOnly:=True
Sheets("Input").Range("O45").FormulaR1C1 = " Clearing Data"

If Sheets("Input").Range("U47").Value = 0 Or Sheets("Input").Range("U48").Value = 0 Or IsEmpty(Sheets("Input").Range("U47")) Or IsE
    Call Reset2_error
    Exit Sub
End If


If Sheets("Input").Range("U47").Value > 328 Then
    Call ROI_error
    Exit Sub
End If


Sheets("rawOG").Range(Sheets("input").Range("A16")).ClearContents
Sheets("Input").Range("O45").ClearContents
End Sub
```

```
Sub Reset_normalize4()

ActiveSheet.protect Password:="vba", UserInterfaceOnly:=True
Sheets("Input").Range("O45").FormulaR1C1 = " Clearing Data"

If Sheets("Input").Range("U47").Value = 0 Or Sheets("Input").Range("U48").Value = 0 Or IsEmpty(Sheets("Input").Range("U47")) Or IsEmpty(Sheets
    Call Reset2_error
    Exit Sub
End If


If Sheets("Input").Range("U47").Value > 328 Then
    Call ROI_error
    Exit Sub
End If

Sheets("raw").Range(Sheets("input").Range("A16")).ClearContents
Sheets("raw0").Range(Sheets("input").Range("A16")).ClearContents
Sheets("rawOG").Range(Sheets("input").Range("A16")).ClearContents
Sheets("Input").Range("O45").FormulaR1C1 = " Not normalized"
End Sub
```

```
Sub Reset_normalize5()

ActiveSheet.protect Password:="vba", UserInterfaceOnly:=True
Sheets("Input").Range("O45").FormulaR1C1 = " Clearing Data"

If Sheets("Input").Range("U47").Value = 0 Or Sheets("Input").Range("U48").Value = 0 Or IsEmpty(Sheets("Input").Range("U47")) Or IsEmpty(Sheets
    Call Reset2_error
    Exit Sub
End If


If Sheets("Input").Range("U47").Value > 328 Then
    Call ROI_error
    Exit Sub
End If

Sheets("raw").Range(Sheets("input").Range("A16")).ClearContents
Sheets("raw0").Range(Sheets("input").Range("A16")).ClearContents

End Sub
```

```
Sub clearall()

Call reset_new
Call Reset_normalize4

End Sub
```

```
Sub normalpercent()
'
'
Dim percent As Double, normrng As Range, percentrng As Range
Set normrng = Sheets("raw").Range("I107:LX107")
Set percentrng = Sheets("input").Range("p53")
'
For percent = 0.0001 To 1 Step 0.0001
    percentrng.Value = percent
        For Each Cell In normrng
            If Cell.Value = 0 Then
                Exit For
            Else
                percentrng = 0
                Exit For
            End If
        Next Cell
        If percent > 0 Then Exit For
Next percent
'
percentrng = percent * 10
'
'
End Sub
```

```
Sub search_stim()

'
'To search for stims on heatmaps
'
'
Dim stim As Integer, stim_row As Integer, c As String, cr As String
Dim variable
c = "F"

        'For Each cell In Sheets("input").Range("C7:C107")
            'If Not cell.Value = ActiveSheet.Range("A3") Then
                'Call search_stim_error
                'Exit Sub
            'End If
        'Next cell

        If IsEmpty(Sheets("input").Range("G3")) Then
            Call heatmapsearch_error
            Exit Sub
            Else

            If IsError(ActiveSheet.Range("A3")) = True Then
                Call search_stim_error
                Exit Sub
            End If

            If ActiveSheet.Range("A3") = 0 Then
                Call heatmapsearch_error
            End If
'
            For stim = 1 To 100
                If ActiveSheet.Range("A3") = stim Then
                    stim_row = stim + 7
                    cr = c + CStr(stim_row)
                    ActiveSheet.Range("C111:C25150").Select
                    Selection.Find(What:=Sheets("Input").Range(cr), After:=ActiveCell, LookIn:=xlFormulas, _
                    LookAt:=xlPart, SearchOrder:=xlByRows, SearchDirection:=xlNext, _
                    MatchCase:=False, SearchFormat:=False).Activate
                    cells(3, 2).Select
                End If
            Next stim
        End If
'

End Sub
```

```
Sub click_stim1()

    ActiveSheet.Range("C111:C25150").Select

    If Err.Number = 0 Then
        Selection.Find(What:=Sheets("Input").Range("F8"), After:=ActiveCell, LookIn:=xlFormulas, _
        LookAt:=xlPart, SearchOrder:=xlByRows, SearchDirection:=xlNext, _
        MatchCase:=False, SearchFormat:=False).Activate
        cells(3, 2).Select
    Else
    Call heatmapsearch_error
    End If

End Sub
Sub click_stim2()

    ActiveSheet.Range("C111:C25150").Select

    If Err.Number = 0 Then
        Selection.Find(What:=Sheets("Input").Range("F9"), After:=ActiveCell, LookIn:=xlFormulas, _
        LookAt:=xlPart, SearchOrder:=xlByRows, SearchDirection:=xlNext, _
        MatchCase:=False, SearchFormat:=False).Activate
        cells(3, 2).Select
    Else
    Call heatmapsearch_error
    End If

End Sub
Sub click_stim3()

    ActiveSheet.Range("C111:C25150").Select

    If Err.Number = 0 Then
        Selection.Find(What:=Sheets("Input").Range("F10"), After:=ActiveCell, LookIn:=xlFormulas, _
        LookAt:=xlPart, SearchOrder:=xlByRows, SearchDirection:=xlNext, _
        MatchCase:=False, SearchFormat:=False).Activate
        cells(3, 2).Select
    Else
    Call heatmapsearch_error
    End If

End Sub
Sub click_stim4()

    ActiveSheet.Range("C111:C25150").Select

    If Err.Number = 0 Then
        Selection.Find(What:=Sheets("Input").Range("F11"), After:=ActiveCell, LookIn:=xlFormulas, _
        LookAt:=xlPart, SearchOrder:=xlByRows, SearchDirection:=xlNext, _
        MatchCase:=False, SearchFormat:=False).Activate
        cells(3, 2).Select
    Else
    Call heatmapsearch_error
    End If

End Sub
```

```
Sub click_stim5()

    ActiveSheet.Range("C111:C25150").Select

    If Err.Number = 0 Then
        Selection.Find(What:=Sheets("Input").Range("F12"), After:=ActiveCell, LookIn:=xlFormulas, _
        LookAt:=xlPart, SearchOrder:=xlByRows, SearchDirection:=xlNext, _
        MatchCase:=False, SearchFormat:=False).Activate
        cells(3, 2).Select
    Else
    Call heatmapsearch_error
    End If

End Sub
```

```
Sub click_stim6()

    ActiveSheet.Range("C111:C25150").Select

    If Err.Number = 0 Then
        Selection.Find(What:=Sheets("Input").Range("F13"), After:=ActiveCell, LookIn:=xlFormulas, _
        LookAt:=xlPart, SearchOrder:=xlByRows, SearchDirection:=xlNext, _
        MatchCase:=False, SearchFormat:=False).Activate
        cells(3, 2).Select
    Else
    Call heatmapsearch_error
    End If

End Sub
```

```
Sub heatmap_bring_up()

        If IsEmpty(Sheets("input").Range("G3")) Then
            Call heatmap_up_error
            Exit Sub
            Else
        ActiveSheet.Range(Sheets("input").Range("AK8")).Select
            Selection.Find(What:=Sheets("input").Range("F8").Value, After:=ActiveCell, LookIn:=xlFormulas, _
                LookAt:=xlPart, SearchOrder:=xlByRows, SearchDirection:=xlNext, _
                MatchCase:=False, SearchFormat:=False).Activate
        cells(3, 2).Select
        End If

End Sub
```

```
Sub search_stim2()
'

'To search for stims on heatmaps from Dashboard sheet
'
'
Dim stim As Integer, stim_row As Integer, c As String, cr As String
Dim variable
c = "F"
Dim heatmap As String
Dim heatmap2 As String
'Set myrange = Sheets("dashboard").Range("A2:B4")

        If IsError(ActiveSheet.Range("P4")) = True Then
            Call search_stim_error
            Exit Sub
        End If
'

heatmap = Sheets("dashboard").Range("Q4")
heatmap2 = Sheets("dashboard").Range("A6")
'Sheets("dashboard").Range("O1") = heatmap2

If IsEmpty(Sheets("input").Range("G3")) Then
    Call heatmapsearch_error
    Exit Sub
    Else

    If Sheets("dashboard").Range("Q4") = heatmap Then
        For stim = 1 To 100
            If ActiveSheet.Range("P4") = stim Then
                stim_row = stim + 7
                cr = c + CStr(stim_row)
                Sheets(heatmap2).Select
                Sheets(heatmap2).Range("C111:C25150").Select
                Selection.Find(What:=Sheets("Input").Range(cr), After:=ActiveCell, LookIn:=xlFormulas, _
                    LookAt:=xlPart, SearchOrder:=xlByRows, SearchDirection:=xlNext, _
                    MatchCase:=False, SearchFormat:=False).Activate
            cells(3, 2).Select
            End If
        Next stim
     End If
End If
'

End Sub
```

```
Sub resp_overlap()

Sheets("dashboard").Range("I11:I109").FormulaR1C1 = "=IF(OR(R10C11=""Period 1"",R10C11=""Period 2""),IF

End Sub
```

```
Sub tabDashboard()

Sheets("Dashboard").Select

End Sub
```

```
Sub tabInput()

Sheets("Input").Select

End Sub
```

```
Sub tabCharts()

Sheets("charts").Select

End Sub
```

```
Sub tabtables()

Sheets("tables").Select

End Sub
```

```
Sub tabResponders()

Sheets("responders").Select

End Sub
```

```
Sub tabpercent()

Sheets("percent").Select

End Sub
```

```
Sub tabauc()

Sheets("auc").Select

End Sub
```

```
Sub tabraw()

Sheets("raw0").Select

End Sub
```

```
Sub tabrawOG()

Sheets("rawog").Select

End Sub
```

```
Sub tabduration()

Sheets("duration").Select

End Sub
```

```
Sub tabworkflow()

Sheets("workflow").Select

End Sub
```

```
Sub addnew1()

'Dim strName As String
'Dim ws As Worksheet
'Set ws = Worksheets.Add(After:=Worksheets(Worksheets.Count), Type:=xlWorksheet)

Sheets("spreadsheet1").Select

End Sub
```

```
Sub addnew2()

'Dim strName As String
'Dim ws As Worksheet
'Set ws = Worksheets.Add(After:=Worksheets(Worksheets.Count), Type:=xlWorksheet)

Sheets("spreadsheet2").Select

End Sub
```

```
Sub addnew3()

'Dim strName As String
'Dim ws As Worksheet
'Set ws = Worksheets.Add(After:=Worksheets(Worksheets.Count), Type:=xlWorksheet)

Sheets("spreadsheet3").Select

End Sub
```

```
Sub SelectNextSheet()


Dim sht As Worksheet

  Set sht = ActiveSheet
  On Error Resume Next
    Do While sht.Next.Visible <> xlSheetVisible
      If Err <> 0 Then Exit Do
        Set sht = sht.Next
    Loop
      sht.Next.Activate
  On Error GoTo 0

End Sub
```

```
Sub SelectPreviousSheet()

Dim sht As Worksheet

  Set sht = ActiveSheet

  On Error Resume Next
    Do While sht.Previous.Visible <> xlSheetVisible
      If Err <> 0 Then Exit Do
        Set sht = sht.Previous
    Loop
      sht.Previous.Activate
  On Error GoTo 0

End Sub
```

```
Sub Run_error()

MsgBox "Provide at least one stimulation with at least one ROI starting with row 1 in the Stim Table.", vbokay

End Sub
```

```
Sub ROI_error()

MsgBox "The number of ROIs should be between 1 and 328.", vbokay

End Sub
```

```
Sub maxframes_error()

MsgBox "Number of frames must be less than 25,000.", vbokay

End Sub
```

```
Sub period_frame_error()

MsgBox "Period 1 should be before Period 2 and they should not overlap in time.", vbokay

End Sub
```

```
Sub period_frame_error2()

MsgBox "If there's only one period, it should be Period 1 not Period 2.", vbokay

End Sub
```

```
Sub period_frame_error3()

MsgBox "The names of the periods cannot be the same.", vbokay

End Sub
```

```
Sub Reset2_error()

MsgBox "To clear data, the number frames and ROIs should be integers greater than 0.", vbokay

End Sub
```

```
Sub Basal_window_error()

MsgBox "A stim's basal window should not overlap with the prior stim's response window. See the trial duration table, and con

End Sub
```

```
Sub Basal_window_error2()

MsgBox "The start of the basal window cannot exist before time = 0. Consider decreasing the basal window duration.", vbokay


End Sub
```

```
Sub normalization_error()

MsgBox "To normalize data, please include at least one ROI and one frame on the rawOG sheet.", vbokay

End Sub
```

```
Sub search_stim_error()

MsgBox "The stim name is incorrect.", vbokay


End Sub
```

```
Sub maxframe_error()

MsgBox "The end of the last trial cannot excede total duration of frames included in file.", vbokay

End Sub
```

```
Sub heatmap_up_error()

MsgBox "The Heatmap is empty.", vbokay

End Sub
```

```
Sub heatmapsearch_error()

MsgBox "The heatmap is empty or the stim isn't present.", vbokay

End Sub
```

```
Sub not_normal()

MsgBox "The raw data is not normalized to 1.", vbokay

End Sub
```

```
Sub not_normal2()

MsgBox "The raw data is not normalized to 0.", vbokay
```

```
Sub duptrial_error()

MsgBox "No stim trial names can be the same.", vbokay

End Sub
```

```
Sub datanotnorm()

MsgBox "Data is not normalized.", vbokay

End Sub
```

```
Sub maxROI_error()

MsgBox "Each trial's number of ROIs should be less than or equal to total ROIs in file.", vbokay

End Sub
```

Appendix D Two-Photon Imaging Settings

BitsPerPixel = 8

DimensionOrder = XYCZT

IsInterleaved = false

IsRGB = false

LittleEndian = true

PixelType = uint8

Series 0 Name = part 1

SizeC = 1

SizeT = 4000

SizeX = 1024

SizeY = 512

SizeZ = 1

ChannelDescription|BitInc = 0

ChannelDescription|BytesInc = 0

ChannelDescription|ChannelTag = 0

ChannelDescription|DataType = 0

ChannelDescription|IsLUTInverted = 0

ChannelDescription|LUTName = Green

ChannelDescription|Max = 2.550000e+002

ChannelDescription|Min = 0.000000e+000

ChannelDescription|Resolution = 8

ChannelScalingInfo|Automatic = 0

ChannelScalingInfo|BlackValue = 0

ChannelScalingInfo|GammaValue = 1

ChannelScalingInfo|WhiteValue = 1

DimensionDescription|BitInc = 0

DimensionDescription|BytesInc = 524288

DimensionDescription|DimID = 4

DimensionDescription|Length = 1.739637e+003

DimensionDescription|NumberOfElements = 4000

DimensionDescription|Origin = 0.000000e+000

DimensionDescription|Unit = s

HardwareSetting|FilterSettingRecord|AOTF (458) #1 = 0

HardwareSetting|FilterSettingRecord|AOTF (458) #2 = 0

HardwareSetting|FilterSettingRecord|AOTF (476) #1 = 0

HardwareSetting|FilterSettingRecord|AOTF (476) #2 = 0

HardwareSetting|FilterSettingRecord|AOTF (488) #1 = 0

HardwareSetting|FilterSettingRecord|AOTF (488) #2 = 0

HardwareSetting|FilterSettingRecord|AOTF (514) #1 = 0

HardwareSetting|FilterSettingRecord|AOTF (514) #2 = 0

HardwareSetting|FilterSettingRecord|AOTF (543) #1 = 0

HardwareSetting|FilterSettingRecord|AOTF (543) #2 = 0

HardwareSetting|FilterSettingRecord|AOTF (633) #1 = 0

HardwareSetting|FilterSettingRecord|AOTF (633) #2 = 0

HardwareSetting|FilterSettingRecord|Attenuation MP #1 = Min

HardwareSetting|FilterSettingRecord|Attribute = Stain

HardwareSetting|FilterSettingRecord|ClassName = CSpectropheatometerUnit

HardwareSetting|FilterSettingRecord|Constant Power Lambda Begin #1 = 0

HardwareSetting|FilterSettingRecord|Constant Power Lambda End #1 = 0

HardwareSetting|FilterSettingRecord|Constant Power Mode #1 = 0

HardwareSetting|FilterSettingRecord|Data = 0

HardwareSetting|FilterSettingRecord|Description = SP Mirror Channel 1 (stain)

HardwareSetting|FilterSettingRecord|Dummy Name (Obj.) #1 = Dummy1

HardwareSetting|FilterSettingRecord|EOM (940) #1 = 1

HardwareSetting|FilterSettingRecord|EOM (940) #2 = 0

HardwareSetting|FilterSettingRecord|Excitation Beam Splitter FW #1 = RT 30/70

HardwareSetting|FilterSettingRecord|Hardware Type No. #1 = 7

HardwareSetting|FilterSettingRecord|Laser output power #1 = -11.1111111111111

HardwareSetting|FilterSettingRecord|Laser output power #2 = 1411.00W (940nm)

HardwareSetting|FilterSettingRecord|Laser wavelength #1 = 458

HardwareSetting|FilterSettingRecord|Laser wavelength #2 = 543

HardwareSetting|FilterSettingRecord|Laser wavelength #3 = 633

HardwareSetting|FilterSettingRecord|Laser wavelength #4 = 940

HardwareSetting|FilterSettingRecord|MP Gain #1 = 52.0008102268635

HardwareSetting|FilterSettingRecord|MP Offset #1 = 61.9989318684672

HardwareSetting|FilterSettingRecord|Magnification-Changer #1 = SCANx

HardwareSetting|FilterSettingRecord|Multifunction Port (MFP) #1 = SP 665

HardwareSetting|FilterSettingRecord|Notch Filter Wheel 2 #1 = MP2 SP 700

HardwareSetting|FilterSettingRecord|Numerical aperture (Obj.) #1 = 1

HardwareSetting|FilterSettingRecord|ObjectName = SP Mirror Channel 1

HardwareSetting|FilterSettingRecord|Objective #1 = HCX APO L 20.0x1.00 WATER

HardwareSetting|FilterSettingRecord|Order number (Obj.) #1 = 11507701

HardwareSetting|FilterSettingRecord|PMT 1 #1 = Inactive

HardwareSetting|FilterSettingRecord|PMT HyD6 #1 = Inactive

HardwareSetting|FilterSettingRecord|PMT HyD7 #1 = Active

HardwareSetting|FilterSettingRecord|PMT HyD7 (AcquisitionMode) #1 = Standard

HardwareSetting|FilterSettingRecord|PMT HyD7 (Gain) #1 = 100

HardwareSetting|FilterSettingRecord|PMT HyD7 (OverloadState) #1 = OK

HardwareSetting|FilterSettingRecord|PMT Trans #1 = Inactive

HardwareSetting|FilterSettingRecord|Phase #1 = -33.4767681391623

HardwareSetting|FilterSettingRecord|Polarization FW #1 = Empty

HardwareSetting|FilterSettingRecord|Position #1 = 1

HardwareSetting|FilterSettingRecord|Power State #1 = Off

HardwareSetting|FilterSettingRecord|Power State #2 = Off

HardwareSetting|FilterSettingRecord|Power State #3 = Off

HardwareSetting|FilterSettingRecord|Power State #4 = On

HardwareSetting|FilterSettingRecord|RLD_Settings #1 = 500

HardwareSetting|FilterSettingRecord|Refraction index #1 = 1.33

HardwareSetting|FilterSettingRecord|Rotation Direction #1 = 1

HardwareSetting|FilterSettingRecord|SMD-Phase #1 = 0

HardwareSetting|FilterSettingRecord|SP Mirror Channel 1 (left) #1 = 485

HardwareSetting|FilterSettingRecord|SP Mirror Channel 1 (right) #1 = 695

HardwareSetting|FilterSettingRecord|Scan Field Rotation #1 = 95.004500450045

HardwareSetting|FilterSettingRecord|Scan Speed #1 = 600

HardwareSetting|FilterSettingRecord|Spectrum Position #1 = 35.0002923761511

HardwareSetting|FilterSettingRecord|System Number #1 = 5100001689

HardwareSetting|FilterSettingRecord|TLD_Settings #1 = -1

HardwareSetting|FilterSettingRecord|Target Slider #1 = Target Park

HardwareSetting|FilterSettingRecord|VariantType = 8

HardwareSetting|FilterSettingRecord|X Scan Actuator #1 = Active

HardwareSetting|FilterSettingRecord|X Scan Actuator (Gain) #1 = 1.20000045776385

HardwareSetting|FilterSettingRecord|X Scan Actuator (Offs.) #1 = 8.67361737988404E-19

HardwareSetting|FilterSettingRecord|X Scan Actuator (POS) #1 = 0

HardwareSetting|FilterSettingRecord|Y Scan Actuator #1 = Active

HardwareSetting|FilterSettingRecord|Y Scan Actuator (Gain) #1 = 1.20000045776385

HardwareSetting|FilterSettingRecord|Y Scan Actuator (Offs.) #1 = 8.67361737988404E-19

HardwareSetting|FilterSettingRecord|Y Scan Actuator (POS) #1 = 0

HardwareSetting|FilterSettingRecord|Y-Phase #1 = 0

HardwareSetting|FilterSettingRecord|inverse flag topo #1 = 1

HardwareSetting|Name = default

HardwareSetting|ScannerSettingRecord|SystemType #1 = TCS SP5

HardwareSetting|ScannerSettingRecord|bAFUseFixSliceNumber #1 = 0

HardwareSetting|ScannerSettingRecord|bAdaptiveFocusControlActive #1 = 0

HardwareSetting|ScannerSettingRecord|bEnableRoiScan #1 = 0

HardwareSetting|ScannerSettingRecord|bIs3DLimitedRoiScanEnable #1 = 0

HardwareSetting|ScannerSettingRecord|bIsSequential #1 = 0

HardwareSetting|ScannerSettingRecord|bIsSeriesScanAutofocusActive #1 = 0

HardwareSetting|ScannerSettingRecord|bMinimizeMode #1 = 1

HardwareSetting|ScannerSettingRecord|bStepSizeConstant #1 = 0

HardwareSetting|ScannerSettingRecord|bStepSizerActivated #1 = 1

HardwareSetting|ScannerSettingRecord|bUseMPShutter #1 = 1

HardwareSetting|ScannerSettingRecord|bUseVisibleShutter #1 = 0

HardwareSetting|ScannerSettingRecord|bValidBegin #1 = 0

HardwareSetting|ScannerSettingRecord|bValidEnd #1 = 0

HardwareSetting|ScannerSettingRecord|csLutName00 #1 = Green

HardwareSetting|ScannerSettingRecord|csLutName01 #1 = Gray

HardwareSetting|ScannerSettingRecord|csLutName02 #1 = Blue

HardwareSetting|ScannerSettingRecord|csLutName03 #1 = Green

HardwareSetting|ScannerSettingRecord|csScanMode #1 = xyzt

HardwareSetting|ScannerSettingRecord|dAdaptiveFocusControlAutonomousOffset #1 = -2

HardwareSetting|ScannerSettingRecord|dblAFCOffset #1 = -2

HardwareSetting|ScannerSettingRecord|dblAFFocusRange #1 = 0.00008

HardwareSetting|ScannerSettingRecord|dblPinhole #1 = 4.45357212763785E-05

HardwareSetting|ScannerSettingRecord|dblPinholeAiry #1 = 0.999033649994583

HardwareSetting|ScannerSettingRecord|dblSizeX #1 = 6.15079130445208E-04

HardwareSetting|ScannerSettingRecord|dblSizeY #1 = 3.07238940036658E-04

HardwareSetting|ScannerSettingRecord|dblSizeZ #1 = 0

HardwareSetting|ScannerSettingRecord|dblStepSize #1 = 0.00000005

HardwareSetting|ScannerSettingRecord|dblVoxelX #1 = 6.01250371891699E-07

HardwareSetting|ScannerSettingRecord|dblVoxelY #1 = 6.01250371891699E-07

HardwareSetting|ScannerSettingRecord|dblZWidePos #1 = 0.0087386586

HardwareSetting|ScannerSettingRecord|dblZoom #1 = 1.20000045776385

HardwareSetting|ScannerSettingRecord|dwChannelMask #1 = 33554432

HardwareSetting|ScannerSettingRecord|dwLogiChMask #1 = 8

HardwareSetting|ScannerSettingRecord|eAFAnalyseType #1 = 1

HardwareSetting|ScannerSettingRecord|eAFSubsystem #1 = 0

HardwareSetting|ScannerSettingRecord|eAFWorkflowTimelapse #1 = 2

HardwareSetting|ScannerSettingRecord|eAFWorkflowXY #1 = 2

HardwareSetting|ScannerSettingRecord|eAFZUseMode #1 = 2

HardwareSetting|ScannerSettingRecord|eDataSource #1 = 0

HardwareSetting|ScannerSettingRecord|eDirectional #1 = 2

HardwareSetting|ScannerSettingRecord|eDirectionalY #1 = 1

HardwareSetting|ScannerSettingRecord|eSequentialMode #1 = 0

HardwareSetting|ScannerSettingRecord|eZUseMode #1 = 2

HardwareSetting|ScannerSettingRecord|m_bConstantIntegrationTimeActive #1 = 0

HardwareSetting|ScannerSettingRecord|nAFFixSliceNumber #1 = 0

HardwareSetting|ScannerSettingRecord|nAFPrecision #1 = 2

HardwareSetting|ScannerSettingRecord|nAFWorkflowTimelapseIterator #1 = 1

HardwareSetting|ScannerSettingRecord|nAFWorkflowXYIterator #1 = 1

HardwareSetting|ScannerSettingRecord|nAccumulation #1 = 1

HardwareSetting|ScannerSettingRecord|nAverageFrame #1 = 1

HardwareSetting|ScannerSettingRecord|nAverageLine #1 = 1

HardwareSetting|ScannerSettingRecord|nBegin #1 = 0

HardwareSetting|ScannerSettingRecord|nBit #1 = 8

HardwareSetting|ScannerSettingRecord|nChannels #1 = 1

HardwareSetting|ScannerSettingRecord|nDelayTime_ms #1 = 435

HardwareSetting|ScannerSettingRecord|nEnd #1 = 0

HardwareSetting|ScannerSettingRecord|nFormatInDimension #1 = 1024

HardwareSetting|ScannerSettingRecord|nFormatOutDimension #1 = 512

HardwareSetting|ScannerSettingRecord|nLineAccumulation #1 = 1

HardwareSetting|ScannerSettingRecord|nLines #1 = 1.19999980926525

HardwareSetting|ScannerSettingRecord|nPages #1 = 1.19999980926514

HardwareSetting|ScannerSettingRecord|nRepeatActions #1 = 4000

HardwareSetting|ScannerSettingRecord|nSections #1 = 1

Image name = part 1

Location = E:\Experiments\2P\2020\03192020\this\03192020Experiment.lif

Reverse X orientation = false

Reverse Y orientation = true

(Fiji Is Just) ImageJ 2.0.0-rc-69/1.52p; Java 1.8.0_66 [64-bit]; Windows 10 10.0; 3503MB of 29300MB (11%)

Title: 03192020Experiment.lif - part 1

Width: 615.6804 microns (1024)

Height: 307.8402 microns (512)

Size: 2GB

X Resolution: 1.6632 pixels per micron

Y Resolution: 1.6632 pixels per micron

Voxel size: 0.6013x0.6013x0.0500 micron^3

ID: -11

Bits per pixel: 8 (color LUT)

Display range: 0-255

Frame: 46/4000 (t:46/4000 - part 1)

Frame interval: 0.43502 sec

No threshold

ScaleToFit: false

Uncalibrated

Path: E:\Experiments\2P\2020\03192020\this\03192020Experiment.lif

Screen location: 332,156 (1920x1080)

Coordinate origin: 0,0,0

No overlay

No selection

Appendix E Additional Work Performed

This next section outlines some of the additional work performed in addition to the Two-photon imaging. In a separate project, in an effort to determine which LT primary afferents can drive responses in lamina I projection neurons, it includes the optogenetic activation of Trk B down hair fibers, and Trk C LT afferents, while recording in the dorsal root ganglia and lamina 1 of the spinal cord.

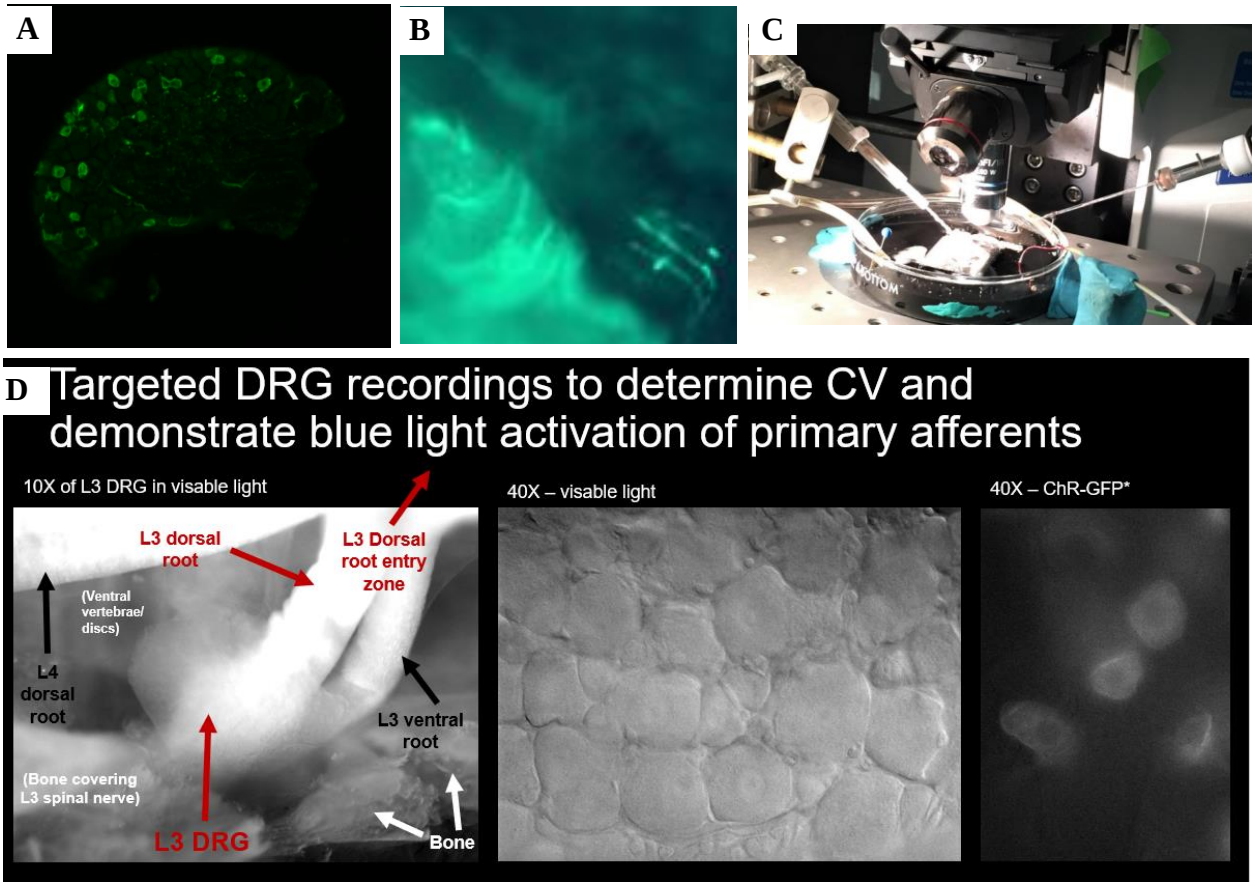

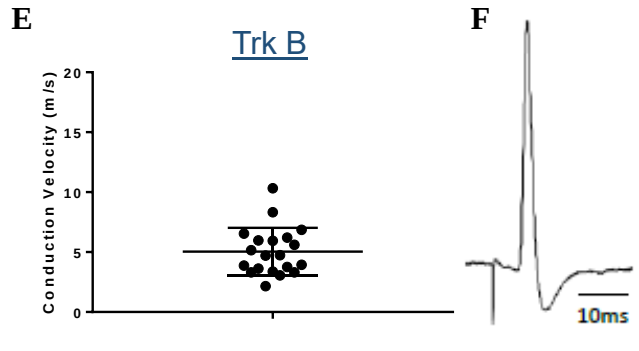

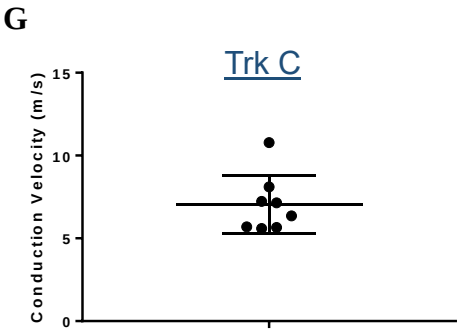

A: DRG with TRKB+ neurons

B: Lanceolate endings

C: Targeting DRG recording in ex vivo prep

D: Targeting DRG recording in ex vivo prep

E: Trk B conduction velocities

F: Blue Light evoked -AP

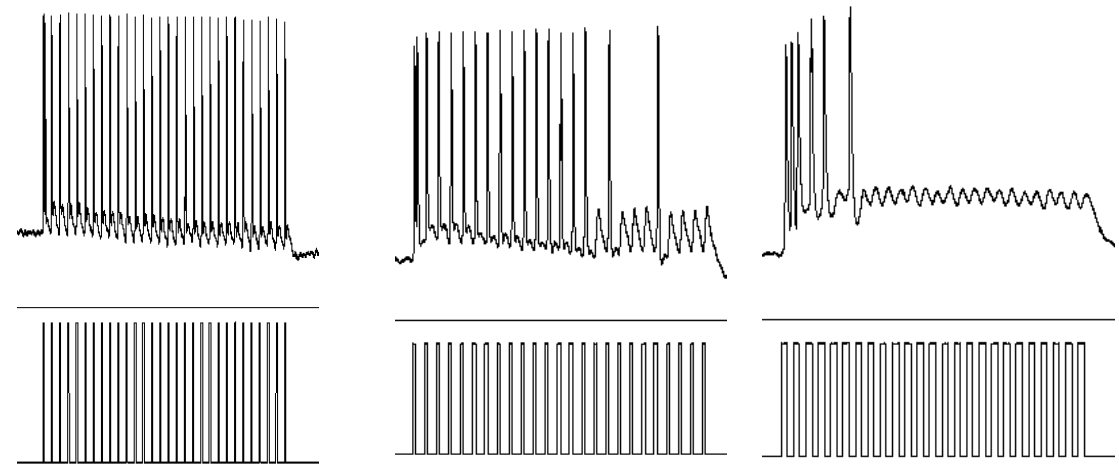

Cell #1

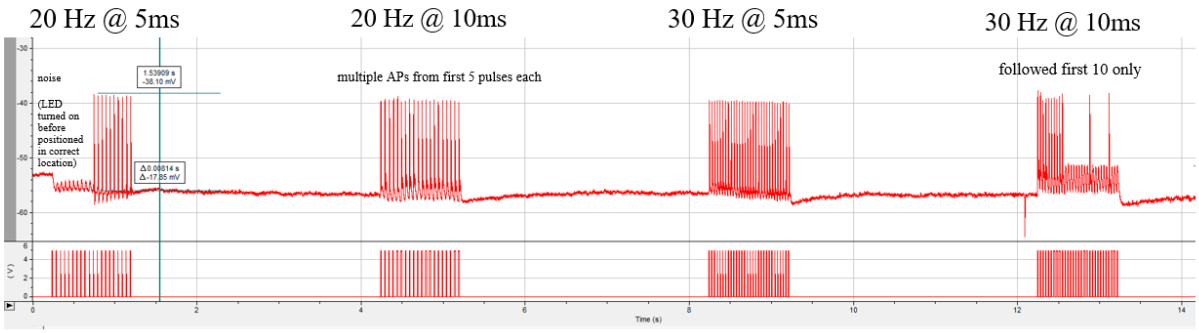

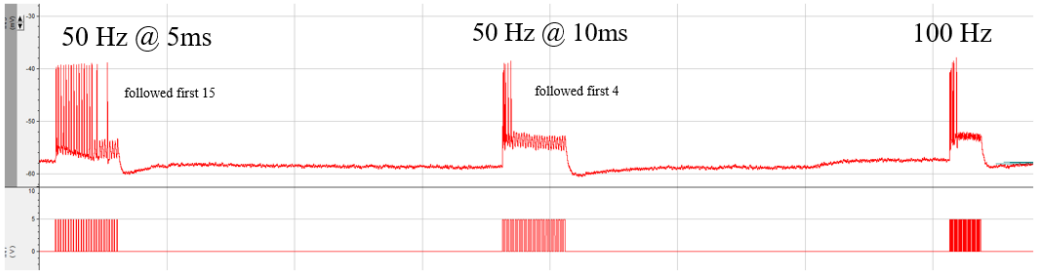

Testing of different blue light frequency and durations to see how TrkB and TrkC can follow optogenetic stimulation

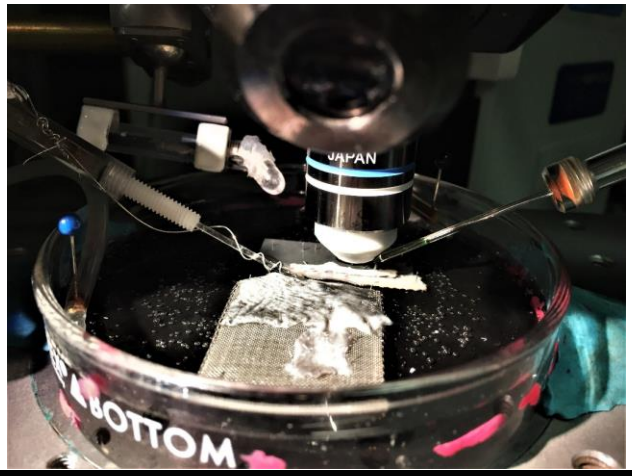

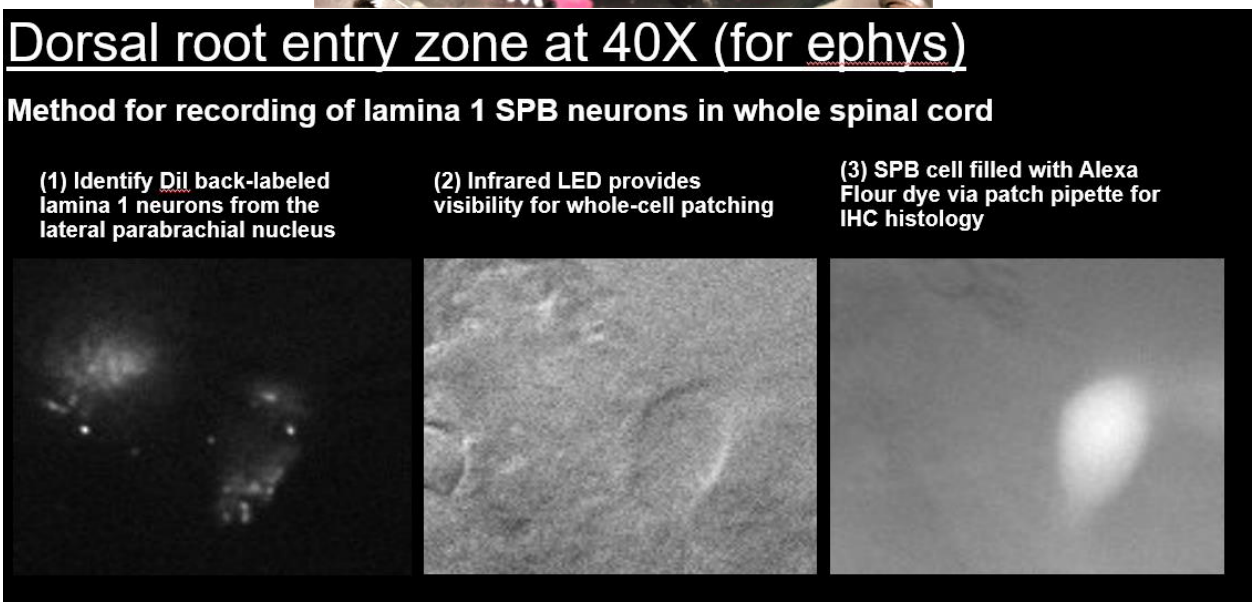

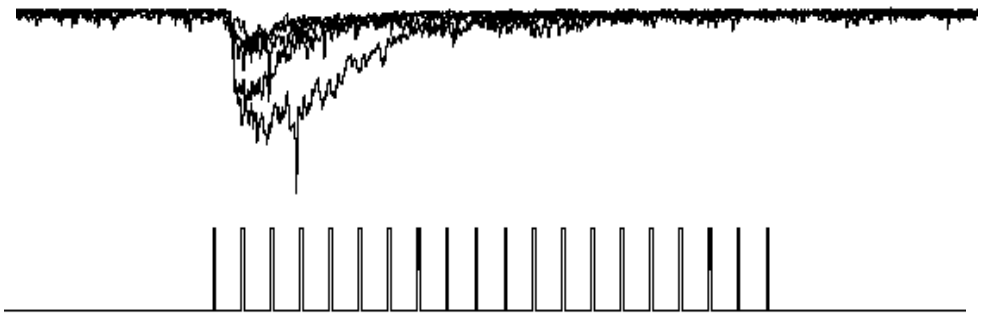

20 5ms blue light pulses at 20Hz on L2 DRG

Lamina I back-labeled spinoparabrachial patch clamp recordings in ex vivo prep

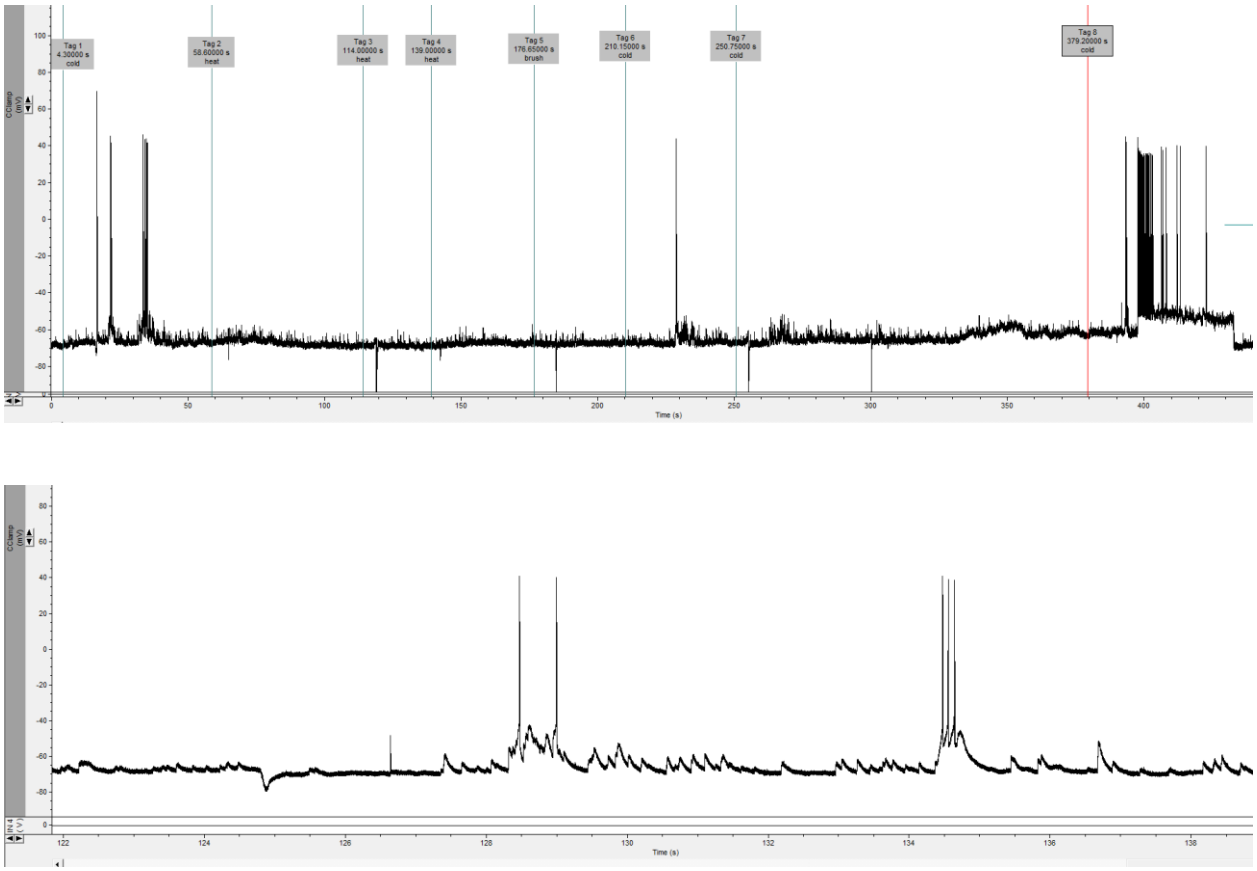

Cold responses in lamina I neuron. Note that the timing of the grey notes are offset from the actual stimulation. These are cold responses.

Bibliography

1. Allard, J. (2019). Physiological properties of the lamina I spinoparabrachial neurons in the mouse. *J Physiol*, *597*(7), 2097-2113. https://doi.org/10.1113/JP277447
2. Andrew, D. (2009). Sensitization of lamina I spinoparabrachial neurons parallels heat hyperalgesia in the chronic constriction injury model of neuropathic pain. *J Physiol*, *587*(Pt 9), 2005-2017. https://doi.org/10.1113/jphysiol.2009.170290
3. Andrew, D. (2010). Quantitative characterization of low-threshold mechanoreceptor inputs to lamina I spinoparabrachial neurons in the rat. *J Physiol*, *588*(Pt 1), 117-124. https://doi.org/10.1113/jphysiol.2009.181511
4. Averill, S., McMahon, S. B., Clary, D. O., Reichardt, L. F., & Priestley, J. V. (1995). Immunocytochemical localization of trkA receptors in chemically identified subgroups of adult rat sensory neurons. *Eur J Neurosci*, *7*(7), 1484-1494. https://doi.org/10.1111/j.1460-9568.1995.tb01143.x
5. Baccei, M. L., & Fitzgerald, M. (2004). Development of GABAergic and glycinergic transmission in the neonatal rat dorsal horn. *J Neurosci*, *24*(20), 4749-4757. https://doi.org/10.1523/JNEUROSCI.5211-03.2004
6. Bessou, P., & Perl, E. R. (1969). Response of cutaneous sensory units with unmyelinated fibers to noxious stimuli. *J Neurophysiol*, *32*(6), 1025-1043. https://doi.org/10.1152/jn.1969.32.6.1025
7. Bester, H., Chapman, V., Besson, J. M., & Bernard, J. F. (2000). Physiological properties of the lamina I spinoparabrachial neurons in the rat. *J Neurophysiol*, *83*(4), 2239-2259. https://doi.org/10.1152/jn.2000.83.4.2239
8. Beyer, C., Roberts, L. A., & Komisaruk, B. R. (1985). Hyperalgesia induced by altered glycinergic activity at the spinal cord. *Life Sci*, *37*(9), 875-882. https://doi.org/10.1016/0024-3205(85)90523-5
9. Blomqvist, A., Ma, W., & Berkley, K. J. (1989). Spinal input to the parabrachial nucleus in the cat. *Brain Res*, *480*(1-2), 29-36. https://doi.org/10.1016/0006-8993(89)91563-1
10. Boylan, C. B., Davis, K., Bennett-Clarke, C. A., & Rhoades, R. W. (1996). Neonatal damage to the rat's infraorbital nerve upregulates both galanin and neuropeptide Y in individual vibrissae-related primary afferent axons. *Exp Brain Res*, *112*(3), 475-484. https://doi.org/10.1007/BF00227953
11. Boyle, K. A., Gutierrez-Mecinas, M., Polgar, E., Mooney, N., O'Connor, E., Furuta, T., Watanabe, M., & Todd, A. J. (2017). A quantitative study of neurochemically defined populations of inhibitory interneurons in the superficial dorsal horn of the mouse spinal cord. *Neuroscience*, *363*, 120-133. https://doi.org/10.1016/j.neuroscience.2017.08.044
12. Bracci, E., Ballerini, L., & Nistri, A. (1996). Localization of rhythmogenic networks responsible for spontaneous bursts induced by strychnine and bicuculline in the rat isolated spinal cord. *J Neurosci*, *16*(21), 7063-7076. https://doi.org/10.1523/JNEUROSCI.16-21-07063.1996

13. Brown, A. G. (1981). *Organization in the Spinal Cord: The Anatomy and Physiology of Identified Neurones*. Springer London. https://books.google.com/books?id=ZRpIAQAAIAAJ
14. Brown, P. B., & Fuchs, J. L. (1975). Somatotopic representation of hindlimb skin in cat dorsal horn. *J Neurophysiol*, *38*(1), 1-9. https://doi.org/10.1152/jn.1975.38.1.1
15. Brown, P. B., & Koerber, H. R. (1978). Cat hindlimb tactile dermatomes determined with single-unit recordings. *J Neurophysiol*, *41*(2), 260-267. https://doi.org/10.1152/jn.1978.41.2.260
16. Burgess, P. R., & Perl, E. R. (1967). Myelinated afferent fibres responding specifically to noxious stimulation of the skin. *J Physiol*, *190*(3), 541-562. https://doi.org/10.1113/jphysiol.1967.sp008227
17. Campbell, J. N., Meyer, R. A., & LaMotte, R. H. (1979). Sensitization of myelinated nociceptive afferents that innervate monkey hand. *J Neurophysiol*, *42*(6), 1669-1679. https://doi.org/10.1152/jn.1979.42.6.1669
18. Casser, H. R., & Schaible, H. G. (2015). [Musculoskeletal pain]. *Schmerz*, *29*(5), 486-488, 490-485. https://doi.org/10.1007/s00482-015-0046-9 (Muskuloskeletaler Schmerz.)
19. Chen, T. W., Wardill, T. J., Sun, Y., Pulver, S. R., Renninger, S. L., Baohan, A., Schreiter, E. R., Kerr, R. A., Orger, M. B., Jayaraman, V., Looger, L. L., Svoboda, K., & Kim, D. S. (2013). Ultrasensitive fluorescent proteins for imaging neuronal activity. *Nature*, *499*(7458), 295-300. https://doi.org/10.1038/nature12354
20. Cheunsuang, O., Maxwell, D., & Morris, R. (2002). Spinal lamina I neurones that express neurokinin 1 receptors: II. Electrophysiological characteristics, responses to primary afferent stimulation and effects of a selective mu-opioid receptor agonist. *Neuroscience*, *111*(2), 423-434. https://doi.org/10.1016/s0306-4522(02)00035-0
21. Cheunsuang, O., & Morris, R. (2000). Spinal lamina I neurons that express neurokinin 1 receptors: morphological analysis. *Neuroscience*, *97*(2), 335-345. https://doi.org/10.1016/s0306-4522(00)00035-x
22. Christensen, B. N., & Perl, E. R. (1970). Spinal neurons specifically excited by noxious or thermal stimuli: marginal zone of the dorsal horn. *J Neurophysiol*, *33*(2), 293-307. https://doi.org/10.1152/jn.1970.33.2.293
23. Craig, A. D., & Dostrovsky, J. O. (2001). Differential projections of thermoreceptive and nociceptive lamina I trigeminothalamic and spinothalamic neurons in the cat. *J Neurophysiol*, *86*(2), 856-870. https://doi.org/10.1152/jn.2001.86.2.856
24. Craig, A. D., & Kniffki, K. D. (1985). Spinothalamic lumbosacral lamina I cells responsive to skin and muscle stimulation in the cat. *J Physiol*, *365*, 197-221. https://doi.org/10.1113/jphysiol.1985.sp015767
25. Culberson, J. L., & Brown, P. B. (1984). Projections of hindlimb dorsal roots to lumbosacral spinal cord of cat. *J Neurophysiol*, *51*(3), 516-528. https://doi.org/10.1152/jn.1984.51.3.516
26. Deng, J., Zhou, H., Lin, J. K., Shen, Z. X., Chen, W. Z., Wang, L. H., Li, Q., Mu, D., Wei, Y. C., Xu, X. H., & Sun, Y. G. (2020). The Parabrachial Nucleus Directly Channels Spinal Nociceptive Signals to the Intralaminar Thalamic Nuclei, but Not the Amygdala. *Neuron*, *107*(5), 909-923 e906. https://doi.org/10.1016/j.neuron.2020.06.017

27. Ellrich, J., & Makowska, A. (2007). Nerve growth factor and ATP excite different neck muscle nociceptors in anaesthetized mice. *Cephalalgia*, *27*(11), 1226-1235. https://doi.org/10.1111/j.1468-2982.2007.01431.x
28. Fang, X., McMullan, S., Lawson, S. N., & Djouhri, L. (2005). Electrophysiological differences between nociceptive and non-nociceptive dorsal root ganglion neurones in the rat in vivo. *J Physiol*, *565*(Pt 3), 927-943. https://doi.org/10.1113/jphysiol.2005.086199
29. Fitzgerald, M. (1985). The post-natal development of cutaneous afferent fibre input and receptive field organization in the rat dorsal horn. *J Physiol*, *364*, 1-18. https://doi.org/10.1113/jphysiol.1985.sp015725
30. Fitzgerald, M., & Jennings, E. (1999). The postnatal development of spinal sensory processing. *Proc Natl Acad Sci U S A*, *96*(14), 7719-7722. https://doi.org/10.1073/pnas.96.14.7719
31. Foster, E., Wildner, H., Tudeau, L., Haueter, S., Ralvenius, W. T., Jegen, M., Johannssen, H., Hosli, L., Haenraets, K., Ghanem, A., Conzelmann, K. K., Bosl, M., & Zeilhofer, H. U. (2015). Targeted ablation, silencing, and activation establish glycinergic dorsal horn neurons as key components of a spinal gate for pain and itch. *Neuron*, *85*(6), 1289-1304. https://doi.org/10.1016/j.neuron.2015.02.028
32. Gasser, H. S. (1941). The Classification of Nerve Fibers. *The Ohio Journal of Science. v41 n3 (May, 1941), 145-159*. https://kb.osu.edu/handle/1811/3153?show=full
33. Gauriau, C., & Bernard, J. F. (2002). Pain pathways and parabrachial circuits in the rat. *Exp Physiol*, *87*(2), 251-258. https://doi.org/10.1113/eph8702357
34. Gotch, F. (1891). On The Mammalian Nervous System: Its Functions, And Their Localization Determined By An Electrical Method.
35. Gradwell, M. A., Callister, R. J., & Graham, B. A. (2020). Reviewing the case for compromised spinal inhibition in neuropathic pain. *J Neural Transm (Vienna)*, *127*(4), 481-503. https://doi.org/10.1007/s00702-019-02090-0
36. Gutierrez-Mecinas, M., Furuta, T., Watanabe, M., & Todd, A. J. (2016). A quantitative study of neurochemically defined excitatory interneuron populations in laminae I-III of the mouse spinal cord. *Mol Pain*, *12*. https://doi.org/10.1177/1744806916629065
37. Hachisuka, J., Omori, Y., Chiang, M. C., Gold, M. S., Koerber, H. R., & Ross, S. E. (2018). Wind-up in lamina I spinoparabrachial neurons: a role for reverberatory circuits. *Pain*, *159*(8), 1484-1493. https://doi.org/10.1097/j.pain.0000000000001229
38. Han, J. J. (2021). Synchron receives FDA approval to begin early feasibility study of their endovascular, brain-computer interface device. *Artif Organs*, *45*(10), 1134-1135. https://doi.org/10.1111/aor.14049
39. Handwerker, H. O., Anton, F., & Reeh, P. W. (1987). Discharge patterns of afferent cutaneous nerve fibers from the rat's tail during prolonged noxious mechanical stimulation. *Exp Brain Res*, *65*(3), 493-504. https://doi.org/10.1007/BF00235972
40. Harding, E. K., Boivin, B., & Salter, M. W. (2020). Intracellular Calcium Responses Encode Action Potential Firing in Spinal Cord Lamina I Neurons. *J Neurosci*, *40*(23), 4439-4456. https://doi.org/10.1523/JNEUROSCI.0206-20.2020
41. Hoheisel, U., & Mense, S. (1990). Response behaviour of cat dorsal horn neurones receiving input from skeletal muscle and other deep somatic tissues. *J Physiol*, *426*, 265-280. https://doi.org/10.1113/jphysiol.1990.sp018137

42. Hoheisel, U., Mense, S., Simons, D. G., & Yu, X. M. (1993). Appearance of new receptive fields in rat dorsal horn neurons following noxious stimulation of skeletal muscle: a model for referral of muscle pain? *Neurosci Lett*, *153*(1), 9-12. https://doi.org/10.1016/0304-3940(93)90064-r
43. Hoheisel, U., Unger, T., & Mense, S. (2005). Excitatory and modulatory effects of inflammatory cytokines and neurotrophins on mechanosensitive group IV muscle afferents in the rat. *Pain*, *114*(1-2), 168-176. https://doi.org/10.1016/j.pain.2004.12.020
44. Hwang, J. H., & Yaksh, T. L. (1997). The effect of spinal GABA receptor agonists on tactile allodynia in a surgically-induced neuropathic pain model in the rat. *Pain*, *70*(1), 15-22. https://doi.org/10.1016/s0304-3959(96)03249-6
45. Hylden, J. L., Anton, F., & Nahin, R. L. (1989). Spinal lamina I projection neurons in the rat: collateral innervation of parabrachial area and thalamus. *Neuroscience*, *28*(1), 27-37.
46. Hylden, J. L., Hayashi, H., Bennett, G. J., & Dubner, R. (1985). Spinal lamina I neurons projecting to the parabrachial area of the cat midbrain. *Brain Res*, *336*(1), 195-198.
47. Hylden, J. L. K., Nahin, R. L., Traub, R. J., & Dubner, R. (1989). Expansion of receptive fields of spinal lamina I projection neurons in rats with unilateral adjuvant-induced inflammation: the contribution of dorsal horn mechanisms. *Pain*, *37*(2), 229-243. https://doi.org/10.1016/0304-3959(89)90135-8
48. Ibuki, T., Hama, A. T., Wang, X. T., Pappas, G. D., & Sagen, J. (1997). Loss of GABA-immunoreactivity in the spinal dorsal horn of rats with peripheral nerve injury and promotion of recovery by adrenal medullary grafts. *Neuroscience*, *76*(3), 845-858. https://doi.org/10.1016/s0306-4522(96)00341-7
49. Iggo, A. (1960). Cutaneous mechanoreceptors with afferent C fibres. *J Physiol*, *152*(2), 337-353. https://doi.org/10.1113/jphysiol.1960.sp006491
50. Jankowski, M. P., & Koerber, H. R. (2010). Neurotrophic Factors and Nociceptor Sensitization. In L. Kruger & A. R. Light (Eds.), *Translational Pain Research: From Mouse to Man*. https://www.ncbi.nlm.nih.gov/pubmed/21882462
51. Jankowski, M. P., Lawson, J. J., McIlwrath, S. L., Rau, K. K., Anderson, C. E., Albers, K. M., & Koerber, H. R. (2009). Sensitization of cutaneous nociceptors after nerve transection and regeneration: possible role of target-derived neurotrophic factor signaling. *J Neurosci*, *29*(6), 1636-1647. https://doi.org/10.1523/JNEUROSCI.3474-08.2009
52. Jankowski, M. P., Rau, K. K., Ekmann, K. M., Anderson, C. E., & Koerber, H. R. (2013). Comprehensive phenotyping of group III and IV muscle afferents in mouse. *J Neurophysiol*, *109*(9), 2374-2381. https://doi.org/10.1152/jn.01067.2012
53. Jankowski, M. P., Rau, K. K., & Koerber, H. R. (2017). Cutaneous TRPM8-expressing sensory afferents are a small population of neurons with unique firing properties. *Physiol Rep*, *5*(7). https://doi.org/10.14814/phy2.13234
54. Jankowski, M. P., Rau, K. K., Soneji, D. J., Anderson, C. E., & Koerber, H. R. (2010). Enhanced artemin/GFRalpha3 levels regulate mechanically insensitive, heat-sensitive C-fiber recruitment after axotomy and regeneration. *J Neurosci*, *30*(48), 16272-16283. https://doi.org/10.1523/JNEUROSCI.2195-10.2010
55. Jankowski, M. P., Soneji, D. J., Ekmann, K. M., Anderson, C. E., & Koerber, H. R. (2012). Dynamic changes in heat transducing channel TRPV1 expression regulate mechanically insensitive, heat sensitive C-fiber recruitment after axotomy and regeneration. *J Neurosci*, *32*(49), 17869-17873. https://doi.org/10.1523/JNEUROSCI.3148-12.2012

56. Keller, A. F., Beggs, S., Salter, M. W., & De Koninck, Y. (2007). Transformation of the output of spinal lamina I neurons after nerve injury and microglia stimulation underlying neuropathic pain. *Mol Pain*, *3*, 27. https://doi.org/10.1186/1744-8069-3-27
57. Koerber, H. R. (1980). Somatotopic organization of cat brachial spinal cord. *Exp Neurol*, *69*(3), 481-492. https://doi.org/10.1016/0014-4886(80)90046-1
58. Koerber, H. R., & Brown, P. B. (1982). Somatotopic organization of hindlimb cutaneous nerve projections to cat dorsal horn. *J Neurophysiol*, *48*(2), 481-489. https://doi.org/10.1152/jn.1982.48.2.481
59. Koerber, H. R., Druzinsky, R. E., & Mendell, L. M. (1988). Properties of somata of spinal dorsal root ganglion cells differ according to peripheral receptor innervated. *J Neurophysiol*, *60*(5), 1584-1596. https://doi.org/10.1152/jn.1988.60.5.1584
60. Koerber, H. R., & Woodbury, C. J. (2002). Comprehensive phenotyping of sensory neurons using an *ex vivo* somatosensory system. *Physiol Behav*, *77*(4-5), 589-594. https://doi.org/10.1016/s0031-9384(02)00904-6
61. Koga, K., Kanehisa, K., Kohro, Y., Shiratori-Hayashi, M., Tozaki-Saitoh, H., Inoue, K., Furue, H., & Tsuda, M. (2017). Chemogenetic silencing of GABAergic dorsal horn interneurons induces morphine-resistant spontaneous nocifensive behaviours. *Sci Rep*, *7*(1), 4739. https://doi.org/10.1038/s41598-017-04972-3
62. Kumazawa, T., & Perl, E. R. (1978). Excitation of marginal and substantia gelatinosa neurons in the primate spinal cord: indications of their place in dorsal horn functional organization. *J Comp Neurol*, *177*(3), 417-434. https://doi.org/10.1002/cne.901770305
63. Laferriere, A., Millecamps, M., Xanthos, D. N., Xiao, W. H., Siau, C., de Mos, M., Sachot, C., Ragavendran, J. V., Huygen, F. J., Bennett, G. J., & Coderre, T. J. (2008). Cutaneous tactile allodynia associated with microvascular dysfunction in muscle. *Mol Pain*, *4*, 49. https://doi.org/10.1186/1744-8069-4-49
64. Lawson, S. N., Crepps, B. A., & Perl, E. R. (1997). Relationship of substance P to afferent characteristics of dorsal root ganglion neurones in guinea-pig. *J Physiol*, *505 (Pt 1)*(Pt 1), 177-191. https://doi.org/10.1111/j.1469-7793.1997.00177.x
65. Li, J., & Baccei, M. L. (2017). Functional Organization of Cutaneous and Muscle Afferent Synapses onto Immature Spinal Lamina I Projection Neurons. *J Neurosci*, *37*(6), 1505-1517. https://doi.org/10.1523/JNEUROSCI.3164-16.2016
66. Light, A. R., Sedivec, M. J., Casale, E. J., & Jones, S. L. (1993). Physiological and morphological characteristics of spinal neurons projecting to the parabrachial region of the cat. *Somatosens Mot Res*, *10*(3), 309-325.
67. Light, A. R., Trevino, D. L., & Perl, E. R. (1979). Morphological features of functionally defined neurons in the marginal zone and substantia gelatinosa of the spinal dorsal horn. *J Comp Neurol*, *186*(2), 151-171. https://doi.org/10.1002/cne.901860204
68. Loomis, C. W., Khandwala, H., Osmond, G., & Hefferan, M. P. (2001). Coadministration of intrathecal strychnine and bicuculline effects synergistic allodynia in the rat: an isobolographic analysis. *J Pharmacol Exp Ther*, *296*(3), 756-761. https://www.ncbi.nlm.nih.gov/pubmed/11181903
69. Mackintosh, J. A., Choi, H. Y., Bae, S. H., Veal, D. A., Bell, P. J., Ferrari, B. C., Van Dyk, D. D., Verrills, N. M., Paik, Y. K., & Karuso, P. (2003). A fluorescent natural product for ultra sensitive detection of proteins in one-dimensional and two-dimensional gel electrophoresis. *Proteomics*, *3*(12), 2273-2288. https://doi.org/10.1002/pmic.200300578

70. Malan, T. P., Mata, H. P., & Porreca, F. (2002). Spinal GABA(A) and GABA(B) receptor pharmacology in a rat model of neuropathic pain. *Anesthesiology*, *96*(5), 1161-1167. https://doi.org/10.1097/00000542-200205000-00020
71. Mantyh, P. W., Rogers, S. D., Honore, P., Allen, B. J., Ghilardi, J. R., Li, J., Daughters, R. S., Lappi, D. A., Wiley, R. G., & Simone, D. A. (1997). Inhibition of hyperalgesia by ablation of lamina I spinal neurons expressing the substance P receptor. *Science*, *278*(5336), 275-279.
72. McMahon, S. B., & Wall, P. D. (1985). The distribution and central termination of single cutaneous and muscle unmyelinated fibres in rat spinal cord. *Brain Res*, *359*(1-2), 39-48. https://doi.org/10.1016/0006-8993(85)91410-6
73. Mense, S. (1993). [Neurobiological mechanisms of muscle pain referral.]. *Schmerz*, *7*(4), 241-249. https://doi.org/10.1007/BF02529860 (Neurobiologische Mechanismen der Ubertragung von Muskelschmerz.)
74. Mitchell, K., Spike, R. C., & Todd, A. J. (1993). An immunocytochemical study of glycine receptor and GABA in laminae I-III of rat spinal dorsal horn. *J Neurosci*, *13*(6), 2371-2381. https://doi.org/10.1523/JNEUROSCI.13-06-02371.1993
75. Molander, C., & Grant, G. (1985). Cutaneous projections from the rat hindlimb foot to the substantia gelatinosa of the spinal cord studied by transganglionic transport of WGA-HRP conjugate. *J Comp Neurol*, *237*(4), 476-484. https://doi.org/10.1002/cne.902370405
76. Molander, C., & Grant, G. (1986). Laminar distribution and somatotopic organization of primary afferent fibers from hindlimb nerves in the dorsal horn. A study by transganglionic transport of horseradish peroxidase in the rat. *Neuroscience*, *19*(1), 297-312. https://doi.org/10.1016/0306-4522(86)90023-0
77. Molander, C., & Grant, G. (1987). Spinal cord projections from hindlimb muscle nerves in the rat studied by transganglionic transport of horseradish peroxidase, wheat germ agglutinin conjugated horseradish peroxidase, or horseradish peroxidase with dimethylsulfoxide. *J Comp Neurol*, *260*(2), 246-255. https://doi.org/10.1002/cne.902600208
78. Molander, C., Xu, Q., & Grant, G. (1984). The cytoarchitectonic organization of the spinal cord in the rat. I. The lower thoracic and lumbosacral cord. *J Comp Neurol*, *230*(1), 133-141. https://doi.org/10.1002/cne.902300112
79. Molander, C., Xu, Q., Rivero-Melian, C., & Grant, G. (1989). Cytoarchitectonic organization of the spinal cord in the rat: II. The cervical and upper thoracic cord. *J Comp Neurol*, *289*(3), 375-385. https://doi.org/10.1002/cne.902890303
80. Molliver, D. C., Radeke, M. J., Feinstein, S. C., & Snider, W. D. (1995). Presence or absence of TrkA protein distinguishes subsets of small sensory neurons with unique cytochemical characteristics and dorsal horn projections. *J Comp Neurol*, *361*(3), 404-416. https://doi.org/10.1002/cne.903610305
81. Molliver, D. C., Wright, D. E., Leitner, M. L., Parsadanian, A. S., Doster, K., Wen, D., Yan, Q., & Snider, W. D. (1997). IB4-binding DRG neurons switch from NGF to GDNF dependence in early postnatal life. *Neuron*, *19*(4), 849-861. https://doi.org/10.1016/s0896-6273(00)80966-6
82. Moore, D. S., G.P. McCabe and B.A. Craig. (2014). *Introduction to the Practice of Statistics* (8th ed.). W.H. Freeman and Company. https://www.coursehero.com/file/22178147/Syllabus/

83. Narikawa, K., Furue, H., Kumamoto, E., & Yoshimura, M. (2000). In vivo patch-clamp analysis of IPSCs evoked in rat substantia gelatinosa neurons by cutaneous mechanical stimulation. *J Neurophysiol*, *84*(4), 2171-2174. https://doi.org/10.1152/jn.2000.84.4.2171
84. Polgar, E., Wright, L. L., & Todd, A. J. (2010). A quantitative study of brainstem projections from lamina I neurons in the cervical and lumbar enlargement of the rat. *Brain Res*, *1308*(5), 58-67. https://doi.org/10.1016/j.brainres.2009.10.041
85. Pomeranz, B., Wall, P. D., & Weber, W. V. (1968). Cord cells responding to fine myelinated afferents from viscera, muscle and skin. *J Physiol*, *199*(3), 511-532. https://doi.org/10.1113/jphysiol.1968.sp008666
86. Prescott, S. A. (2015). Synaptic inhibition and disinhibition in the spinal dorsal horn. *Prog Mol Biol Transl Sci*, *131*, 359-383. https://doi.org/10.1016/bs.pmbts.2014.11.008
87. Raja, S. N., Meyer, R. A., & Campbell, J. N. (1988). Peripheral mechanisms of somatic pain. *Anesthesiology*, *68*(4), 571-590. https://doi.org/10.1097/00000542-198804000-00016
88. Rexed, B. (1952). The cytoarchitectonic organization of the spinal cord in the cat. *J Comp Neurol*, *96*(3), 414-495. https://doi.org/10.1002/cne.900960303
89. Rexed, B. (1954). A cytoarchitectonic atlas of the spinal cord in the cat. *J Comp Neurol*, *100*(2), 297-379. https://doi.org/10.1002/cne.901000205
90. Rivero-Melian, C. (1996). Organization of hindlimb nerve projections to the rat spinal cord: a choleragenoid horseradish peroxidase study. *J Comp Neurol*, *364*(4), 651-663. https://doi.org/10.1002/(SICI)1096-9861(19960122)364:4<651::AID-CNE4>3.0.CO;2-2
91. Rivero-Melian, C., & Grant, G. (1991). Choleragenoid horseradish peroxidase used for studying projections of some hindlimb cutaneous nerves and plantar foot afferents to the dorsal horn and Clarke's column in the rat. *Exp Brain Res*, *84*(1), 125-132. https://doi.org/10.1007/BF00231767
92. Ruscheweyh, R., & Sandkuhler, J. (2005). Long-range oscillatory Ca2+ waves in rat spinal dorsal horn. *Eur J Neurosci*, *22*(8), 1967-1976. https://doi.org/10.1111/j.1460-9568.2005.04393.x
93. Sandkuhler, J. (2009). Models and mechanisms of hyperalgesia and allodynia. *Physiol Rev*, *89*(2), 707-758. https://doi.org/10.1152/physrev.00025.2008
94. Satoh, O., & Omote, K. (1996). Roles of monoaminergic, glycinergic and GABAergic inhibitory systems in the spinal cord in rats with peripheral mononeuropathy. *Brain Res*, *728*(1), 27-36. https://www.ncbi.nlm.nih.gov/pubmed/8864294
95. Schaible, H. G., Schmidt, R. F., & Willis, W. D. (1987). Convergent inputs from articular, cutaneous and muscle receptors onto ascending tract cells in the cat spinal cord. *Exp Brain Res*, *66*(3), 479-488. https://doi.org/10.1007/BF00270680
96. Sessle, B. J., Hu, J. W., Amano, N., & Zhong, G. (1986). Convergence of cutaneous, tooth pulp, visceral, neck and muscle afferents onto nociceptive and non-nociceptive neurones in trigeminal subnucleus caudalis (medullary dorsal horn) and its implications for referred pain. *Pain*, *27*(2), 219-235. https://doi.org/10.1016/0304-3959(86)90213-7
97. Silverman, J. D., & Kruger, L. (1988). Acid phosphatase as a selective marker for a class of small sensory ganglion cells in several mammals: spinal cord distribution, histochemical properties, and relation to fluoride-resistant acid phosphatase (FRAP) of rodents. *Somatosens Res*, *5*(3), 219-246. https://doi.org/10.3109/07367228809144628

98. Sivilotti, L., & Woolf, C. J. (1994). The contribution of GABAA and glycine receptors to central sensitization: disinhibition and touch-evoked allodynia in the spinal cord. *J Neurophysiol*, *72*(1), 169-179. https://doi.org/10.1152/jn.1994.72.1.169
99. Snider, W. D., & McMahon, S. B. (1998). Tackling pain at the source: new ideas about nociceptors. *Neuron*, *20*(4), 629-632. https://doi.org/10.1016/s0896-6273(00)81003-x
100. Todd, A. J. (1996). GABA and glycine in synaptic glomeruli of the rat spinal dorsal horn. *Eur J Neurosci*, *8*(12), 2492-2498. https://doi.org/10.1111/j.1460-9568.1996.tb01543.x
101. Todd, A. J., & Sullivan, A. C. (1990). Light microscope study of the coexistence of GABA-like and glycine-like immunoreactivities in the spinal cord of the rat. *J Comp Neurol*, *296*(3), 496-505. https://doi.org/10.1002/cne.902960312
102. Todd, A. J., Watt, C., Spike, R. C., & Sieghart, W. (1996). Colocalization of GABA, glycine, and their receptors at synapses in the rat spinal cord. *J Neurosci*, *16*(3), 974-982. https://doi.org/10.1523/JNEUROSCI.16-03-00974.1996
103. Torsney, C., & Fitzgerald, M. (2002). Age-dependent effects of peripheral inflammation on the electrophysiological properties of neonatal rat dorsal horn neurons. *J Neurophysiol*, *87*(3), 1311-1317. https://doi.org/10.1152/jn.00462.2001
104. Warwick, C., Salsovic, J., Hachisuka, J., Smith, K. M., Sheahan, T. D., Chen, H., Ibinson, J., Koerber, H. R., & Ross, S. E. (2022). Cell type-specific calcium imaging of central sensitization in mouse dorsal horn. *Nat Commun*, *13*(1), 5199. https://doi.org/10.1038/s41467-022-32608-2
105. Woodbury, C. J., & Koerber, H. R. (2003). Widespread projections from myelinated nociceptors throughout the substantia gelatinosa provide novel insights into neonatal hypersensitivity. *J Neurosci*, *23*(2), 601-610. https://doi.org/10.1523/JNEUROSCI.23-02-00601.2003
106. Woodbury, C. J., Ritter, A. M., & Koerber, H. R. (2000). On the problem of lamination in the superficial dorsal horn of mammals: a reappraisal of the substantia gelatinosa in postnatal life. *J Comp Neurol*, *417*(1), 88-102. https://doi.org/10.1002/(sici)1096-9861(20000131)417:1<88::aid-cne7>3.0.co;2-u
107. Zieglgansberger, W., & Herz, A. (1971). Changes of cutaneous receptive fields of spino-cervical-tract neurones and other dorsal horn neurones by microelectrophoretically administered amino acids. *Exp Brain Res*, *13*(2), 111-126. https://doi.org/10.1007/BF00234080

5.0 The End

The End.